UNCLASSIFIED UNLIMITED

DRES

CONTRACT REPORT 29/89

DEVELOPMENT OF A LIPID - MEMBRANE COATED FIBER - OPTIC TRANSDUCER FOR SELECTIVE DETECTION OF HAZARDOUS ORGANIC COMPOUNDS

U.J. Krull

University of Toronto

April 1989

DEFENCE RESEARCH ESTABLISHMENT SUFFIELD, RALSTON, ALBERTA

UNCLASSIFIED

SECTION 1

Initial work with lipid membranes showed that the structures could remain stable in vesicular form for periods of weeks to months. This was not true of planar membranes, and necessitated development of strategies for stabilization on solid flat surfaces. Excitation and capture of radiation from fluorophores located within lipid membranes indicated that the signal which could be obtained was very limited in intensity. An intrinsic fibre optic device was devised for this work which combined the advantages of surface stabilization with the signal integration capacity and efficiency of evanescent excitation. Preparation of lipid films was routinely accomplished by compression of lipid monolayers at the air-water interface of a Langmuir-Blodgett thin film balance. These films could be subsequently transferred to solid substrates by forcing the substrate through the air-water interface at slow and fast casting speeds, under conditions of constant surface pressure. Transfer ratios, wettability measurements, X-ray photoelectron spectroscopy and fluorescence studies confirmed that lipid monolayers could be transferred to the surfaces of quartz fibres. Superior transfer characteristics were achieved if the quartz surface was first derivatized to deposit a hydrophobic C-18 hydrocarbon layer. The film transfer at slow casting speeds (1 mm/min) would retain the structure established on the surface of the Langmuir-Blodgett trough, and would guarantee that the lipid headgroup zone was oriented away from the solid substrate, thereby maximizing the stability and longevity of the membrane. Technical details of this work have been reported in the scientific literature (1-3).

The intrinsic mode of fluorescence signal generation was characterized by the selective interactions of concanavalin A with saccharides at the surface of quartz fibres. The technical details of this work are included in the section entitled "Selective interactions of concanavalin A at lipid membranes on the surface of an optical fibre". The work established that maximum fluorescence signal intensity could be collected by observing wavelength-shifted radiation eminating from the fibre due to intrinsic capture of fluorescence. Selective interactions of concanavalin A attached to lipid membranes were observed in the presence of dextran, indicating that the protein could operate as a receptor. Another form of receptor, based on a lipid bearing a saccharide terminus, was irreversibly located in the lipid membrane and was shown to quantitatively bind concanavalin A. This work was done to investigate the feasibility of use of the intrinsic mode of fibre optic sensing for applications using lipid membranes. The poor reproducibility of quantitative results and the limitations of sensitivity should not be construed as major difficulties since the work reported for concanavalin A was not optimized to address these technical issues. Multidimensional signal analysis and new portable equipment described later in this report indicate that a reliable device may be constructed.

SECTION 2

Details of the extraction, characterization and reconstitution of AChR have been previously submitted. A summary of these procedures and of the structure and function of AChR is included in the section entitled, "Chemical transduction with fluorescent lipid membranes using selective interactions of acetylcholine receptor and acetylcholinesterase". This work was used to establish that fluorescent lipid membranes could be employed as generic transducers for selective chemical reactions between widely different "receptor" systems.

Alterations of the physical structure of vesicles and monolayers of phospholipids and soybean lecithin were monitored by measurement of the average fluorescent intensity changes from nitrobenzoxadiazole-phosphatidyl ethanolamine (NBD-PE) located in the lipid matrices. This probe was intimately dispersed at 1 - 2 mole percent concentrations in lipid membranes and had an emission sensitive to local environmental structure. Alterations of the structure of soybean lecithin vesicles were induced by the selective interaction of AChR with the agonist carbamylcholine and antagonist a-bungarotoxin (4,5). Structural changes of vesicles composed of a 7:3 mole ratio mixture of dipalmitoyl phosphatidylcholine (DPPC) to dipalmitoyl phosphatidic acid (DPPA) were observed for selective interactions between acetylcholinesterase (AChE) and acetylcholine. Selectivity was demonstrated for both the receptor and enzyme by observing the results from experiments using denatured protein, and by results from numerous control and blank experiments. Enhancement of fluorescence emission from the lipid membranes containing active protein provided transduction of the selective binding events of

the receptor and enzyme. A maximum sensitivity of about 30% enhancement per uM carbamylcholine, and 10 nM detection limits for the toxin were observed for the receptor. These results are exciting since the physiological action of the receptor is not known to be associated with major conformational changes on interaction with agonist or antagonist. Quantitative results for the reaction of AChE with acetylcholine are not available, but the data indicates that sub-micromolar detection should be possible. The action of the AChE reaction is significantly different from that associated with AChR, and involves alteration of membrane structure by surface activity of hydronium ion when acetylcholine is hydrolysed to choline and acetic acid. Fluorescence microscopy was used to establish that the receptor and enzyme could be incorporated into lipid monolayers, and provided information about potential mechanisms of fluorescence enhancement. These studies show that lipid membranes containing NBD-PE can be used as generic transducers of protein-ligand interactions.

The most recent results investigating alterations of fluorescence from acidic membranes have been derived from stearic acid monolayers that have been reproducibly transferred from an air-water interface to a quartz surface by L-B dip casting techniques. Acidification of the environment of the stabilized stearic acid monolayers containing NBD-PE has shown large fluorescence intensity enhancements. Work is proceeding with deposition of AChE to these surfaces to prepare a prototype assembly of a device suitable for device development and demonstration of the principle of operation.

SECTION 3

A major problem encountered by every chemical sensor is that of interference effects due to drift and non-selective interactions. Fluorescence techniques provide a significant advantage in reproducible and reliable sensing due to the multidimensional form of the information available in the experiment. A combination of analyses of intensity, lifetime and wavelength (perhaps polarization-not attempted to date) can permit unique identification of selective binding events, and also interference. Even further information is available in the generic transduction experiment using lipid membranes since analytical signals could be derived from both the membrane as well as fluorescently labelled selective receptor. Experimentation has been initiated to determine the viability of a chemometrics approach in solving some of the problems encountered with noise and selectivity as associated with transduction using lipid membranes.

Concurrent analysis of fluorescence intensity using variable wavelength windows for signal integration from lipid vesicles containing NBD-labelled AChR and NBD-labelled lipid indicates that selective interactions with carbamylcholine can be reproducibly measured. The technique involves ratioing of signal intensities from the response windows of NBD-AChR and NBD-lipid, and eliminates variability due to laser noise, photobleaching and inconsistency between vesicle preparations, to provide uM detection limits. Concurrent analysis of fluorescence intensity and lifetime at varoius wavelengths from the new probe 4-dicyanomethylene-1,2,3,4-tetrahydromethylquinoline indicates that

phase structure alterations in lipid membranes (induced by temperature variations) can be determined from a probe located in the headgroup region of lipid vesicles. This has been extended to the generic transduction mechanism involving fluorescent lipid membranes, where the NBD label from NBD-PE is located in the headgroup region of lipid membranes. A generic approach to detection of selective interactions has been investigated by observation of fluorescence intensity and lifetime changes from the two lifetime components of NBD-PE in lipid vesicles that also contained AChR. Detection and differentiation of selective interactions between carbamylcholine and a-bungarotoxin were possible by correlation with intensity and lifetime at different emission wavelengths. Details of this work are described in the following section entitled,"Fluorescence wavelength, intensity and lifetime for multidimensional transduction of selective interactions of acetylcholine receptor by lipid membranes".

CONCLUSION

Development work continues in the area of device construction. The fluorescence signals derived from monolayers of chemically selective lipids are clearly available, but exist at low intensities. Much of the work reported herein has overcome this signal-to-noise limitation by using laser sources for excitation and photomultiplier tubes for detection. The cost, size and power constraints associated with the equipment make the development of portable field units impractical. Work is now progressing in the construction of a field unit based on the following components:

-flash tube excitation source; emission in blue/green region suitable for NBD-PE and many other probes; cyclic use allows minimization of energy consumption and possibility of lifetime work

-intrinsic fibre optic sensor coated with DPPA/DPPC/NBD-PE membrane containing AChE; in flowing solution cell for dynamic response investigations

-Semiconductor avalanche photodiode detector (capable of single photon counting, RCA C30902E, cost approx. $90); provides high sensitivity while minimizing weight and power consumption

This work is now being done outside of the contract for which this report is being submitted. Continued research and development in this area will therefore be a function of other external funding and time constraints. We intend to provide a summary of this further development work to DRES when significant progress has been made.

Literature Publications (previously submitted)

1. U.J. Krull, R.S. Brown, R.F. DeBono and B.D. Hougham, Towards a fluorescent chemoreceptive lipid membrane-based optrode. TALANTA, 35: 129, 1988.

2. U.J. Krull, R.S. Brown and A. Safarzadeh-Amiri, Optical transduction of chemoreceptive events: towards a fiber-optic biosensor. PROC. SPIE-INT. SOC. OPT. ENG., 906: 49, 1988.

3. U.J. Krull, J.D. Brennan, R.S. Brown and E.T. Vandenberg, Phase structure modulation of fluorescent lipid membranes for selective chemical transduction. PROC. SPIE-INT. SOC. OPT. ENG., in press, 1989.

4. R.S. Brown, U.J. Krull and B.D. Hougham, Selective biochemical interactions of acetylcholine receptor on the surface of an optical fiber. In "Biotechnology Research and Applications", G. Gavora, D.F. Gerson, J. Luong, A. Storer and J.H. Woodley, eds., Elsevier Applied Science Pub., England, 1988, p. 195.

5. U.J. Krull, R.S. Brown, K. Dyne, B.D. Hougham and E.T. Vandenberg, Acetylcholine receptor-mediated optical transduction from lipid membranes. In "Chemical Sensors and Microinstrumentation", R. Murray, ed., American Chemical Society Symposium Series, in press, 1989.

SECTION 1

Selective Interactions of Concanavalin A at Lipid Membranes on the Surface of an Optical Fibre

Lipid membranes have great potential to provide useful surfaces for development of electrochemical and optical biosensors.[1,2] These structures can support a wide range of different biological materials such as enzymes, antibodies and receptors in a matrix within which they remain biochemically active. The high degree of biochemical activity coupled with the ultra-thin physical dimensions of the membrane provides for relatively large and very rapid interfacial signal development. A representative example of such a process is the selective complexation by the lectin concanavalin A (Con A) of polysaccharide at bilayer or monolayer lipid membranes.[3] Con A is a globular protein containing saccharide, ion (co-factors) and hydrophobic binding sites.[4,5] The maximum dimensions of Con A are approximately 4.0 nm × 3.9 nm as determined by crystal structure studies at 0.2 nm resolution.[6] Con A non-selectively adsorbs to bilayer and monolayer lipid membranes, and can bind polysaccharides such as dextran or glycogen to form aggregates which tend to alter the physical structure of the lipid matrix on a time scale of hundreds of milliseconds.[3,7]

The selective interactions of Con A at lipid membranes provide an interesting model for testing the ability to derive analytical signals by electrochemical and by optical methods. Optical methods such as fluorescence spectroscopy provide an inherently sensitive detection technique, while concurrently eliminating the problems of mixed potentials and charging currents often associated with electrochemical experiments.

Total internal reflectance fluorescence is a sensitive technique for detecting the presence of biochemical species at an interface. The solution of Maxwell's wave equations for

conditions of total internal reflection within a waveguide indicate that an exponential decay of electric field intensity of electromagnetic radiation propagates beyond an interface defined by two materials of different refractive index (presumes refractive index of waveguide n_1 > external coating n_2).[9,10] At these conditions the external electric field intensity, I, varies with perpendicular distance from the surface, z, as:

$$I(z) = I(\theta) \exp(-2z/d_P) \qquad (1)$$

where $I(\theta)$ represents the electric field intensity at the interface and d_P is a characteristic penetration depth defined as the perpendicular distance from the interface at which the electric field intensity has reduced to $1/e$ of the original value at the interface. The value of d_P can be calculated for any particular wavelength of radiation, λ, from the following relationship:

$$d_P = \frac{\lambda/n_1}{2\pi (\sin^2\theta - (n_2/n_1)^2)^{1/2}} \qquad (2)$$

where θ represents the angle of incidence at the interface of the electromagnetic radiation propagating through the waveguide by total internal reflection.

The use of evanescent excitation for an intrinsic optrode configuration in which a lipid membrane is deposited on the surface of an optical fiber offers the advantages of; mechanical stabilization of the membrane, increased effective pathlength for optical excitation (particularly on a multi-mode optical fiber) and analytical sampling that is restricted to the chemically selective interface.[11]

Biochemical interfaces have been studied fluorometrically by evanescent excitation techniques. These investigations have

established aspects of quantitative selective binding, and the kinetics and mechanisms of binding processes such as those involving immunochemical systems.[12-14] Relatively little work has been done at optical wavelengths for investigation of lipid membranes and associated protein-mediated selective interactions. Recent experimental work has confirmed that lipid membranes containing fluorescent lipid species at 1 to 2 mole % concentrations can be detected in an intrinsic fiber-optic sensing configuration following surface deposition by Langmuir-Blodgett monolayer transfer.[11] The intensity of the fluorescence signals collected in these experiments was very limited, suggesting that the technique may not be suitable for development of transducers based on fluorescent lipid membranes. Furthermore, the experiments did not attempt to evaluate the fluorescence response from any selective binding interactions, and did not clearly demonstrate any advantages that could be gained from the use of lipid membranes.

This paper reports the results of experimentation which investigated mechanical configurations for optimization of collection of fluorescent radiation from lipid membranes deposited on quartz optical fibers. A selective binding interaction using complexation of Con A with saccharide residues was chosen to illustrate: fluorescent signal acquisition from a chemically-selective lipid monolayer; the use of a lipid membrane as a structural support for adsorbed selective protein; and the use of an irreversibly bound receptor site supported in the lipid matrix in the form of the saccharide residue of a glycolipid for complexation with the lectin.

EXPERIMENTAL

Reagents

Materials used for lipid membrane preparation were egg phosphatidyl choline, EPC, cholesterol, C, (Avanti Biochemicals, Birmingham, AL) and monosialoganglioside from bovine brain, G_{M1}, 95% (Sigma Chemical Co., St. Louis, MO), and were used without further purification. Vesicular solutions of EPC/C were formed by first preparing an ethanolic solution of the lipid species, followed by evaporation of the ethanol to leave a dry film and then suspension in an aqueous buffer solution containing 10mM TRIS buffer, 10^{-4} M $CaCl_2$, 10^{-4} M $MnCl_2$ at pH 7.0. The EPC/C ratio was selected to be 70/30 mole percent, and sufficient buffer was added to achieve a concentration of 1.3 mg/mL. Vesicles of EPC/C/G_{M1} were prepared by a similar procedure to a concentration of 1.4 mg/mL with a mole percent ratio of constituents of approximately 50/30/20, respectively. Similar mole ratio solutions of EPC/C and EPC/C/G_{M1} were prepared in hexane for formation of monolayers on a Langmuir-Blodgett trough, (Lauda Model 1974, Sybron Brinkman, Toronto). An alkylating solution for preparation of fiber surfaces prior to dip casting experiments consisted of 0.1% octadecyltrichlorosilane (95%, Aldrich Chemical Company, Milwaukee, Wisconsin, USA), 80% hexadecane, 12% carbon tetrachloride and 8% chloroform. Pyrene-butyryl concanavalin A, (Py-Con A), and fluorescein isothiocyanate dextran, (FITC-dextran, MW 4000), were used as received (Molecular Probes, Eugene, OR) and were dissolved in aqueous buffered solution as used for vesicular work. All solvents were reagent grade, and water was obtained from a

Milli-Q cartridge filter system of minimal resistivity of 18 MΩ.cm (Millipore, Mississauga, Canada).

Apparatus

Vesicle aggregation induced by selective and non-selective binding events was monitored by measurement of optical density alterations at 455 nm of aqueous solutions in a standard 1cm pathlength quartz cuvette as determined using a DU-50 absorption spectrophotometer (Beckmann). Vesicular solutions were dispersed with a Vibra-Cell Model 250 probe-tip sonicator (Sonics and Materials, Inc., Danbury, CT) set at 40 W power, after suspension of vesicles in aqueous solution and before experiments were initiated. Fluorescence from optical fibers (silica core fibers, 400 μm, Tasso, Montreal, Canada) was induced by a nitrogen laser (LN 103, Photochemical Research Associates, London, ON Canada), and the emitted radiation was processed by a monochromator (Bentham M300, Optikon, Waterloo, ON, Canada) and photomultiplier tube detector (R928, Hamamatsu). The output from the photomultiplier was passed to a gated-integrator/boxcar averager (Stanford Research Systems) which was operated with a sampling gate width of 40 nsec. The fluorescence acquisition equipment was operated in the two configurations shown in Fig. 1.

Procedures

Vesicle experiments

These experiments were done as controls to establish that lipid membranes containing G_{M1} would be capable of selectively binding Con A. The light scattering experiments followed the agglomeration of vesicles caused by cross-linking mediated by the lectin. Vesicular solutions were sonicated for 20 minutes at

room temperature before experiments were initiated. Vesicle solution was mixed with an equal volume of aqueous solution containing Con A at 1.3 mg/mL concentration, and the optical density of the solution was measured periodically for 60 minutes. Solutions were checked for homogeneous suspension of aggregates before each measurement.

Fluorescence experiments

The ability of the equipment to collect fluorescence radiation in the two configurations shown in Fig. 1 was established with a sample consisting of an optical fiber which had been coated with Py-Con A by non-selective adsorption from an aqueous buffered solution containing 10^{-8} M Py-Con A. The termini of all fibers were polished by use of a rotary sander with a series of successively finer polishing grits.

Non-selective adsorption of Py-Con A was investigated for a series of different fiber surfaces. The four surfaces of length of 3 cm consisted of : a) untreated fiber surfaces as exposed when the sheath and cladding were removed with a mechanical wire stripping device (all fibers were initially cleaned by 24 hour NOCROMIX (Godax, New York) wash followed by NaOH neutralization and water rinse); b) fiber surfaces which had been coated by Langmuir-Blodgett lipid monolayer casting deposition (speed: 0.7 mm/min) using the appropriate lipid mixtures held at a constant pressure of 30 mN . m^{-1};[15] c) alkylated surfaces prepared by immersion of the fibers into the silane solution for 60 minutes with vigorous agitation every 10 minutes; d) alkylated surfaces which were further modified by deposition of a lipid monolayer. All of these fibers were supported in a cuvette containing Py-Con A in buffered aqueous solution. Experimentation continued in

some cases by addition of FITC-dextran as an aqueous solution to the sample cuvette to achieve final solution concentrations of 10^{-6} M of polysaccharide.

RESULTS AND DISCUSSION

The utility of the technique of total internal reflection can be understood from equation (2), which indicates that optical intensity of excitation radiation and penetration depth adjustment for sampling near an interface can be controlled by appropriate selections of excitation wavelength, incident angle and refractive indices. Fig. 2 provides some examples of theoretical results calculated from equations (1) and (2) for the nitrogen laser source. The experiments described in this work make use of a broad and uncontrolled range of angles of incidence in a multimode distribution at fixed wavelength (337.1 nm) and relatively invariant refractive index ratio. The calculations indicate that lipid monolayers (4 to 5 nm thickness) alkylated surfaces coated with lipid monolayers (7 to 10 nm) and films incorporating lipid monolayers with Con A and dextran (5 to 20 nm), will all be exposed to relatively high excitation intensities of the laser radiation given that the refractive index of the organic layers will be in the range of 1.45 to 1.5. While most descriptions of intrinsic mode optrodes have used an evanescent spectroscopic model, it should be noted that films of many biological materials such as lipids and proteins have an index of refraction close to that of the quartz optical fibers (approx. 1.5). If the refractive indices of the waveguide and organic layer were matched, internal reflection would not occur at the fiber/coating interface. Optical excitation of the

organic layer would be due to the fact that the coating would act as a physical extension of the quartz waveguide. Even though the evanescent field would then propagate beyond the coating/ambient (aqueous solution) interface, there would still be a high degree of surface selectivity, and bulk solution interference should be minimal.

Collection of fluorescence can be established in the two configurations shown in Fig 3. A collection strategy where radiation is collected in a perpendicular orientation along the surface of the fiber (Fig. 3a) would be efficient in a conventional spectrofluorimetric experiment using a standard 1-cm quartz cuvette. The fluorescence generated in a TIRF experiment does scatter in a perpendicular orientation, but can also couple back into the waveguide under certain conditions. Equation (2) represents the penetration of electric field intensity across an interface indicating decay of intensity in an exponential manner. A thick (relative to d_p) and homogeneous fluorescent film exposed to such an evanescent wave would emit radiation at intensities which would follow an exponential decay from the interface, since fluorescence intensity is proportional to excitation power. This would generate the equivalent of an external component of a new evanescent wave (longer wavelength), which could couple with the waveguide across the refractive index interface to produce a high electric field strength within the waveguide.[14,16] The presence of such a process could provide for collection of a majority of the fluorescence by the waveguide, and would enable detection to be based on sampling of the fluorescence as shown in Fig. 3b. It is not clear that a monolayer lipid membrane or protein film which provides fluorescence in a localized plane can satisfy the

conditions of equation (2) and provide significant capture of fluorescence within a waveguide.

Experimental results indicate a dramatic difference in the collection efficiencies of the optical configurations shown in Fig. 1. Observation of fluorescence in an orientation perpendicular to an optical fiber (Fig.1b) coated with Py-Con A provided a signal magnitude of up to 100-fold less than that obtained from coupling of fluorescence into the fiber (Fig.1a). The efficiency of perpendicular collection was limited to such a degree that the distinctive fluorescence profile of the pyrene moiety could not be resolved by the instrumentation used in this work. The same equipment could readily provide a distinctive spectral profile for pyrene when used in the configuration of Fig. 1a, as shown in Fig. 4. Note that the use of the bright nitrogen laser source provided excellent wavelength separation of fluorescence from excitation radiation, even though the laser wavelength was well removed from the wavelength of maximum absorption of the fluorophore. The efficiency of signal collection due to coupling of fluorescence into a fiber does not prove that the effect is necessarily due to the process of equation (2). If the refractive indices of the fiber and organic film were closely matched, then the coupling of fluorescence into the waveguide would be very efficient. In this case the fluorescence would be produced within the waveguide and would remain in the structure if the propagation angle was greater than the critical angle for total internal reflection.

Concanavalin A as a Receptor

Analysis of the adsorption of Py-Con A onto various fiber surfaces indicated no clear preference of non-selective adsorption of the protein onto quartz, alkylated quartz or EPC/C-coated fibers. The pH of the solution used in these experiments induces the formation of a quaternary protein structure which takes the form of a tetrameric association of Con A. The complex is physically massive (approx. 100 KD) and contains a minimum of 4 hydrophobic binding sites, as well as numerous areas of relatively high polarity. These attributes combine to provide the protein with a capacity to deposit non-selectively onto many different surfaces. Attachment of the protein at significant concentrations to EPC/C membranes was consistent with previous work,[3] and the usefulness of the evanescence technique was clearly indicated by elimination of extraneous absorption and fluorescence due to Py-Con A in the bulk aqueous solution or on the sample cuvette surfaces when the system was operated in the configuration shown in Fig. 1a. The Py-Con A on the EPC/C membrane was able to complex FITC-dextran, which was added incrementally directly to the solution in the sample cuvette supporting the optical fiber. A response curve for this experiment demonstrating selective complexation by analysis of the FITC signal is shown in Fig. 5. The results were collected after 20 minutes of incubation to allow equilibration of interactions in solution between free Py-Con A and FITC-dextran, and are suitable only for analysis of trends since quantitative determination of the amount of Py-Con A and FITC-dextran in dynamic equilibrium on the surface of the fiber was not attempted. The Py-Con A selectively partitions to the

surface and may be greater than 100 fold more concentrated than in bulk solution.[3] The concentration-response curve for interaction of Py-Con A with FITC-dextran shows that selective binding occurs (results are corrected for bulk solution concentration of FITC-dextran), and the results may indicate the approach of saturation as a non-linear response of low sensitivity is seen at 10^{-6} M FITC-dextran. Blank experiments using only FITC-dextran indicated that this material did not selectively adsorb to any of the optical fiber surfaces that were investigated.

G_{M1} as a Receptor

Glycolipids have been extensively investigated as membrane-intrinsic molecular receptors in model membrane studies of lectin- mediated agglutination.[17,18] Gangliosides such as G_{M1} have been used in vesicular form and have been incorporated into PC/C lipid vesicles to provide surfaces coated with saccharide residues suitable for lectin binding. The agglutination of vesicles by lectin has been followed by observation of changes of light scattering. A series of experiments using vesicular agglutination were done in this work to demonstrate the ability of G_{M1} to act as a receptor for both Con A and pyrene labelled Con A. The G_{M1} was present at high molar concentrations (20 mole %) in (EPC/C) vesicles, and the vesicles were used at room temperature to insure that glycolipid diffusion could take place on the surface of the membranes. A series of experiments were designed to investigate aggregation or fusion of vesicles with and without G_{M1} in combination with the absence of any protein, in the presence of non-selective protein (bovine serum albumin,

BSA), in the presence of Con A (previously associated with vesicle fusion)[19] and in the presence of Py-Con A. The results of these experiments are summarized in Fig. 6. The trends of light scattering variation indicate that little change occurs when BSA is present or when Con A is absent, but some EPC/C vesicle interaction is induced by the presence of the lectin. A greater rate and extent of interaction occurs when G_{M1} is available, and the results confirm that both Con A and pyrene-labelled Con A are selectively complexed by the glycolipid.

Lipid membranes of EPC/C containing G_{M1} and devoid of the glycolipid were deposited onto silylated optical fibers by the Langmuir-Blodgett casting technique and were retained in aqueous solution. Experimental compression curves for these monolayers are shown in Fig. 7, and indicate that large differences in physical compressibility and therefore structure are not observed for the different membranes. Incremental additions of Py-Con A to EPC/C membranes indicated non-selective adsorption of the protein to the membrane. The presence of G_{M1} caused a general trend of enhancement of the pyrene signal relative to the results for non-selective adsorption. Quantitative correction of the background signal due to non-selective Py-Con A adsorption to the surfaces could not be done by signal subtraction using fibers coated with EPC/C but without G_{M1}. It was not possible to accurately match the non-selective binding properties of different fibers. Results for selective Py-Con A adsorption to EPC/C/G_{M1} membranes are shown in Fig. 8 and represent response trends after a 30 minute incubation period with background correction by estimation of contributions to the analytical

signal from non-selective adsorption. The results indicate that the lipid membrane does contain an intrinsic selective receptor, but that the analytical system is not very sensitive or reproducible.

CONCLUSIONS

Chemically-selective lipid membranes can be prepared at the surface of an optical fiber for investigation of binding interactions by monitoring of fluorescence intensity in an intrinsic sensor configuration. The use of Con A as a selective receptor or an analyte provided limitations in analytical reproducibility and sensitivity due to non-selective adsorption to the sensing surface. This clearly identifies one of the serious limitations of fiber optic biosensors when used exclusively for fluorescence intensity measurement at a fixed analytical wavelength. The analytical potential of fluorescence lies in the correction or isolation of an analytical signal from noise by use of multidimensional signal acquisition in the form of concurrent information of wavelength, intensity, lifetime and perhaps polarization. A further limitation exposed in this work is that lipid membranes as used herein can provide useful matrices for certain receptors (eg. G_{M1}), but are not widely applicable to many different situations if the analyte must be fluorescently labelled. This is not necessarily the case since many different biochemical reactions can perturb the structure of lipid membranes indicating that a fluorescent lipid membrane could be a generic transducer of selective binding events. Aspects of generic transduction and multidimensional analysis of

fluorescence from lipid membranes will be presented in an associated manuscript in this journal.

Acknowledgements

The authors wish to thank the Natural Sciences and Engineering Research Council of Canada, the Canadian Defense Research Establishment, the Ontario Ministry of the Environment and Imperial Oil Canada for financial support of this work.

REFERENCES

1. U. J. Krull and M. Thompson, IEEE TRANS. ELECTRON DEVICES, 1985, 32, 1180.
2. U. J. Krull, R. S. Brown, K. Dyne, B. D. Hougham and E. T. Vandenberg in CHEMICAL SENSORS AND MICROINSTRUMENTATION, R. Murray (ed.), American Chemical Society Symposium Series, in press.
3. U. J. Krull, R. S. Brown, R. N. Koilpillai, R. Nespolo, A. Safarzadeh-Amiri and E. T. Vandenberg, ANALYST, 1989, 114, 33.
4. K. D. Hardman and I. J. Goldstein in IMMUNOCHEMISTRY OF PROTEINS, M. Z. Atazzi (ed.), Vol. 2, p. 373, Plenum Press, New York, 1977.
5. G. M. Edelman and J. L. Wang, J. BIOL. CHEM., 1978, 253, 3016.
6. G. N. Reeke Jr., J. W. Becker and G. M. Edelman, J. BIOL. CHEM., 1975, 250, 1525.

7. M. Thompson, H. E. Wong and W. H. Dorn, ANAL. CHIM. ACTA, 1987, 200, 319.

8. M. Thompson, U. J. Krull, L. I. Bendell-Young, I. Lundstrom and C. Nylander, ANAL. CHIM. ACTA, 1985, 173, 129.

9. S. A. Rockhold, R. D. Quinn, R. A. Van Wagenen, J. D. Andrade and M. Reichert, J. ELECTROANAL. CHEM., 1983, 150, 261.

10. M. Reichert, S. Rockhold, R. A. Van Wagenen and J. D. Andrade in INTERFACIAL ASPECTS OF BIOMEDICAL POLYMERS, J. D. Andrade, (ed.), Vol. 2, Plenum Press, New York, 1986.

11. U. J. Krull, R. S. Brown, R. F. DeBono and B. D. Hougham, TALANTA, 1988, 35, 129.

12. J. D. Andrade, R. A. Van Wagenen, D. E. Gregonis, K. Newby and J.-N. Lin, IEEE TRANS ELECTRON DEVICES, 1985, 32, 1175.

13. N. L. Thompson and D. Axelrod, BIOPHYS. J., 1983, 43, 103.

14. J. F. Place, R. M. Sutherland and C. Dahne, BIOSENSORS, 1985, 1, 321.

15. W. M. Heckl, M. Thompson and H. Mohwald, LANGMUIR, 1989, 5, 290.

16. N. J. Harrick and G. I. Loeb, ANAL. CHEM., 1973, 45, 687.

17. C. W. M. Grant and M. W. Peters, BIOCHIM. BIOPHYS. ACTA, 1984, 779, 403.

18. F. A. Quiocho, ANN. REV. BIOCHEM., 1986, 55, 287.

19. J. Van Der Bosch and H. M. McConnell, PROC. NATL. ACAD. SCI. USA, 1975, 72, 4409.

FIGURE CAPTIONS

Figure 1. Experimental optical configurations used for collection of fluorescence from quartz optical fibers using: a) detector a for end-on detection of radiation coupled into fiber; b) detector b side-on collection of radiation scattered from fiber.

Figure 2. Calculated relationships of evanescent field a) penetration depth (d_p) and b) intensity at various distances from a fiber surface for coatings of various indeces of refraction based on equation (2), using a fiber index of refraction of 1.5 and a propagated wavelength of 337 nm.

Figure 3. General strategies for collection of fluorescence from waveguides showing a) light scattering and b) capture of radiation within the light-guide.

Figure 4. Fluorescence intensity measurements from pyrene-concanavalin A adsorbed on the surface of a quartz fiber in the end-on fluorescence collection configuration a) after adsorption to the fiber surface and b) background spectrum from uncoated fiber.

Figure 5. Concentration-response curve based on relative fluorescence intensity increases for selective binding of pyrene-concanavalin A (located on a phospholipid-cholesterol monolayer) with fluorescein isothiocyanate dextran.

Figure 6. Lipid vesicle aggregation studies determined by light scattering at 455 nm using monosialoganglioside as a selective binding agent for concanavalin A. (□) Phospholipid-cholesterol vesicles in the presence of concanavalin A or pyrene-concanavalin A: (◇) Phospholipid-cholesterol vesicles containing ganglioside in the presence of concanavalin A or pyrene-concanavalin A: (△)

Lipid vesicles containing the ganglioside G_{M1}: (▽) Lipid vesicles containing the protein BSA in the presence of concanavalin A. Variability between vesicle preparations limits absolute comparisons of reaction rates.

The results confirm that the presence of ganglioside assists vesicle aggregation in the presence of Con A.

Figure 7. Pressure-area curves showing results from monolayers of A: 50/50 mole percent mixture of phosphatidyl choline and cholesterol B: 70/30 mole percent mixture of phosphatidyl choline and cholesterol C: 50/30/20 mole percent mixture of phosphatidyl choline, cholesterol and ganglioside. Monolayers were transferred to quartz fibers at constant pressure of 30 mN.m-1.

Figure 8. Concentration-response curve based on relative fluorescence intensity increases from quartz fibers coated with lipid monolayers containing phosphatidylcholine, cholesterol and ganglioside for selective binding of pyrene-concanavalin A, (results corrected for non-selective adsorption of pyrene-concanavalin A).

Fig 1

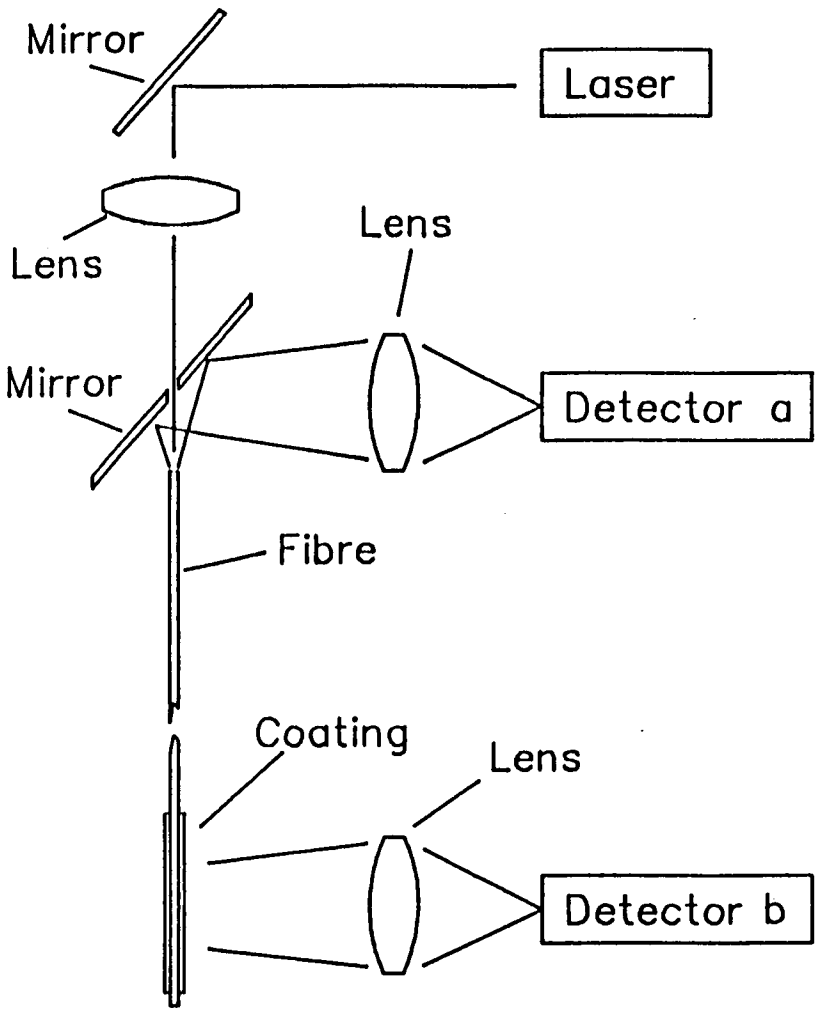
Mirror
Laser
Lens
Lens
Mirror
Detector a
Fibre
Coating
Lens
Detector b

Fig 2a.

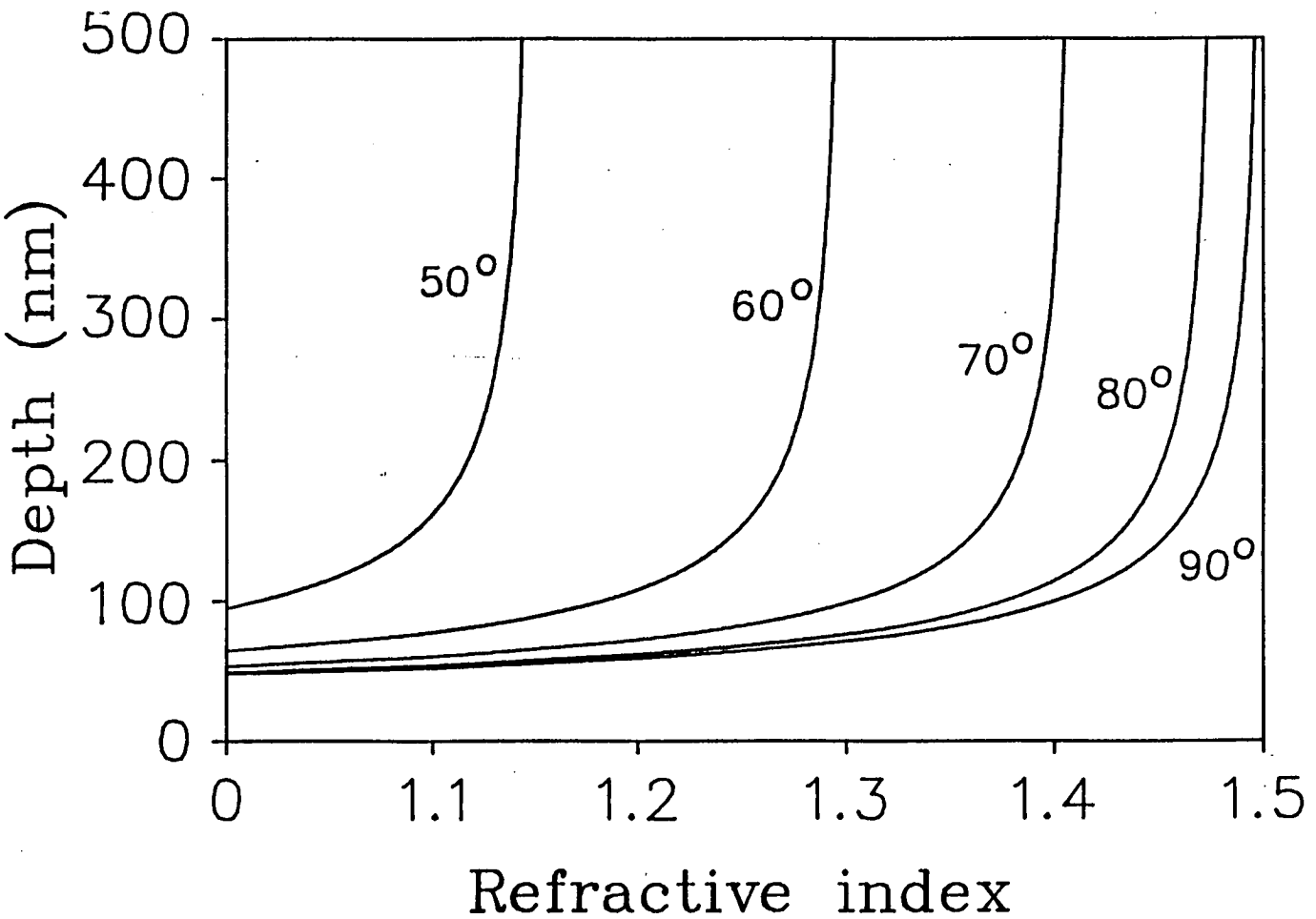
500
400
300
200
100
0
Depth (nm)
50°
60°
70°
80°
90°
0
1.1
1.2
1.3
1.4
1.5
Refractive index

Fig 2b

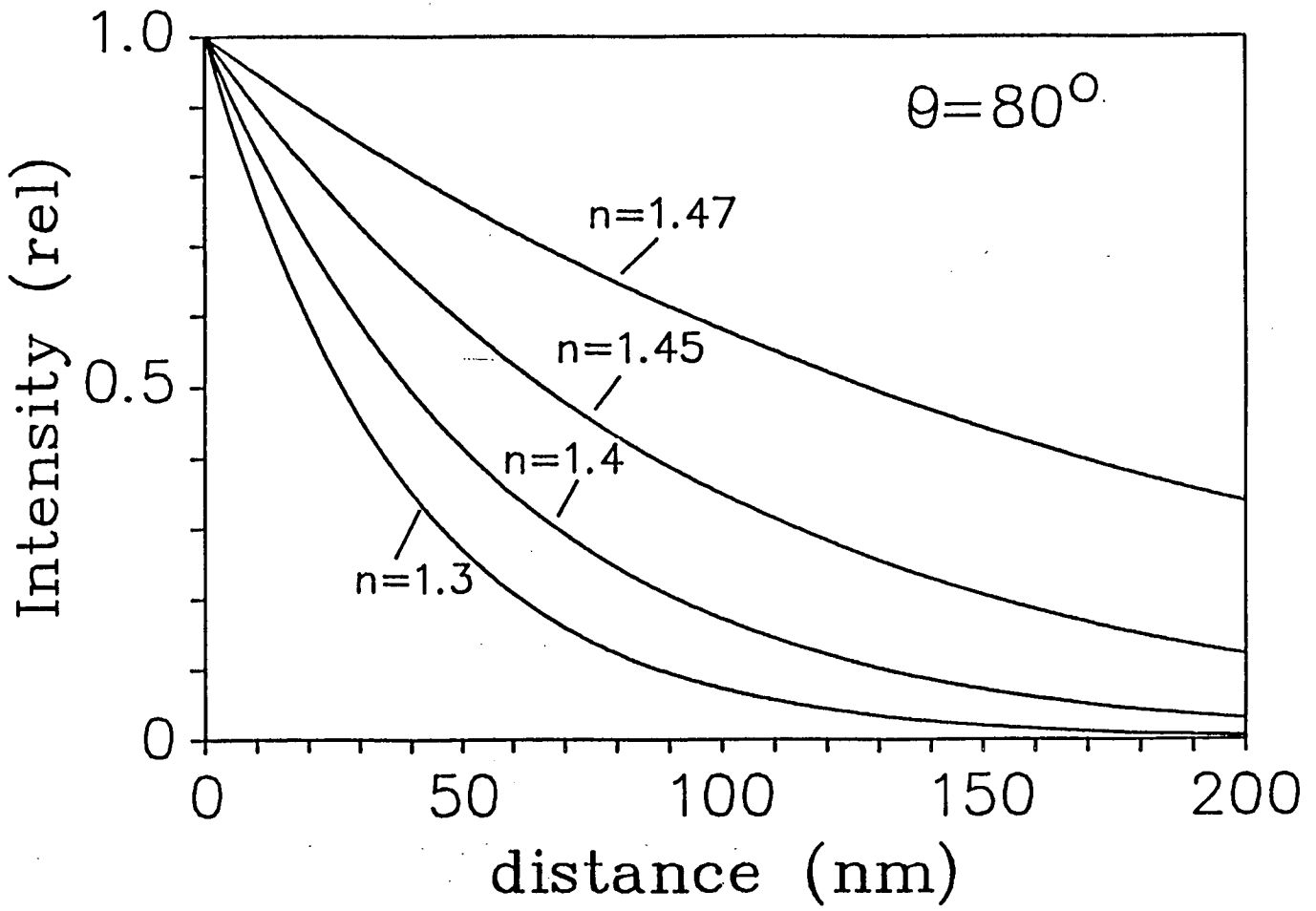
1.0
0.5
0
Intensity (rel)
θ=80°
n=1.47
n=1.45
n=1.4
n=1.3
0
50
100
150
200
distance (nm)

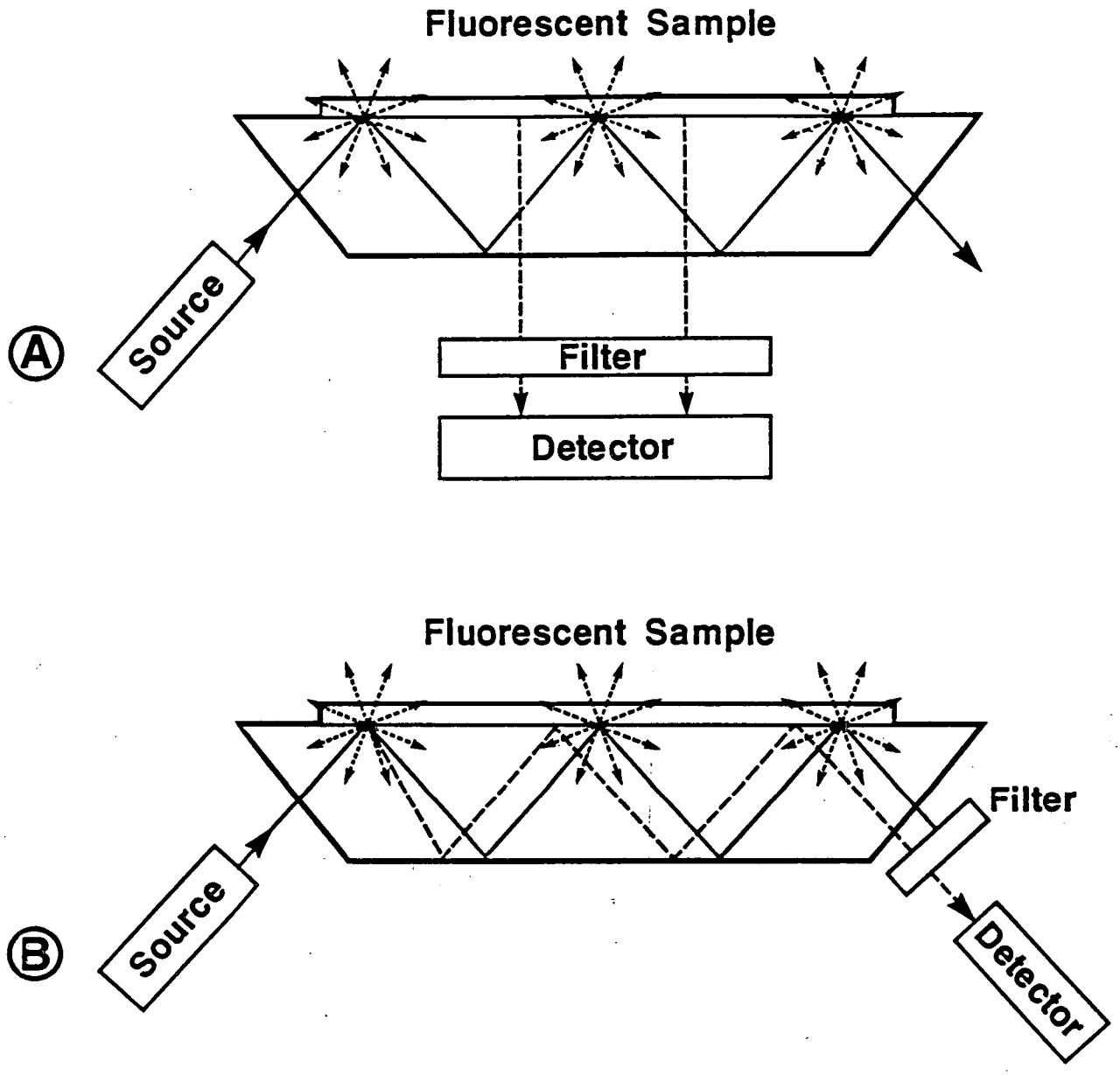
Fluorescent Sample
A
Source
Filter
Detector
Fluorescent Sample
B
Source
Filter
Detector

Fig 3

Fig. 4

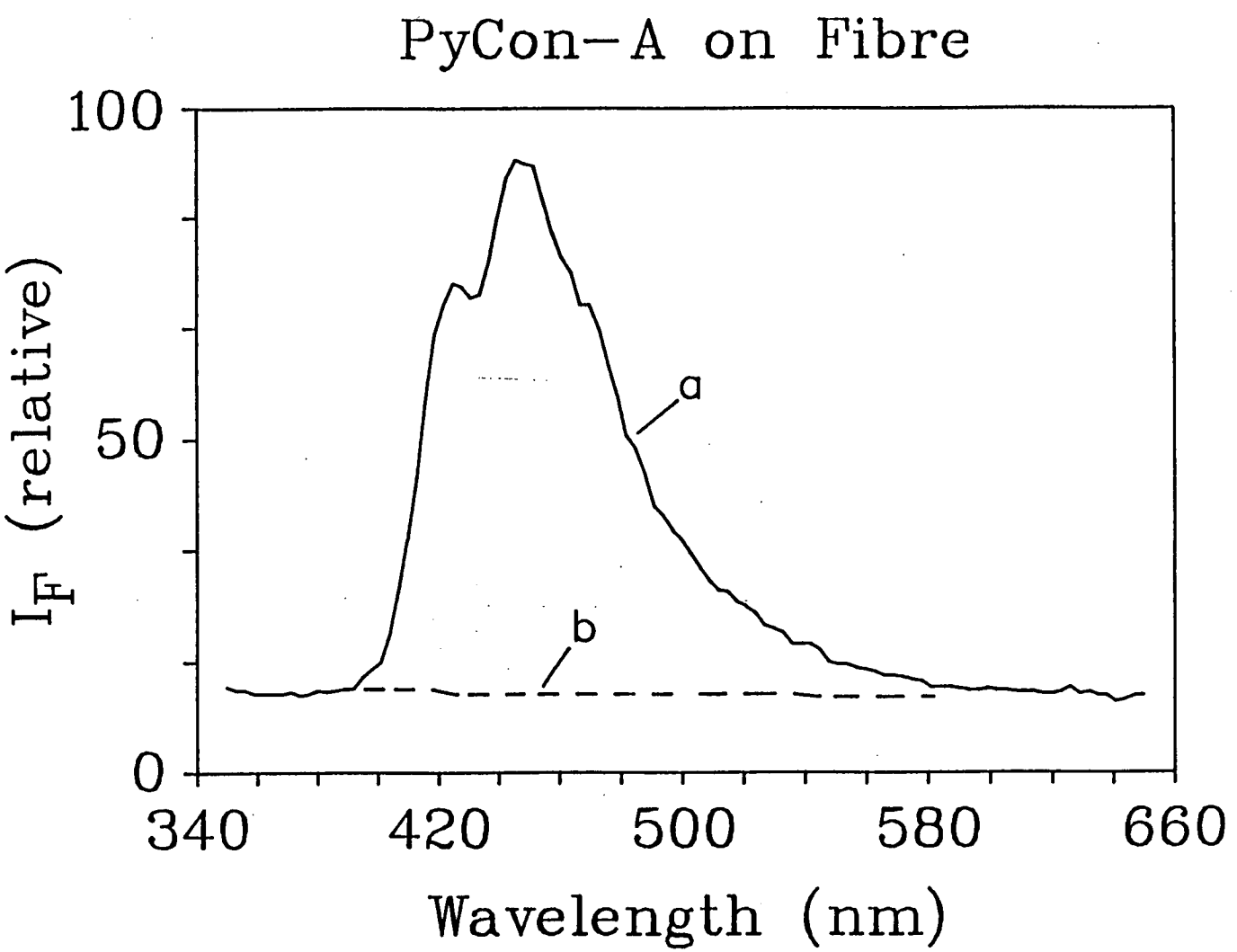
PyCon-A on Fibre
100
50
0
I_F (relative)
a
b
340
420
500
580
660
Wavelength (nm)

Fig. 15

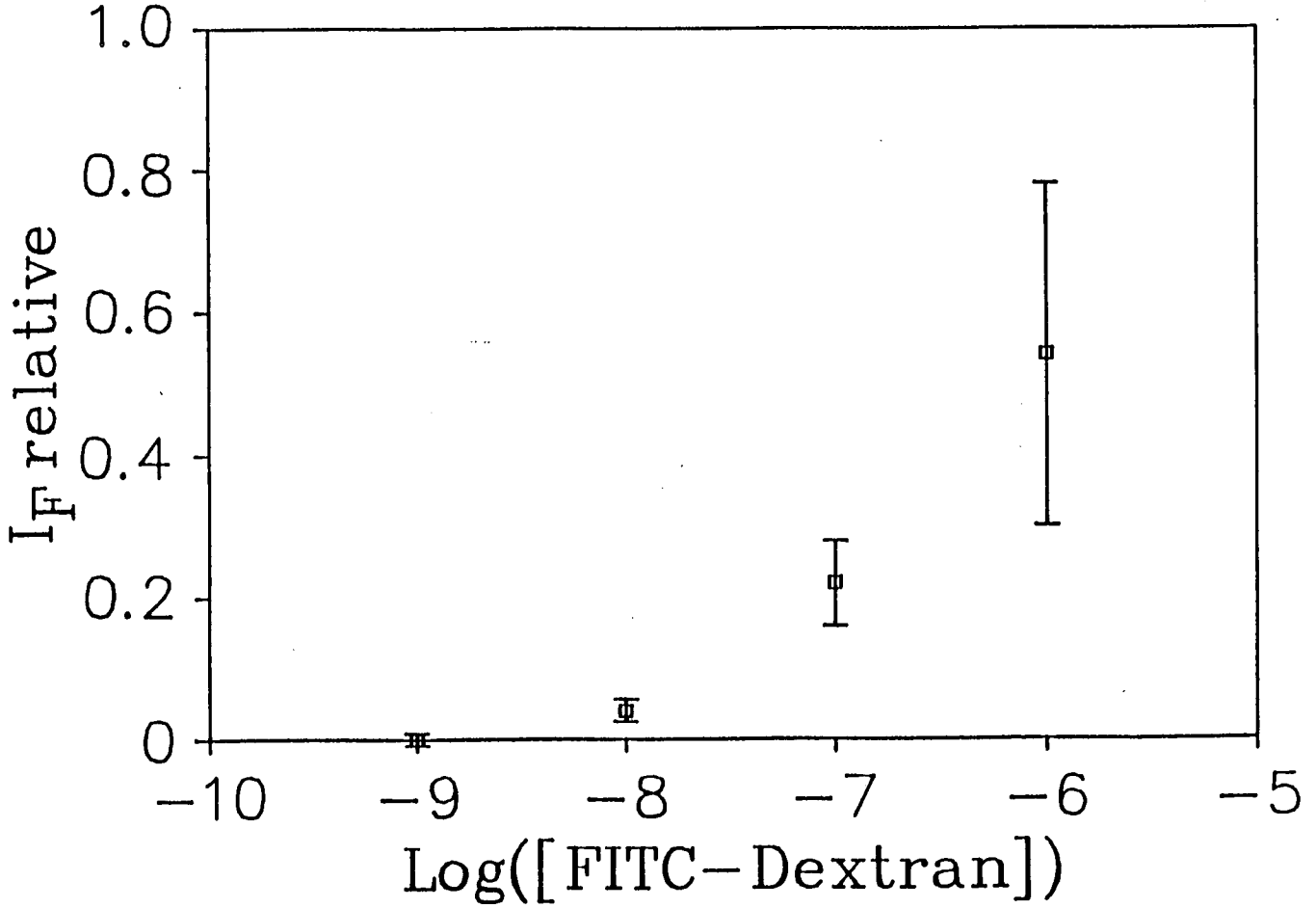

Fig. 6.

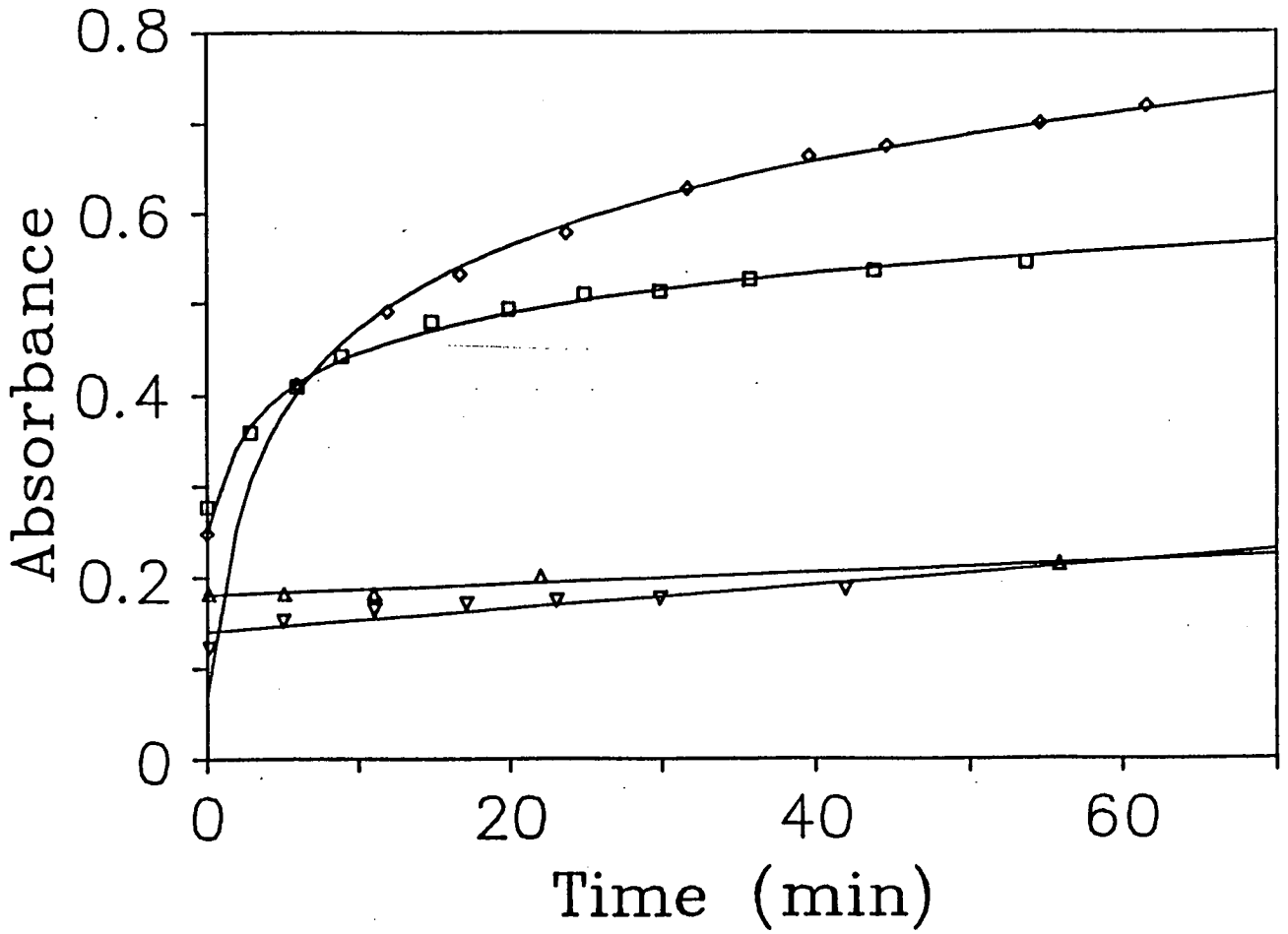

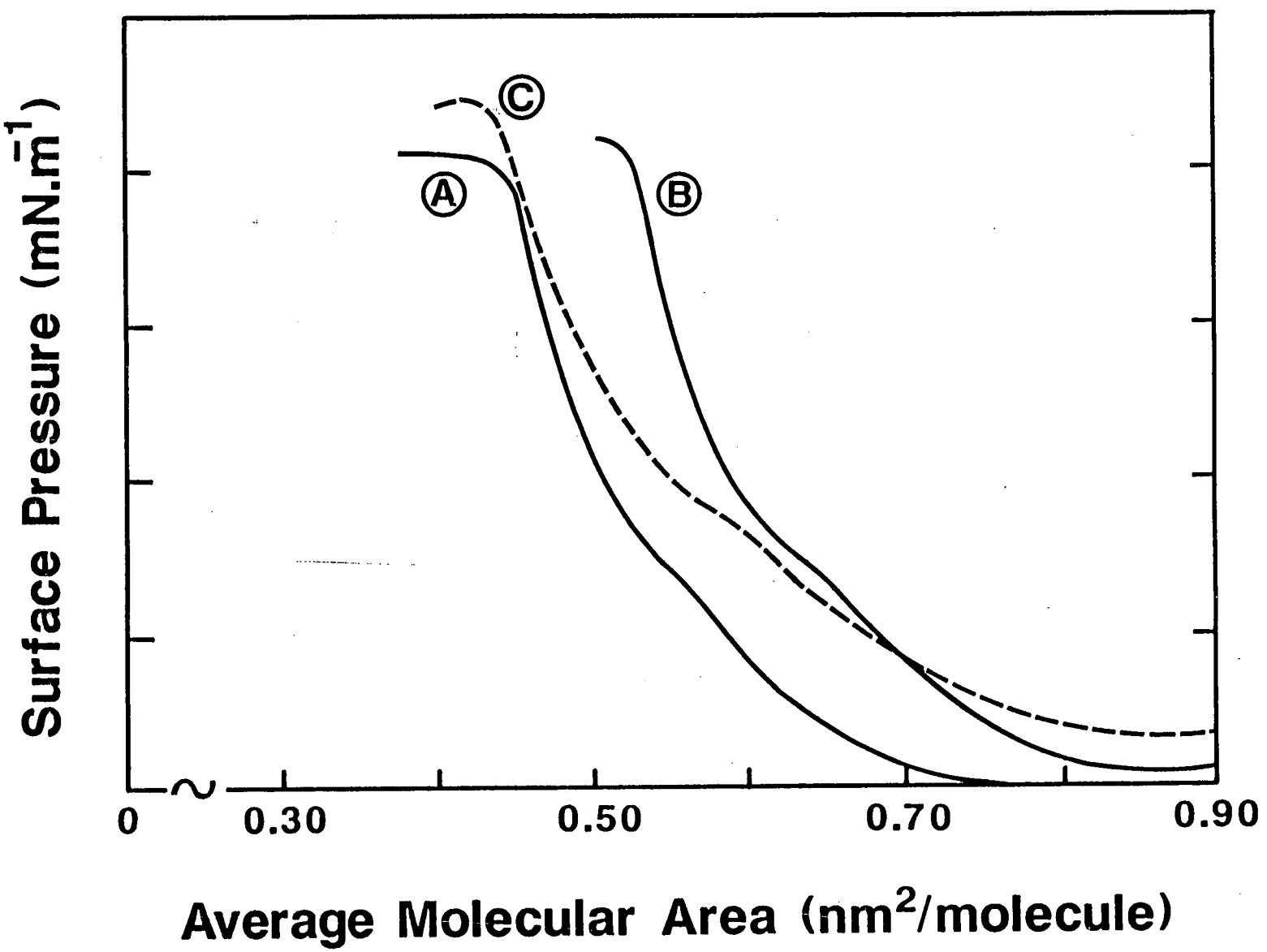
Surface Pressure (mN.m^{-1})
C
A
B
0
0.30
0.50
0.70
0.90
Average Molecular Area (nm^2/molecule)

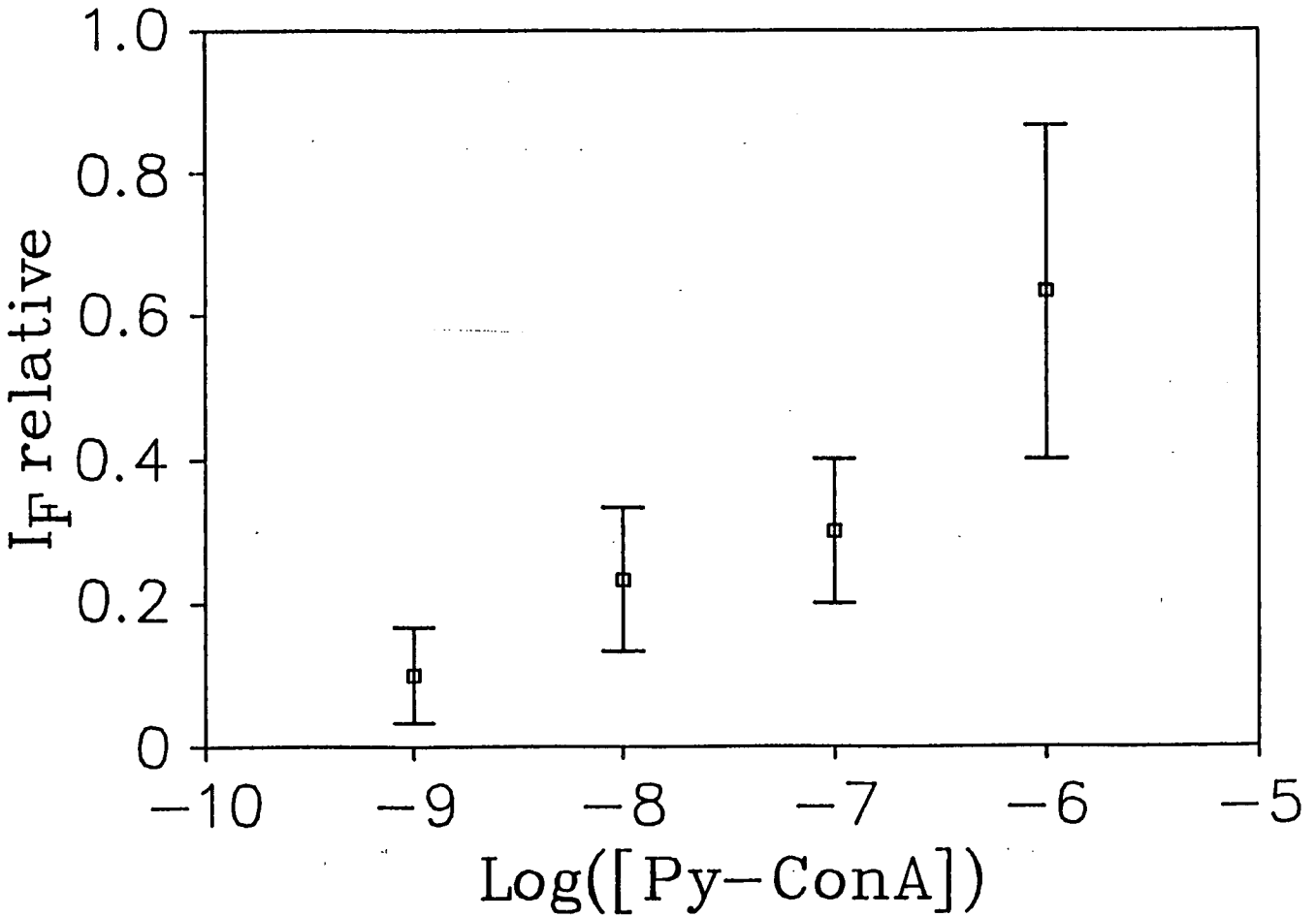
1.0
0.8
0.6
0.4
0.2
0
I_F relative
−10
−9
−8
−7
−6
−5
Log([Py−ConA])

SECTION 2

Chemical Transduction with Fluorescent Lipid Membranes Using Selective Interactions of Acetylcholine Receptor and Acetylcholinesterase

CR 29/89

Development of a Lipid-Membrane Coated Fiber-Optic Transducer for Selective Detection of Hazardous Organic Compounds

DSS File #: 24ST.97714-5-5020

Ulrich J. Krull - Chemical Sensors Group - University of Toronto

FINAL REPORT - Period July/86 to April/89

This final report and the attached 3-month report constitute the documentation required for completion of the above-mentioned contract. This report will summarize the results that have been forwarded at three month intervals during the contractual period, and will refer to new technical results which are described in 3 independent sections included in this document.

The intent of the research work of this contract was to investigate the potential of fluorescent lipid membranes as generic transducers of selective biochemical interactions, ultimately leading to the development of a sensitive biosensor for detection of trace concentrations of biological toxins. The work was divided into two main areas:

1) Development of selective reagent chemistry based on extraction, purification and reconstitution of acetylcholine receptor (AChR) into lipid membranes, and development of fluorescent membrane systems suitable for quantitative chemical analysis.

2) Development of device technology for moving the selective chemistry into a practical environment, including aspects of membrane interfacing to optical fibres, multidimensional signal transduction and portable devive construction.

Natural chemoreceptive processes, such as olfaction, gustation and hormone binding to target organs, are often astonishingly selective and sensitive to chemical and biochemical stimulants. The basis for a generic transduction mechanism for biosensor development is exemplified by natural chemoreception. In vivo, the same generic response (eg. Na^+ ion influx or cyclic AMP production) is given by thousands of molecular receptors selective for thousands of analytes. It would be advantageous for artificial sensors to gain such characteristics, as well as the speed and reversibility associated with natural chemical perception.[1,2] A form of artificial chemoreception suitable for development of sensitive chemical sensors can be derived from the physical perturbation of a lipid membrane by "receptor" molecules that participate in selective binding processes.[1] The perturbation can be physical and/or electrostatic, and may be used to transduce the chemical signal of analyte concentration into corresponding electrochemical or optical signals.

Advances in fibre-optic sensing have centered around the development of an "optrode" (optical equivalent of an electrode). These carry their own characteristic advantages, such as freedom from electrical interference, electrical connections and external references (e.g. a reference electrode), as well as disadvantages, such as sensitivity to ambient light. The small optical signals involved in most fibre-optic sensors and the high sensitivity of fluorescence measurements has resulted in fluorescence being adopted as the spectroscopic technique of choice for most optrodes. A fluorescent optical sensing strategy provides many advantages with respect to the electrochemical system when considering lipid membrane transducers. Its greatest asset is the opportunity for simultaneous

analysis using the parameters of wavelength, intensity, polarization and lifetime which can be derived directly from a fluorescently-tagged "receptor", and/or a fluorescent lipid membrane.[3] Thus, the fluorescence signal has much greater dimensionality than the more simple current, potential or frequency measurements made with other common devices. The development of fluorophore-based optrodes is centered on the adaptation of fluorescence assay methods to an optrode configuration.[4] These methods include: 1) direct detection of a fluorescent analyte, as in fluoroimmunoassay; 2) direct interaction of an incorporated fluorophore with an analyte, as in analyte-induced fluorescence quenching; and 3) indirect fluorescence change through analyte-induced perturbation of the fluorophore environment, as discussed in this work. The first scheme is limited to analytes which fluoresce. The second requires analyte influence on fluorescence emission. The third scheme has the greatest potential for development of sensing devices for a variety of analytes not conventionally associated with fluorescence determination. Lipid membrane perturbations by selective binding events or non-selective interactions are routinely studied by fluorescence spectroscopy, where measurement of the spectral characteristics of the emitted radiation provides information about various aspects of the environment of the fluorescing species.

One important aspect of the electrochemical sensing system using lipid membranes is the sensitivity derived from an intrinsic amplification process. A single selective binding event between a "receptor" and one target molecule can result in an increase in transmembrane conduction involving thousands of ions. An analogy in

the optical experiment would necessitate that hundreds or thousands of fluorescent molecules should be influenced by a single selective binding event. This may possibly be achieved through modulation of the phase structure of the lipid membrane by the binding event.[3] To study phase structure in lipid membranes we used the primitive model of a phospholipid monolayer formed at an air-water interface, consisting of a single layer of lipid molecules with polar headgroups at the water surface and acyl chains extending into the air. Recent work with fluorescence microscopy of lipid monolayers at the air-water interface has shown that in membranes of homogeneous as well as heterogeneous lipid composition a number of phases (ie. gaseous, liquid expanded, liquid condensed, gel) can co-exist.[5,6] Fluorescently labelled lipid molecules can be used as probes of phase structure by their partitioning into areas of least structural order. The resulting microscopic fluorescence image often shows areas of brightness and darkness of 10-200 μm diameter as a function of the relative concentration of the fluorescent species available for imaging. It has been shown that these domains within lipid monolayers are sensitive to surface pressure, subphase pH, electrostatic potential and edge active species.[7,8] This provides significant opportunities for domain or phase structure alterations by manipulation of these properties using selective chemical reactions. Analysis of lipid membranes in different phases has shown that large differences in all of the multidimensional parameters associated with fluorescence can be observed, thereby demonstrating that the optical method could achieve an intrinsic amplification of selective binding events.[3]

The major goal of this research is the adaptation of a "receptor"

fluoroassay technique using the lipid membrane as a transducer for eventual incorporation into an optrode. This work reports transduction of selective binding events of two very different types of "receptor" as monitored by the fluorescence response derived from perturbations of the environment of a fluorophore which was directly labelled only to the lipid components of a membrane. Acetylcholine receptor (AChR) is the best characterized molecular receptor with respect to both structure and function. This intrinsic protein is composed of five subunits, all of which traverse the membrane, arranged to form a hollow cylinder.[9] The AChR is found in the post-synaptic membranes where it binds the neurotransmitter acetylcholine and subsequently allows Na^+ into the cell, triggering nerve depolarization or "firing".[10] The electrochemical activity is assumed to result from conformational changes of the AChR on agonist binding, but no major conformational changes have been observed.[9] The AChR is very sensitive to the composition of the surrounding lipid membrane, and has binding sites for various lipids.[11] Lipid/protein interactions may be involved in aggregative events that are related to selective binding of ligands.[12] Recent investigations of AChR, some involving fluorescence studies, have focussed on the interactions of the protein with the surrounding lipid matrix and the effects of the lipid components on the activity of the protein.[13,14] Apparently, some lipid components are tightly associated with the surface of the protein that is exposed to the hydrocarbon region of a supportive BLM.[15] This indicates that effects of selective binding processes along the length of the 11 nm cylinder may be transmitted to the lipid matrix, even though the binding site for the agonist is located 5 nm

beyond the surface of the supportive lipid matrix.

Perturbations of lipid membranes by products of enzyme reactions or antibody-antigen-complement aggregation interactions have been previously reported, and represent processes which modify membrane structure by the introduction of new chemical species to the membrane environment.[16] Another natural membrane-associated protein is acetylcholinesterase (AChE) which hydrolyzes acetylcholine to choline and acetic acid, the latter dissociating at neutral pH to yield hydronium ions. If the surrounding lipid membrane has a net negative charge, protonation of the lipid headgroups may occur, decreasing mutual repulsions of the headgroups and causing the monolayer to contract[17]. This may result in a net increase of packing density and may promote phase separation.

This work reports the use of fluorescent bilayer lipid membrane vesicles as transducers of selective binding events between AChR and agonist/antagonist, and also AChE with substrate. Fluorescence microscopy of lipid monolayers is used to investigate the partitioning of the selective proteins into ordered lipid membranes.

Experimental

Chemicals

Soybean lecithin and cholesterol were obtained from Sigma Chemical Co. (St. Louis, MO, USA) and dipalmitoyl phosphatidylcholine (DPPC) and dipalmitoyl phosphatidic acid (DPPA) from Avanti Polar Lipids (Birmingham, AL, USA). All were used without further purification. The fluorescent material 4-(N-(iodoacetoxy)ethyl-N-methyl)amino-7-nitrobenz-2-oxa-1,3-diazole (IANBD, Molecular Probes, Eugene, OR, USA) was used to label the molecular receptor. The study

of fluorescence which originated from the lipid component of the monolayer and bilayer membranes was based on use of N-(7-nitrobenz-2-oxa-1,3-diazol-4-yl)dipalmitoyl-L-a-phosphatidylethanolamine (NBD-PE, Molecular Probes). Acetylcholinesterase (AChE) fraction XIII, acetylcholine chloride, fluorescein-isothiocyanate isomer I on Celite (FITC/Celite), and dithiothreitol were obtained from Sigma. All other chemicals were reagent grade and used without further purification. Water was purified first by reverse osmosis then by a Milli-Q filtration system (Millipore, Mississauga, ON, Canada) and had a specific resistivity of 18 Mohm.cm.

Apparatus

Fluorescence spectra were obtained using an in-house assembled fluorescence spectrometer consisting of: an atmospheric pressure nitrogen laser (Model LN 103, PRA, London, ON, Canada) for excitation at 337.1 nm; a Bentham M300 monochromator with SMD 3B stepper motor controller (Optikon, Waterloo, ON, CANADA); a Hamamatsu R928 photomultiplier tube (PMT) (Hamamatsu, Bridgewater, NJ, USA) in a linearity-optimized housing (PRA) operated at -1250 V; and a SR 250 Gated integrator/Boxcar averager (SRS, Stanford, CA, USA) operated by an IBM PC through a SR 245 interface. A short length of optical cable placed in the laser output carried a small portion of the excitation pulse directly to a second photomultiplier tube for triggering of the gated integrator. Signal collection was by integrating the PMT output for 30 nsec triggered at the beginning of emission. Ten pulses were averaged for each point. A schematic diagram of the fluorescence microscope system used is shown in Fig. 1. The output of an argon ion laser (Innova 70, Coherent Laser Products, Palo Alto, CA, USA)

operated at 488 nm and 10 mW power, was directed into a Zeiss IM inverted microscope (Carl Zeiss, Oberkochen, FRG) which was mounted such that the objective lens was situated directly above the monolayer. The laser beam was reflected down to the monolayer by a dichroic mirror. The fluorescence emitted from the monolayer was transmitted through the dichroic mirror to a low light level Dage model MTI 66 SIT video camera (Dage Ltd., Michigan City, IN, USA). The camera was linked to an Oculus 300 video grabber card (Coreco Inc., Cleveland, OH, USA) which digitized the image (512 x 480 pixels) for storage and processing using an IBM PC-AT computer. The microscope, film balance and camera were mounted on a gas damped vibration isolation table (Melles Griot, Rochester, NY, USA). The film balance used for monolayer compression was a commercial Lauda model 1974 unit (Sybron-Brinkmann, Toronto, ON, Canada). The probe-tip sonicator was the Vibra-Cell VC 250 adapted with a tapered micro-tip (Sonics & Materials, Danbury, Conn, USA).

Procedures

Labelling of proteins

7.7 mg of AChE was dissolved in 3.85 mL of 10 mM sodium carbonate buffer, pH 9.0, and stirred for 2 hr. A 9.8 mg portion of FITC/Celite was added, and the mixture was stirred overnight. Free FITC was separated from the FITC-AChE on a 1.0 x 15 cm Sephadex G-75-150 column, equilibrated and eluted with 10 mM Tris-HCl, 0.04 M $MgCl_2$, 0.1 M NaCl, pH 7.5. Purification of AChR from Torpedo californica (Pacific Biomarine, Venice, CA, USA) was accomplished by standard methods; by centrifugation[21], sucrose density ultracentrifugation[22], and affinity chromatography on concanavalin A-Sephadex.[18]

Reconstitution with added soybean lecithin was into 10 mM sodium phosphate, pH 7.4, which was then stored as aliquots in liquid nitrogen. Activity of the stock receptor solution was determined by incubation with ^{125}I α-bungarotoxin (α-btx) (ICN Biomedicals Canada Ltd., Montreal, PQ, Canada) to be 1.3 μM in toxin sites.[19] Protein concentration was determined to be 0.3 $mg.mL^{-1}$ as described elsewhere,[20] yielding a specific activity of 4.3 $nmole.mg^{-1}$ in toxin sites. IANBD labeling of the AChR was done according to previous methods.[23] IANBD (Molecular Probes, Eugene, OR, USA) was added in excess as a solid to AChR membranes reduced with dithiothreitol and the solution was stirred on ice and in the dark for two hours.

Vesicle preparation and use

Vesicles containing unlabelled AChE were formed from DPPC/DPPA/NBD-PE. A 5 ml solution of DPPC/DPPA (70/30 mole %) in ethanol was mixed with a concentrated stock solution of NBD-PE in ethanol to produce a solution containing 1 mole % NBD-PE with respect to total lipid concentration. This solution was evaporated under a nitrogen gas stream. The lipid was re-suspended by sonication in 8 mL of 0.1 M KCl containing 2% sodium cholate and adjusted to pH 7.4. A volume of 90 μL of acetylcholinesterase solution was added to 500 μL of lipid solution, and the mixture was placed in dialysis tubing (Spectrapor, 12,000 to 14,000 molecular weight cut-off, VWR Scientific, Rexdale, ON, Canada). Dialysis proceeded against 10 mM Tris buffer, pH 7.4, to remove the cholate detergent. Controls of soybean lecithin and soybean lecithin/bovine serum albumin (BSA) were prepared identically to the AChE sample.

One method of preparation of fluorescent vesicles of unlabelled

AChR involved fusion of vesicles containing the receptor with vesicles containing NBD-PE. A solution of 1 $mg.mL^{-1}$ NBD-PE in HEPES buffer (10 mM HEPES, 35 mM sodium nitrate, pH 7.4) was prepared in vesicle form. 60 µL of this was added to 100 µL of stock AChR solution and sonicated for different periods of time, yielding a final system of vesicles of which approximately 2 mol% of the lipid was NBD-PE, assuming a mean molecular weight of 750 $g.mol^{-1}$ for the soybean lecithin. A second receptor preparation of 2 mol% NBD-PE was produced by addition of the NBD-PE during the reconstitution stage of the AChR purification. The appropriate amount of NBD-PE was added to affinity-purified receptor in 2% sodium cholate detergent before dialysis. The sample was centrifuged at 10,900 g for 15 min after dialysis to remove residual solid NBD-PE.

Vesicular solutions containing AChE and AChR were independently studied by placing the solution in a standard 1-cm quartz cuvette, and observing fluorescence in the region of 500 to 650 nm. Acetylcholine or α-btx was added directly to the cuvette as a titrant solution. "Poisoning" of the receptor was accomplished by pre-incubation with a minimum three-fold excess of α-btx for at least 2 h on ice.

Monolayer preparation and fluorescence microscopy

Phospholipid monolayers were characterized by pressure-area isotherms and concurrent imaging by fluorescence microscopy. Phospholipid monolayers were formed by standard methods[5-8] on the Lauda film balance which contained a subphase of 1000 mL degassed 0.1 M KCl solution adjusted to pH 7.4 with NaOH at room temperature (21 ∓ 1°C). Approximately 70 µL of the phospholipid solution was added dropwise over a period of 90 seconds to the trough surface area of 750

cm^2. After a period of 15 minutes had elapsed to permit solvent evaporation, the monolayer was compressed and expanded repeatedly at a rate of 15 $cm^2.min^{-1}$ until reproducible pressure-area isotherms were obtained. Fluorescently labelled or unlabelled acetylcholinesterase in a 2% sodium cholate, 10 mM Tris buffer, pH 7.4 solution was added to the lipid monolayer by the microdroplet spray technique as described elsewhere.[24] Similarly, AChR monolayers were formed by adding a 2% sodium cholate suspension of AChR vesicles to a previously formed soybean lecithin monolayer. Fluorescence microscope images were accumulated from stationary monolayers at various pressures. Single video frames were grabbed from a video signal of 30 $frames.sec^{-1}$.

Results and Discussion

Response from acetylcholine receptor

A prime focus of this research was to develop a generic strategy for transduction of agonist or antagonist binding to AChR. Recent investigations of the role of membrane lipid components in the function of AChR led us to propose that a fluorescent lipid component of a lipid membrane could be used generically to give a quantitative measure of this binding. Previous experimental work reported by Dunn and Raftery[23] indicated that fluorescently labelled AChR would undergo an enhancement of fluorescence on interaction with agonist. Our work was directed to observation of fluorescence alteration in the presence of unlabelled AChR.

To investigate the response of a system containing only fluorescent lipid components, preparations were made by vesicle fusion

between unlabelled receptor systems and vesicles of the lipid fluorophore NBD-PE. The NBD-PE probe was chosen due to its chemical similarity to the other phospholipids used in these studies, and due to the minimal structural perturbation of the membrane by the fluorescent label located at the headgroup terminus of the lipid. The resultant emission spectrum is shown in Fig. 2 and was identical to AChR-rich membranes labelled with IANBD. Fluorescence enhancement was measured as the increase in peak area observed on addition of the agonist carbamylcholine (carb), which is commonly used to generate an ion-gated response from AChR (Fig. 3A). Selective receptor mediation of the enhancement process was demonstrated by pre-incubation of the receptor system with α-btx. This is a large protein which is a known selective antagonist for AChR. It is binds irreversibly to the receptor near the agonist binding site, prohibiting agonist binding. The expected result of negation of the agonist-induced enhancement was observed. To further confirm receptor mediation of the enhancement, controls were performed using pure lipid vesicles, vesicles with a different protein (bovine serum albumin) and vesicles containing degraded (by extensive sonication, see Table 1) AChR. All of these controls yielded no fluorescence enhancement. In addition, it was observed that the fluorescence signal was enhanced by very low concentrations of the antagonist α-btx as shown in Fig. 4. This indicates an antagonist-associated conformational change which may or may not be similar to the change observed for agonist binding, but which may permit detection of toxin.

Significant difficulties were encountered in the vesicle system with regard to reproducibility and stability of the signal with time. It was suspected that some of the variability was due to incomplete

exchange between the NBD-PE vesicles and the AChR vesicles prior to beginning the agonist addition, resulting in fluorescence changes due to subsequent lipid exchange. To circumvent some of the difficulties of the vesicle fusion technique, incorporation of fluorophore was accomplished by addition of fluorescent lipid to stock lipid before reconstitution of AChR from detergent phase into vesicles. This yielded a more stable signal and a consistent control with α-btx pre-incubation (Fig. 3B). The enhancement versus concentration of agonist was modelled by:

$$F([carb]) = \frac{F(max) \times [carb]}{K_d + [carb]} \qquad \{1\}$$

where F([carb]) is the measured enhancement, F(max) is the limit of enhancement, [carb] is the concentration of the agonist and K_d is the dissociation constant of the complex. Peak areas were obtained from the spectra by integration of the entire peak (500 nm to 650 nm). Fig. 3 indicates a sensitivity of 30%.μM and a limit of detection of 300 nM over a dynamic range of 3 μM with a correlation coefficient of 0.978. The enhancements observed in our experiments resembled those of Dunn et. al.[23] who reported results for labelled AChR with some exceptions. The previous researchers worked in the high-μM to mM agonist concentration region, and attributed the binding phenomenon to a 'low affinity' site on the receptor with a dissociation constant (K_d) of 0.96 mM. However, we observed the same magnitude enhancement while working at concentrations in the low μM regime. The AChR is well known to have low and high affinity binding sites for agonists in the μM and nM range respectively.[25,26] Our response at the low μM

range indicates that our AChR is in the desensitized, high affinity state. This could arise due to heat-inactivation, repeated freeze-thaw cycles of AChR vesicles, or other extreme conditions experienced by the receptor during the course of the experiment. It is exciting that even desensitized AChR can be used for quantitative studies. This lends optimism for the potential use of AChR in the artificial environment of a biosensor.

Response from acetylcholinesterase

The enzyme AChE was used in this work to investigate the possibility of inducing reversible structural transitions within lipid membranes. The enzymatic catalysis of acetylcholine to acetic acid (and choline) could provide a high localized hydronium ion activity at the surface of lipid membranes in which the enzyme is bound. Electrostatic repulsions between acidic functional groups in the headgroup region of the membrane would be decreased by the hydronium ion activity. The structure and fluidity of the membrane would therefore be partially controlled by the dynamic reaction process when acetylcholine was available for the enzymatic reaction to proceed.

Lipid membranes were prepared with relatively high concentrations (30 mole %) of the acidic phospholipid DPPA, providing structural sensitivity to minor pH variations. Vesicles with the fluorescent label NBD-PE were prepared, and enzyme incorporation was accomplished by detergent solubilization and subsequent dialysis. The resulting vesicles were then sonicated to create better size uniformity prior to fluorescence studies. Quantitative analyses of protein concentration and enzyme activity for these vesicles were not established, however spot tests and the results of the fluorescence experiments confirm

that some proportion of the enzyme within the vesicles was biochemically active.

Interaction of vesicles containing AChE with acetylcholine produced a fluorescence enhancement as shown in Fig. 5. The quantitative results are of limited utility in establishing the analytical sensitivity of this transduction system since the absolute quantity of active enzyme has not been established. The results do show a trend of fluorescence enhancement as acetylcholine concentration is increased (linear correlation coefficient shows a poor fit with a value of 0.90). The time course of the fluorescence alteration is particularly revealing since the enhancement sets on very rapidly and continues over a period of many minutes as shown in Fig. 6. The profile of the response curve of Fig. 6 is consistent with the establishment of a pH gradient as a maximal rate for the acetylcholine reaction is achieved, followed by depletion of the substrate in the sample solution. The results confirm the ability of lipid membranes to act as reversible transducers since the fluorescence enhancement is a transient phenomenon. The time course of the response is consistent with the high turnover rate of 25,000 Ach/AChE every second, and the pH after equilibration is expected to be a value of approximately 5 to 6, based on the concentration of acetylcholine available in the sample solution and the buffering action of the lipid headgroups. The final value of fluorescence enhancement was consistent with such a pH change as determined by acetic acid titration experiments using DPPA/DPPC vesicles containing AChE. Blank experiments investigating the influence of acetylcholine and choline on DPPA/DPPC vesicles, and vesicles containing BSA as a replacement for AChE, showed no

enhancement of fluorescence. Likewise, no enhancement was observed when using denatured AChE (heated to 90°C for 2 h before vesicle incorporation). Upon artificial acidification of the sample solution by addition of acetic or hydrochloric acid to bring the pH to 4.0, vesicles with and without AChE both provided a relatively instantaneous increase in fluorescence to the maximal level observed for experiments with acetylcholine. This supports the theory that the fluorescence enhancement arises due to an increase in hydronium ion activity. The mechanism of enhancement may be due to protonation of DPPA headgroups, and/or lateral pressure alterations within the lipid membrane due to osmotic effects experienced by the vesicles. The experiments using millimolar concentrations of the charged choline species did not produce an enhancement, and provides evidence contrary to the osmotic effect hypothesis. Investigations of lipid monolayers (described below) were done to confirm that protonation of DPPA would cause significant structural perturbations of lipid membranes.

Monolayer investigations

The NBD-PE probe has been used to study phase domain structure in membrane systems by classical spectrofluorometric measurements such as enhancement/self-quenching[27] and by the relatively new technique of fluorescence microscopic imaging of lipid monolayers at an air-water interface.[6] Both techniques are possible as a result of the natural tendency of the NBD-PE molecules to partition between phases in a mixed phase system such that they concentrate in the less ordered domains. In the case of microscopy, this allows structures in monolayers to be visualized as bright and dark regions, provided such structures are of μm dimensions.

When in locally concentrated regions, the NBD moities will "self-quench", causing a reduction in the overall measured intensity. Any changes in the relative areas of phase structure types will thus result in a change in the overall intensity. Such changes may be proposed for the system under study as the NBD-PE probe has been shown to indicate perturbation of lipid phase structure by incorporated proteins.[28] Figure 7 shows classical pressure-area curves for DPPA/DPPC/NBD-PE monolayers, with typical fluorescence microscopy images collected at a pressure of 20 $mN.m^{-1}$. At the relatively low pressure of 10 $mN.m^{-1}$ at pH 7.4, the majority of the lipid monolayer was in the liquid-expanded phase where the individual lipid molecules had much lateral freedom of movement. Small domains of varying intensity were observed. At a pressure of 20 $mN.m^{-1}$ at pH 7.4, a larger portion of the monolayer was in liquid condensed phase where lipids were forced into close contact. A very limited number of larger dark domain areas were observed, indicating more extensive areas of condensed phase. To test whether AChE would associate with a lipid monolayer at pH 7.4 and cause structural perturbation, fluorescein-labelled AChE in a detergent solution was introduced into a monolayer of DPPC/DPPA at a pressure of 20 $mN.m^{-1}$. No immediate increase in monolayer pressure was observed, but a pressure increase of less than 5 $mN.m^{-1}$ was seen after 12 h. The presence of a fluorescent image clearly indicated that some of the AChE was incorporated into the membrane, and the negligable pressure increase suggested that the AChE was not interspersed with the lipids in the monolayer, but rather associated with the lipid headgroups at the membrane interface. A representative fluorescence microscopy image obtained from the fluorescence of the enzyme is shown with the

pressure-area curve in Fig. 8. The image is similar to that of the lipid monolayer containing NBD-PE in the absence of protein. Condensed phase domains indicating the absence of protein are roughly spherical and not very abundant, and the extensive bright interspersing regions indicate that the protein selectively associates with fluid regions of the membrane, and has little effect on the interfacial zones between phases.

When the pH of the subphase that supported a DPPA/DPPC monolayer without AchE was decreased from a value of 7.4 to 4.0 (Fig. 7), the fluorescence image at 20 $mN.m^{-1}$ changed from a largely uniform bright field to a field with many darker and brighter domains. The pressure-area curves (using 20 $mN.m^{-1}$ as a reference pressure) and the microscopic images confirm a general condensation of the membrane resulting from acidification of the subphase. The initial uniformity of the images of DPPA/DPPC monolayers at pH 7.4 indicate that electrostatic repulsion of the DPPA headgroups is minimized by homogeneous dispersion with DPPC. At pH 4 the condensed and fluid regions arise from the partial neutralization of negatively charged DPPA headgroups, removing the electrostatic repulsions and allowing separation of the different lipids into condensed domains of relatively pure lipid. These results are consistent with the proposed mechanism of fluorescence enhancement obtained during studies of vesicles containing AChE in the presence of acetylcholine.

A monolayer of soybean lecithin with 2 mol% NBD-PE was investigated by fluorescence microscopy and was observed to have no domain structure at any pressure. AChR vesicles solubilized with detergent were added to monolayers initially at 20 $mN.m^{-1}$ pressure,

and an immediate increase in surface pressure was seen totalling almost 20 mN m^{-1} after 12 h. This was expected since lipid as well as protein had been added to the monolayer. A fluorescence microscope image of this system is shown in Fig. 9, and indicates a uniform dispersion of small bright patches indicating partitioning of NBD-PE molecules. Partitioning due to NBD-PE association with the receptor molecules does not account for this effect, since AChR interactions with the surrounding lipid are known to create a more disordered lipid region to a distance of only a few nanometers.[30] The image scale of this work (resolution ca. 1 μm) indicates that AChR may tend to form aggregates within soybean lecithin monolayers. These results are supported by the addition of IANBD-labelled AChR to a monolayer of soybean lecithin which did not contain NBD-PE. The resulting fluorescent image again showed numerous bright regions 1-10 μm wide in the viewing field, and confirmed that aggregation of the receptor occured. However, the aggregation may be an artifact of the experimental system since a monolayer, rather than teh usual bilayer membrane, was used to support the receptor. If the results are not artifacts, then the physical dimensions of the aggregates in lipid monolayers suggests that the protein-membrane interactions within lipid vesicles may not arise from simple steric interactions, but may propagate over large distances (relative to molecular size) across the membrane surface. This is consistent with electrostatic models of protein-lipid interaction. A long-range perturbation would seem to be necessary to explain the fluorescence enhancement from vesicles observed in the work with AChR, as it is difficult to envision localized molecular perturbation capable of altering the fluorescence emission of a membrane by, in some instances, over 200 percent.[31]

Conclusions

A generic scheme for transduction of protein binding events has been demonstrated based on the ability of fluorescent membrane components to respond to ligand binding with AChR and ligand reaction with AChE. Further investigations of fluorescence lifetime or polarization may provide additional means of signal acquisition and calibration.[32] Preliminary results indicate that the emission lifetime of NBD-PE in experiments using AChR is best modelled by a double exponential fit, where one of the pre-exponential factors of the lifetime components is sensitive to the selective reaction. The results presented indicate that phase domain structure and protein incorporation in lipid monolayers may be characterized using fluorescence microscopy. It remains to use this technology to demonstrate dynamic perturbation of the domain structure by selective interactions of the incorporated proteins. Development of a sensor for neurologically active compounds using the vesicle system characterized here necessitates stabilization of a functional receptor system onto a solid substrate. Possible methods for this stabilization are direct covalent attachment via the protein or the lipid components, fusion of vesicular structures with the substrate,[29] or incorporation of the protein into monolayer at an air/water interface and transfer of the monolayer onto the substrate by Langmuir-Blodgett deposition techniques[33]. Work is presently being directed towards the completion of these two tasks.

We are grateful to the Natural Sciences and Engineering Research Council of Canada, the Canadian Defence Research Establishment, the

Ontario Ministry of the Environment and Imperial Oil Canada for financial support for this work.

References

1. Krull, U.J. and Thompson, M., IEEE Trans. Electron. Dev., 1985, **32**, 1180.
2. Thompson, M. and Dorn, W.H., in "Chemical Sensors", Edmonds, T.E., Editor, Blackie and Sons, Glasgow, 1987.
3. Krull, U.J., Brown, R.S., DeBono, R.F., and Hougham,B.D., Talanta, 1988, **35**, 129.
4. Arnold, M.A., Editor, in "Fiber Optic Chemical Sensors", Talanta, **35(2)**, 1988.
5. Weis, R.M. and McConnell, H.M., Nature (London), 1984, **310**, 47.
6. Heckl, W.M., "Laterale Organization Von Lipidmonoschichten Bei Einbau Von Amphiphilen Fremdstoffen Und Proteinen", Ph.D. Thesis, Department of Physics, Technical University of Munich, 1988, and related publications.
7. McConnell, H.M. and Moy, V.T., J. Phys. Chem., 1988, **92**, 4521.
8. Weis, R.M. and McConnell, H.M., J. Phys. Chem., 1985, **89**, 4453.
9. Changeux, J.-P., Devillers-Thiery, A. and Chemouilli, P., Science, 1984, **225**, 1335.
10. Hille, B., "Ionic Channels of Excitable Membranes", Sinauer Associates, Sunderland, Massachusetts, 1984.
11. Jones, O.T. and McNamee, M.G., Biochem., 1988, **27**, 2364.
12. Tedesco, J.L., Krull, U.J. and Thompson, M., Biosensors, in press.
13. Fong, T.M. and McNamee, M.G., Biochem., 1986, **25**, 830.
14. Zabrecky, J.R. and Raftery, M.A., J. Receptor Res., 1985, **5**, 397.
15. Gonzales-Ros, J.M., Farach, M.C. and Martinez-Carrion, M., Biochem., 1983, **22**, 3807.

16. Thompson, M. and Krull, U.J., Anal. Chim. Acta, 1983, **147**, 1.

17. Heckl, W.M. and Mohwald, H., Ber. Bungenges Phys. Chem., 1986, **90**, 1159.

18. Lindstrom, J., Anholt, R., Einarson, B., Engel, A., Osame, M. and Montal, M., J. Biol. Chem., 1980, 255, 8340.

19. Kohanski, R.A., Andrews, J.P., Wins, P., Eldefrawi, M.E. and Hess, G.P., Anal. Biochem., 1977, **80**, 531.

20. Markwell, M.A.K., Haas, S.M., Tolbert, N.E. and Bieber, L.L., Meth. Enzym., 1981, **72**, 296.

21. Sobel, A., Weber, M. and Changeux, J.-P., Eur. J. Biochem., 1977, **80**, 215, 1977.

22. Sobel, A., Heidmann, T., Cartaud, J. and Changeux, J.-P., Eur. J. Biochem., 1980, **110**, 13-33.

23. Dunn, S.M.J. and Raftery, M.A., Proc. Natl. Acad. Sci., U.S.A., 1982, 79, 6757.

24. Heckl, W.M., Zaba, B.N. and Mohwald, H., Biochim. Biophys. Acta, 1987, **903**, 166.

25. McNamee, M.G. and Ochoa, E.L.M>, Neurosci., 1982, **7**, 2305.

26. Raftery, M.A., Dunn, S.M.J., Conti-Tronconi, B.M., Middlemas, D.S. and Crawford, R.D., Cold Spring Harbor Symp. on Quant. Biol., 1983, **43**, 21.

27. McGrath, A.E., Morgan, C.G. and Radda, G.K., Biochim. Biophys. Acta, 1976, 426, 173.

28. Heckl, W.M., Losche, M., Scheer, H. and Mohwald, H., Biochim Biophys. Acta, 1985, **810**, 73.

29. Watts, T.H., Gaub, H.E. and McConnell, H.M., Nature (London), 1986, **320**, 179.

30. Ellena, J.F., Blazing, M.A. and McNamee, M.G., Biochem., 1983, **22**,

5523.

31. Krull, U.J., Brown, R.S., Dyne, K., Hougham, B.D. and Vandenberg, E.T., in "Chemical Sensors and Microinstrumentation", Murray, R., ed., American Society Symposium Series, in press, 1989.

32. Brown, R.S., Krull, U.J. and Hougham, B.D., in "Biotechnology Research and Applications", Gavora, J., Gerson, .F., Luong, J., Storer, A. and Woodley, J.H., eds., Elsevier Applied Science, New York, 1988.

33. Kuhn, H., Thin Solid Films, 1983, **99**, 1.

Table 1. Demonstration of the loss of ability of acetylcholine receptor to bind with α-bungarotoxin with increasing sonication time

Time of Sonication (min)	α-Btx Binding Activity (nmol.mg^{-1} protein)
0	11.3
5	3.3
10	2.7
20	1.0

Figure Captions

1. Schematic representation of instrumentation used to collect fluorescence images from monolayers at an air-water interface.
2. Fluorescence emission spectrum of NBD-PE (1 mole %) in soybean lecithin vesicles.
3. Concentration-response curves for AChR interaction with carbamylcholine as determined by fluorescence intensity enhancement from lipid vesicles containing 1-2 mole % NBD-PE.
   □-fluorophore incorporated into vesicles containing AChR by means of vesicle fusion; K_d = 0.89 μM, F_{max} = 73.
   ◇-fluorophore uniformly incorporated into vesicles by reconstituting purified AChR into lipid containing NBD-PE; K_d = 11.8 μM, F_{max} = ~~221~~ 190.
4. Spectral response curve for AChR interaction with α-btx (10^{-7} M). Fluorescence intensity enhancement was from NBD-PE incorporated into AChR vesicles, formed by reconstituting purified AChR into lipid containing NBD-PE; a) initial, b) following α-btx addition.
5. Concentration-response curve for AChE interaction with acetylcholine as determined by fluorescence intensity enhancement from lipid vesicles containing NBD-PE.
6. Actual experimental response curve showing time dependence of AChE interaction with acetylcholine as determined by fluorescence intensity enhancement from lipid vesicles containing NBD-PE.
7. Pressure-area curves and fluorescence microscopy images (@ 20 $mN.m^{-1}$) for monolayers of DPPA/DPPC with 1 mole % NBD-PE at (A) pH 7.4 and (B) pH 4.0.
8. Pressure-area curve for a DPPA/DPPC monolayer containing adsorbed

fluorescent FITC-AChE and not labelled with NBD-PE. The accompanying fluorescence microscopy image recorded at ca. 20 $mN.m^{-1}$ shows the localized partitioning of the AChE, and indicates that a structure similar to that seen in Fig. 7 is obtained.

9. Fluorescence microscope image obtained at a pressure of 20 $mN.m^{-1}$ showing aggregative structures in a soybean lecithin monolayer containing 1 mole % NBD-PE after incorporation of AChR. No structure is observed from fluorescent soybean lecithin monolayers in the absence of AChR.

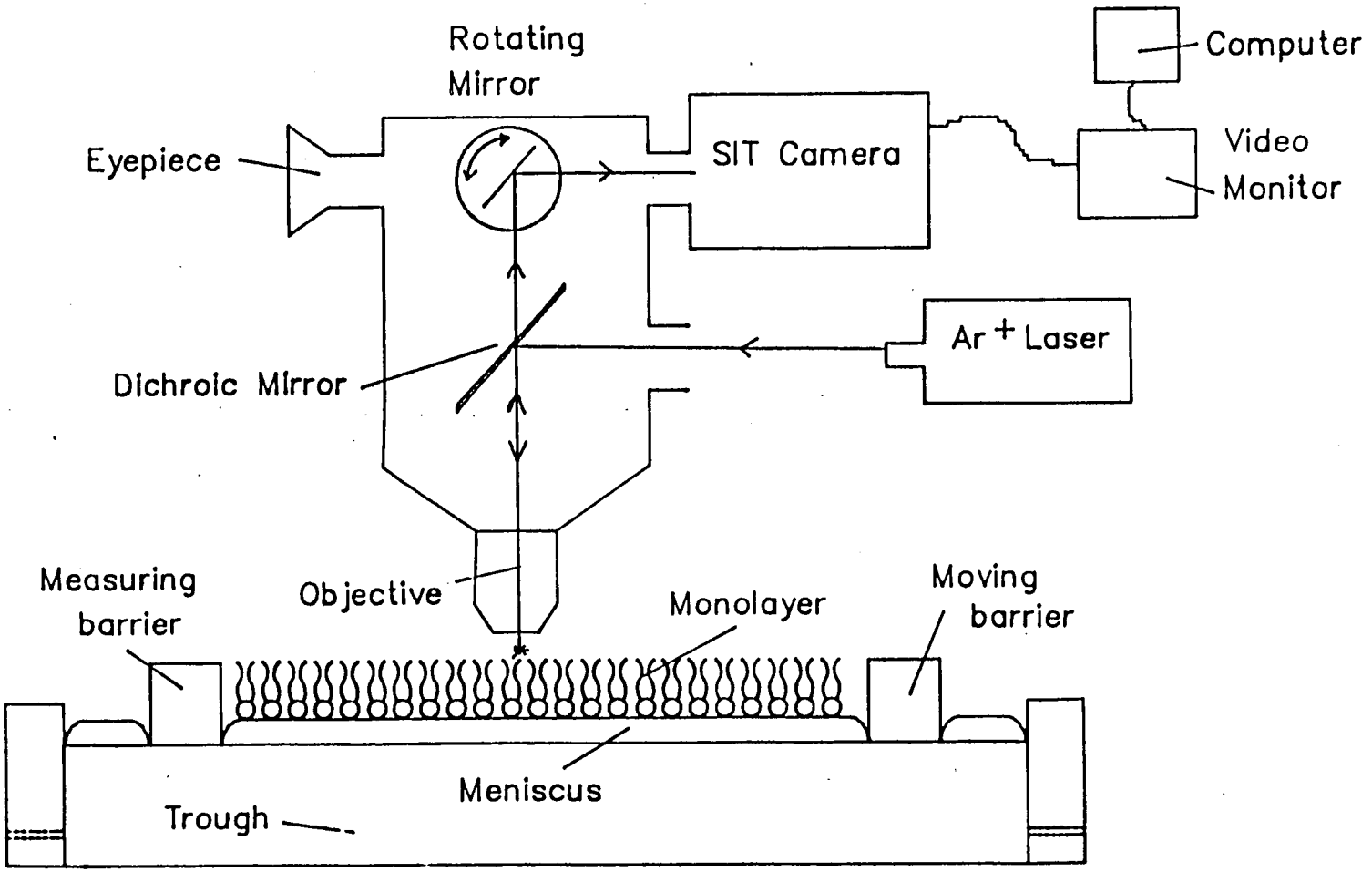
Rotating
Mirror
Computer
Eyepiece
SIT Camera
Video
Monitor
Ar + Laser
Dichroic Mirror
Measuring
barrier
Objective
Monolayer
Moving
barrier
Meniscus
Trough

Fig 1

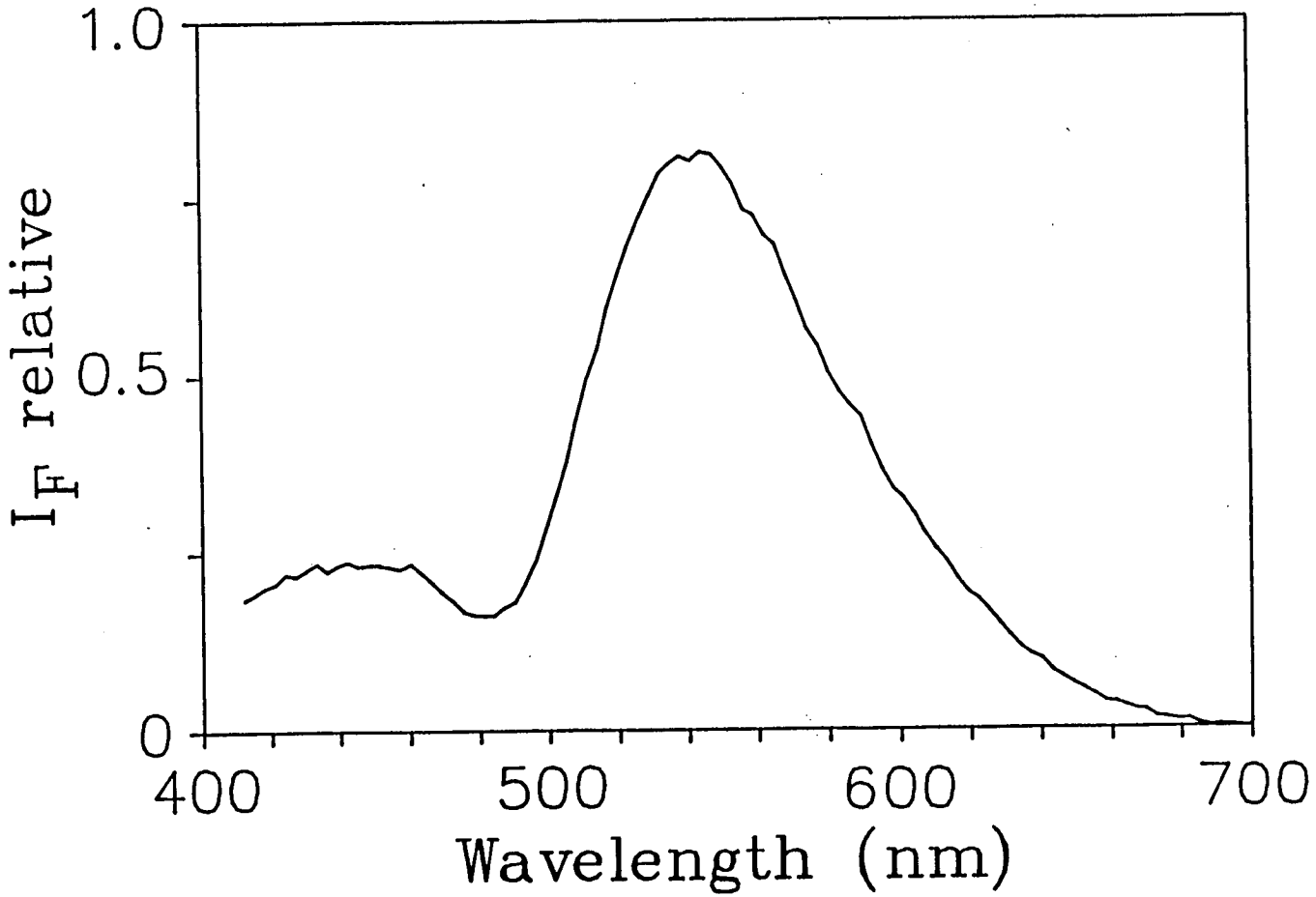

Fig. 2

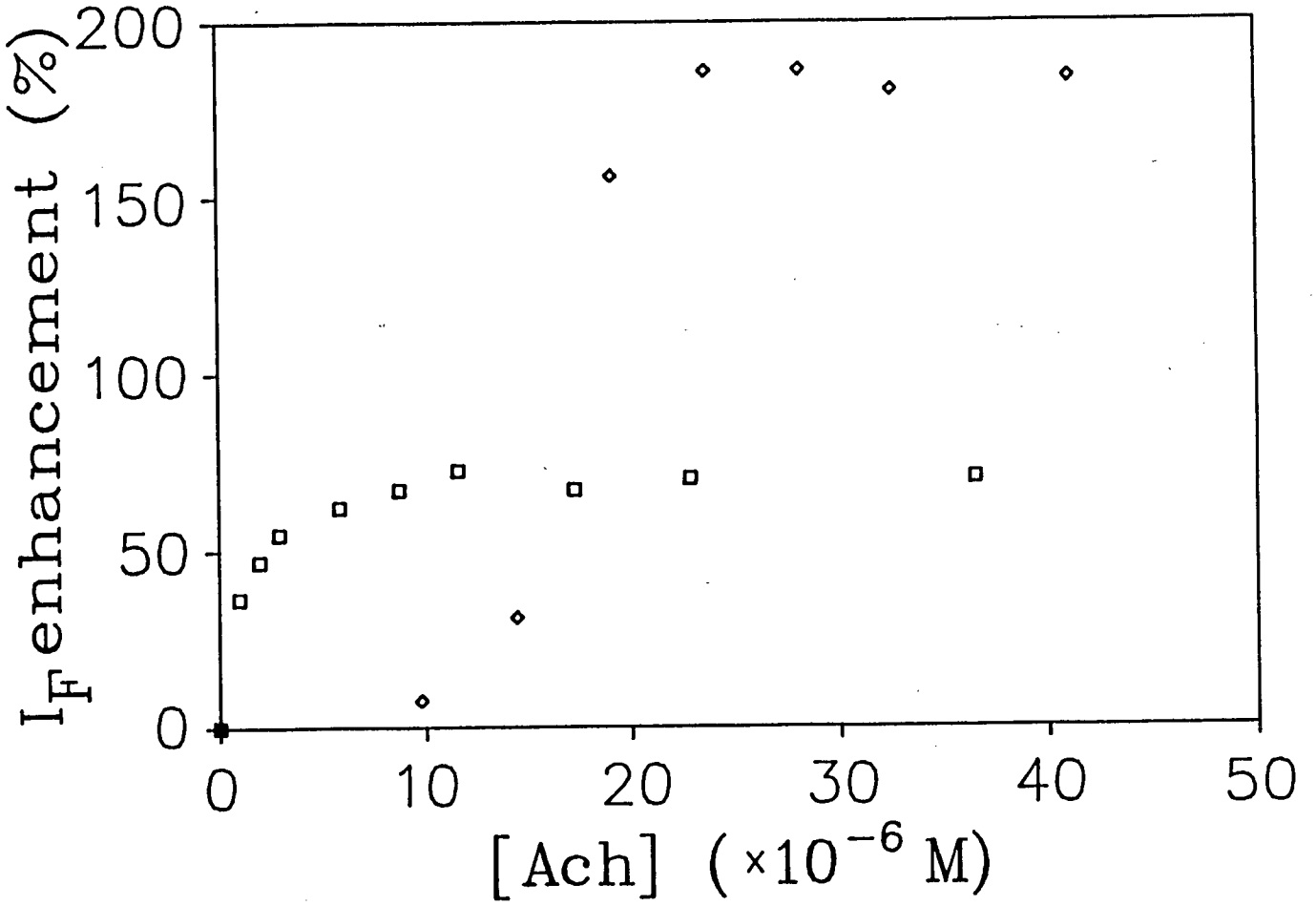

Fig 3

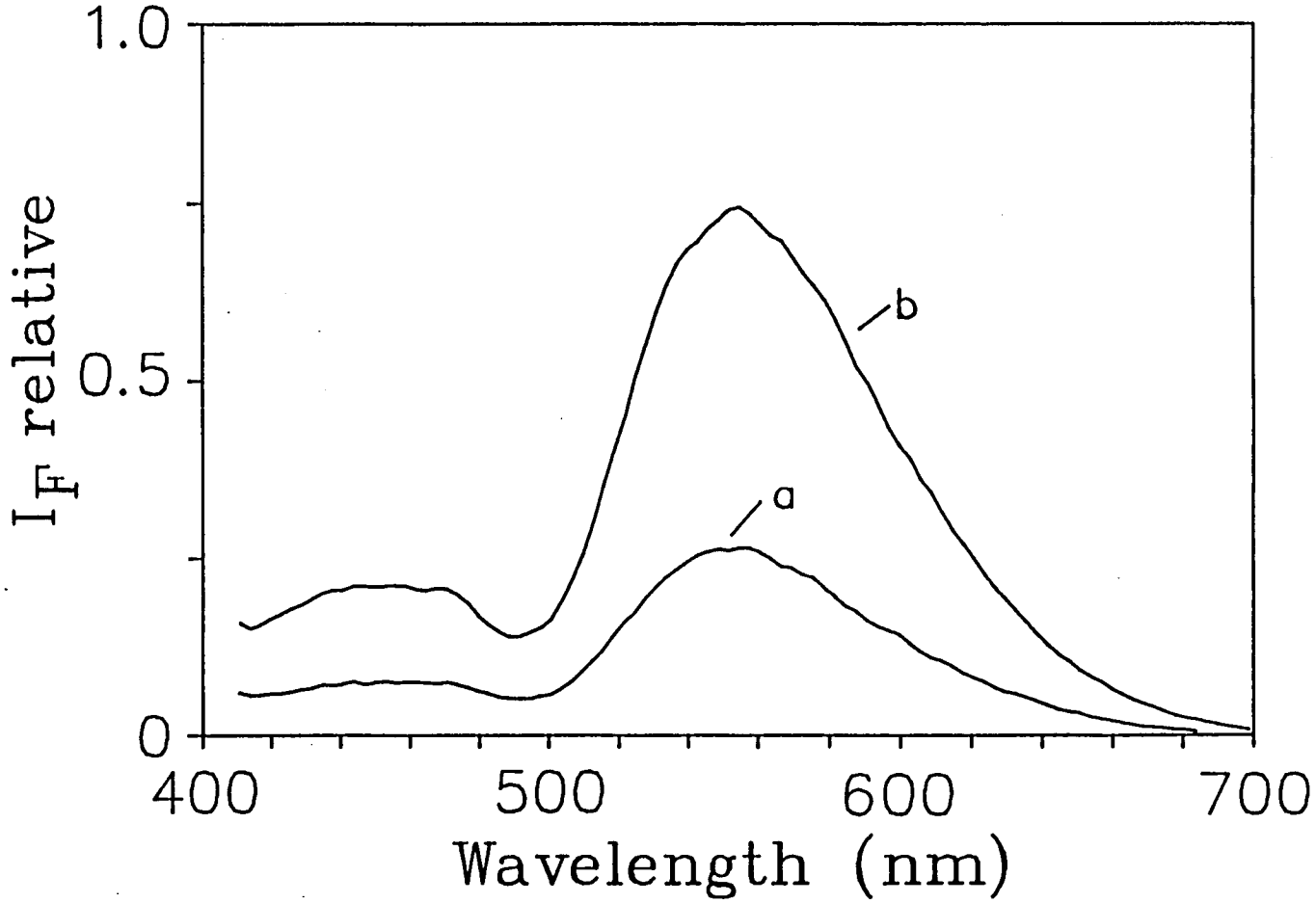

Fig 4

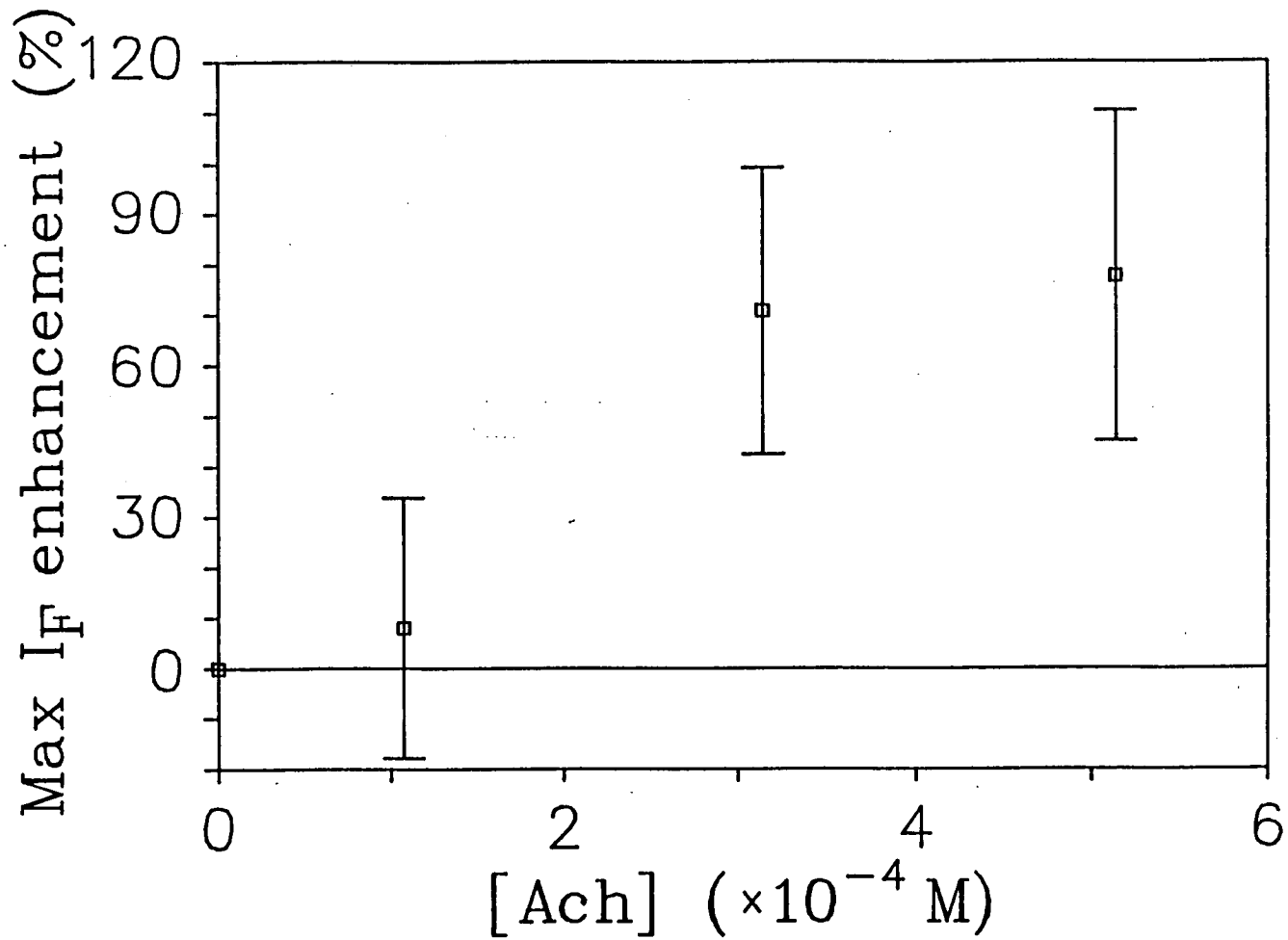

Fig 5

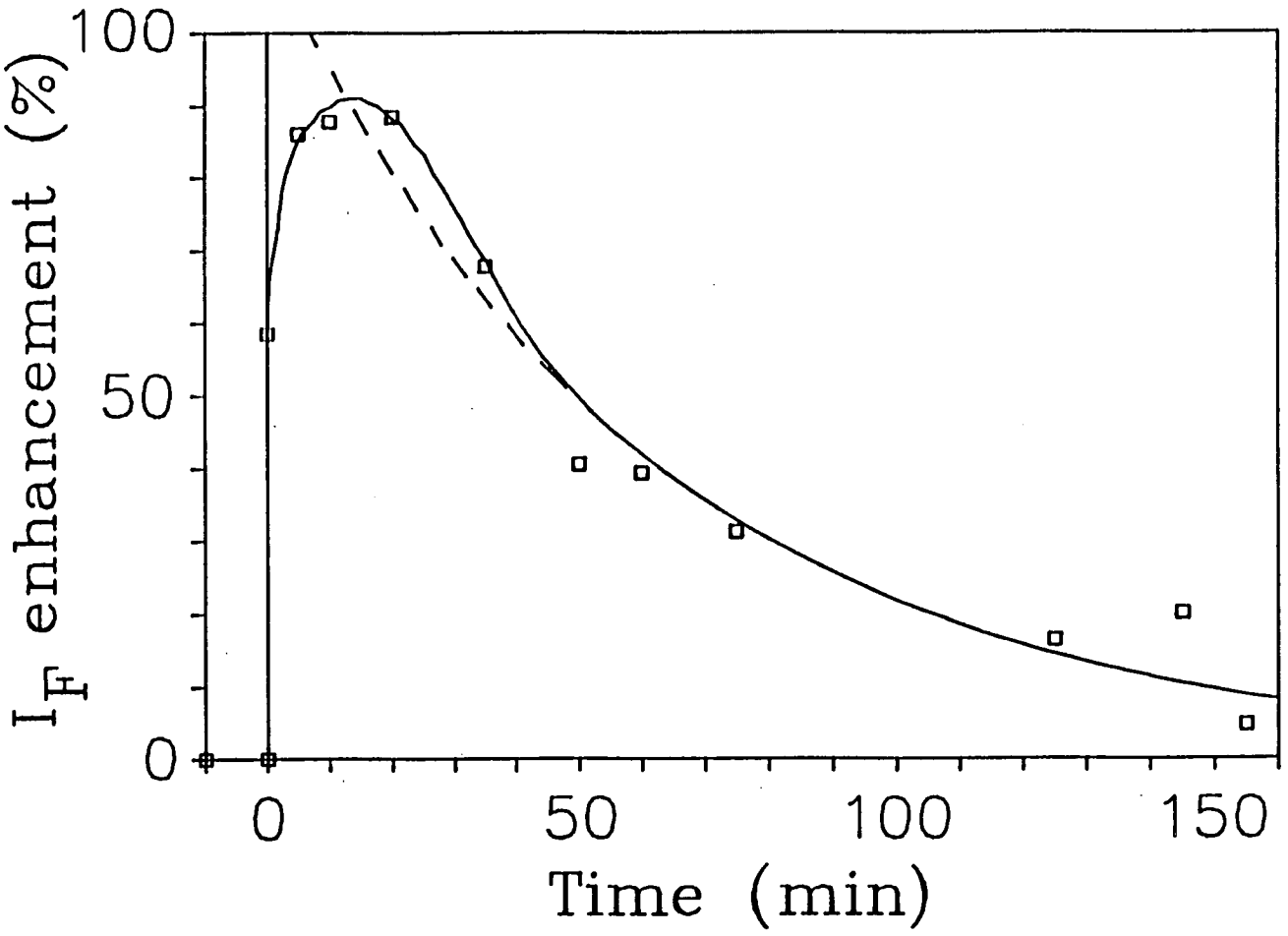

Fig 6

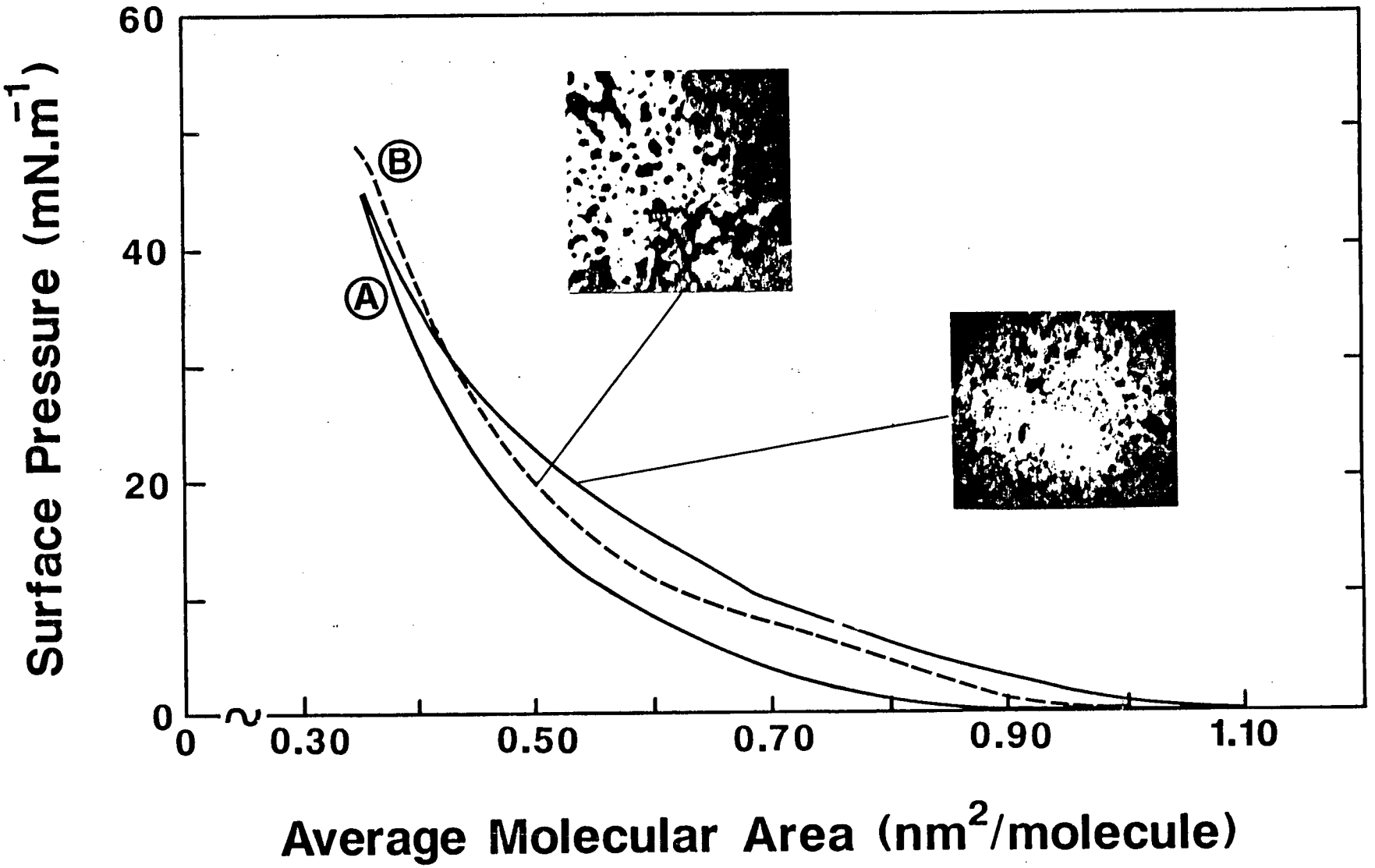
60
40
20
0
0
0.30
0.50
0.70
0.90
1.10
Surface Pressure (mN.m^{-1})
Average Molecular Area (nm^2/molecule)
A
B

Fig 7

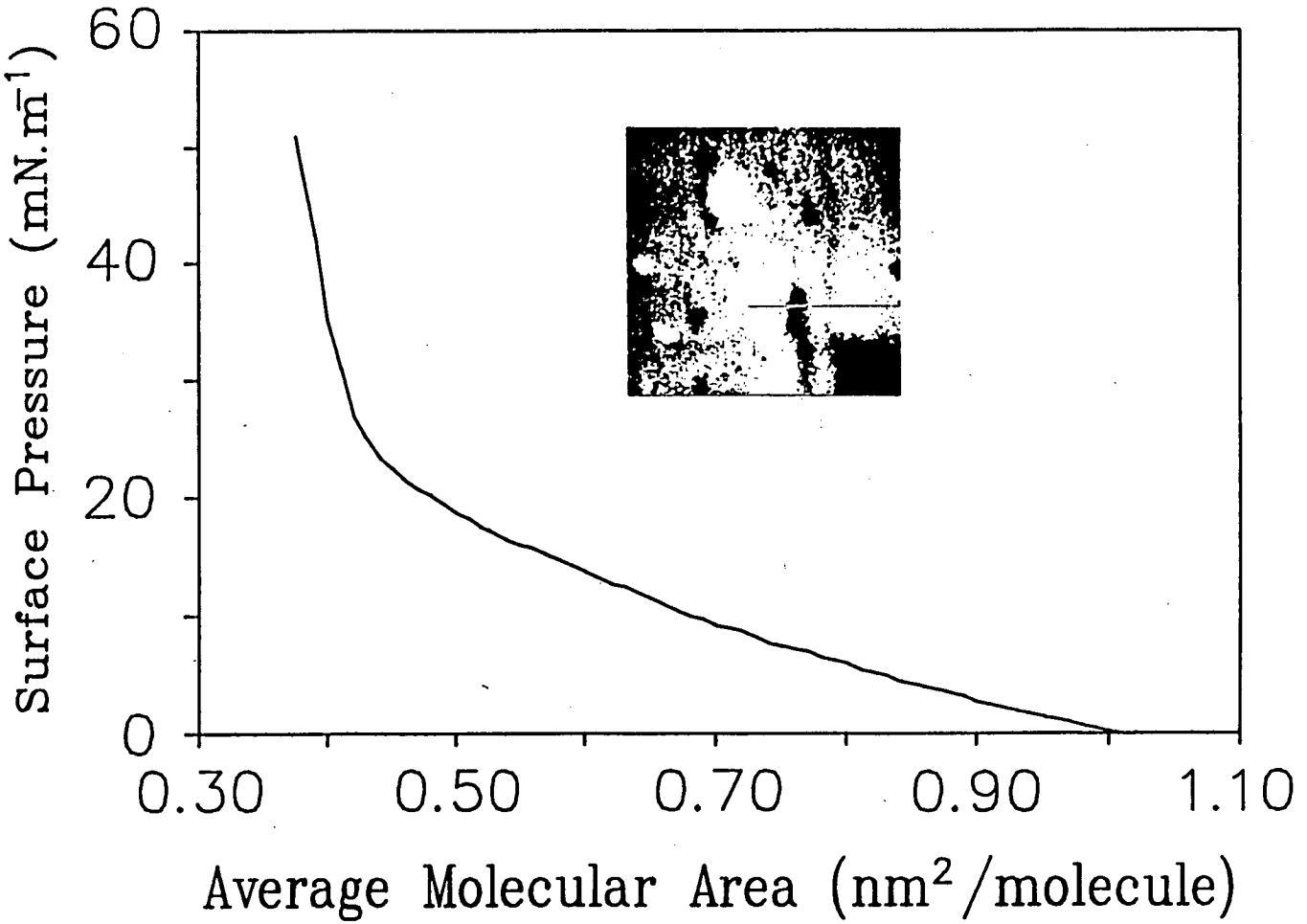
60
40
20
0
Surface Pressure (mN.m⁻¹)
0.30
0.50
0.70
0.90
1.10
Average Molecular Area (nm²/molecule)

Fig 8

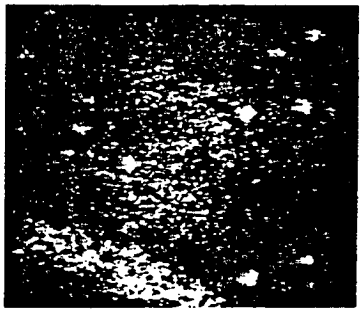

Fig. 9

SECTION 3

Fluorescence Wavelength, Intensity and Lifetime for Multidimensional Transduction of Selective Interactions of Acetylcholine Receptor by Lipid Membranes

INTRODUCTION

Molecular receptor systems are desirable in a biosensing strategy as they exhibit high sensitivity and selectivity, and the formation of receptor-ligand complexes is reversible. Generally, molecular receptors are proteins found embedded in the cell membrane of many cell types. The purpose of these proteins is to detect the presence of certain target molecules, or agonists, in the external environment and mediate some cellular response to the presence of that agonist[1]. Biosensing is possible where the agonist-receptor complexation can be transduced to a measurable signal, as is the case for electrochemical studies of molecular receptors in artificial bilayer lipid membranes.

Natural chemoreception for processes such as neural communication operates using molecular receptors which transduce chemical signals into fast electrochemical events. The rapid response and extreme sensitivity of the gated electrochemical ion translocation provides some "ideal" analytical characteristics, however, for <u>in vitro</u> use this system is limited by background noise and the inability to discern between different agonists. Non-selective binding events and spontaneous ion current transients are filtered and discarded <u>in vivo</u> by processing signals from multiple receptor arrays with respect to frequency and amplitude in a manner analogous to the combination of hardware and software analysis of chemometric approaches[2,3]. This technology represents a horizon of research in the area of sensor development, and presently limits the analytical potential of biosensors based on lipid membrane electrochemistry. However, the application of a chemometric approach is presently possible when operating a biosensor in a fluorescence mode of transduction. The use

of fluorescence offers the opportunity for multidimensional analysis based on concurrent observations of intensity, wavelength, polarization and lifetime, as has been previously introduced for sensor applications by Bright[4], Heiftje[5], and Wolfbeis[6]. The combination of information associated with each of these properties can provide sufficient data for the unique identification of selective binding processes and quantitative evaluation of non-selective interferences[7].

The eventual goal of this research is the adaptation of a molecular receptor fluoroassay for incorporation into a reliable and self-calibrating generic optode which operates using a chemometric approach. The first step is to establish appropriate selective chemistry which can provide multidimensional fluorescence data. Selective interactions resulting in ion gating are common for neurotransmitter receptors, and apparently involve the opening of conductive "pores" or "channels" in the interior of large protein assemblies when binding of agonist occurs[1]. Little perturbation of the lipid environment is expected during gating events since large scale conformational changes of proteins have not been observed with "channel" opening, especially in the absence of an electrochemical gradient across the membrane. However, molecular receptors can have specific physical associations with lipids, and may be involved in aggregative events that are related to selective binding of ligands[8]. This may provide significant perturbation of the lipid membrane, and could provide a generic transduction mechanism which could be monitored by means of fluorescence from probes located within lipid membranes that support the receptor.

Fluorescence spectroscopy provides high sensitivity, requires only small amounts of fluorescent probe (on the order of 10^{-6} M) and causes little (if any) perturbation of lipid membrane environments at mole ratios of 1:100 or less. The main objective of using a fluorescent probe in lipid membranes is to garner information about the polarity, microviscosity and phase behaviour of the lipid environment. We were particularly interested in a probe to study both the steady-state and dynamic physical properties of bilayer lipid membranes. To this end, the probe 4-dicyanomethylene-1,2,3,4-tetrahydromethylquinoline (DCQ) was prepared (Fig. 1), and used to determine the polarity, fluidity and phase behavior of artificial membranes, which indicate how structural changes induced by selective binding events may be transduced[9].

Acetylcholine receptor (AChR) is the best characterized neurotransmitter receptor with respect to both structure and function. The protein is a dimer in a natural environment, where each monomer consists of five discrete protein subunits which together arrange to form a cylinder capable of ion conduction through lipid membranes[10]. It operates as a classical ion gating system, being stimulated by the natural agonist acetylcholine and by many other similar compounds[11]. This report further deals with an investigation of the multidimensional analytical responses derived form perturbations of the lipid membrane by the interactions of acetylcholine receptor with the agonist carbamylcholine and the antagonist α-bungarotoxin (α-BTX). Transduction of selective binding events is monitored by the fluorescence intensity and lifetime obtained from perturbations of the environment of a fluorophore which was either labelled to AChR-rich membranes or to the lipids of the membranes only. In all cases, the

fluorophore and receptor protein were located in bilayer lipid vesicles.

EXPERIMENTAL

Reagents

The fluorescent probe 4-dicyanomethylene-1,2,3,4-tetrahydromethylquinoline (DCQ) was prepared and purified from N-methyl-1,2,3,4-tetahydroquinoline (a gift from Professor I. W. J. Still of this department) and malononitrile according to published procedures[12]. Acetylcholine receptor (AChR) was obtained from Torpedo californica (Pacific Biomarine, Venice, CA) and purified according to standard methods[13-15]. Reconstitution was into soybean lecithin (Sigma Chemical Co., St. Louis, MO) in 10 mM sodium phosphate, pH 7.4, which was then stored as aliquots over liquid nitrogen. Activity of the stock receptor solution was determined by incubation with ^{125}I α-bungarotoxin (α-btx)(ICN Biomedicals Canada Ltd., Montreal, PQ, Canada) to be 1.3 μM in toxin sites[16]. Protein concentration was determined to be 0.3 mg.ml^{-1} as described elsewhere[17], yielding a specific activity of 4.3 nmole.mg^{-1} in toxin sites. The direct protein labelling used the fluorescent probe 4-[N-(iodoacetoxy)ethyl-N-methyl]amino-7-nitrobenz-2-oxa-1,3-diazole (IANBD) (Molecular Probes, Eugene, OR). Studies of fluorescence derived directly from lipid membranes was based on use of N-(7-nitrobenz-2-oxa-1,3-diazol-4-yl)dipalmitoyl-L-α-phospatidyl ethanolamine (NBD-PE) (Molecular Probes). Carbamylcholine was obtained form Sigma, and non-radioactive α-BTX from Miami Serpentarium (Salt Lake City, UT). Solvents were of the highest purity availability commercially and were further purified by standard procedures. All water used was purified first by reverse

osmosis then by a Millipore system (Milli-Q, Type I reagent grade water system), and had a specific resistivity of not less than 18 MΩ.cm . Dimyristoyl phosphatidyl choline (DMPC) was obtained from Avanti Polar Lipids and was used without further purification.

Apparatus

The absorption and emission spectra of DCQ were recorded with a Beckman DU-50 spectrophotometer and with a SLM 4800 spectrofluorimeter, respectively. The spectrofluorimeter used concave holographic monochromators of 2 nm/mm dispersion, and spectra were collected digitally using a 1 nm bandpass. A GG-21 standard block (Helma, Φ_f = 0.494) was used as a standard for relative quantum yield measurements. A thermostated sample holder was used, and temperature was monitored with a Fluke Model 80T-150 probe, which was immersed directly into the sample cell near the irradiation zone. Fluorescence decay times of DCQ were measured by the single-photon counting technique using PRA's system 2000 lifetime apparatus (London, ON, Canada). Fluorescence spectra from vesicles containing AChR were obtained using an in-house assembled fluorescence spectrometer consisting of: an atmospheric pressure nitrogen laser (Model LN 103, PRA) for excitation at 337.1 nm; a Bentham M300 monochromator with SMD 3B stepper motor controller (Optikon, Waterloo, ON, Canada); a Hamamatsu R928 photomultiplier tube (PMT) (Hamamatsu, Bridgewater, NJ) in a linearity-optimized housing (PRA) operated at -1250 V.; and a SR 250 Gated integrator/Boxcar averager (SRS, Stanford, CA) operated by an IBM PC through a SR 245 interface. A short length of optical cable placed in the laser output carried a small portion of the excitation pulse directly to a second photomultiplier tube for triggering of the

gated integrator. Signal collection was by integrating the PMT output for 30 nsec triggered at the beginning of emission. Ten pulses were averaged for each point.

Fluorescence lifetime measurements were obtained using the same in-house assembled fluorescence spectrometer as described above. In this case, the PMT was connected to a LeCroy model 9400 digital storage oscilloscope (DSO)(LeCroy, Chestnut Ridge, NY) using a 50 Ohm input impedance and random interleaved sampling to provide 5 gigasamples.sec^{-1}. The DSO and the monochromator driver were controlled via an IEEE-488 interface by an IBM-PC. The fast pulse of the nitrogen laser (300 ps) allowed for time-resolved emission decay profiles to be obtained from the fluorescent samples.

The data were read as integer values for intensity from the DSO for each bin or time value. This prohibited the standard Poisson weighting used in photon-counting systems. To obtain a measurement of the variance of the data, several values were obtained for each bin and a simple standard deviation was calculated. This value was used in place of the root-of-count value as a weighting parameter. Deconvolution of lifetimes was used an iterative fit, with the weighted least-squares to evaluate "goodness" of the fit. An instrument response ('lamp') function was obtained by sampling the laser pulse scattered from a non-fluorescent solution. Each iteration involved trapezoidal convolution of the exponential model being tested over the instrument response to obtain a fitted curve which could be compared to the observed curve. Fit optimization by Chi-square and least-square minimization was evaluated, with the least-square parameter yielding much better success in achieving convergence of the

fit, especially for noisy data.

Final evaluation was made by observing the autocorrelation function. The general inability to achieve a truly flat autocorrelation suggested a poor instrument response function, indicating that a better profile might be obtained from a the emission of a standard solution at a wavelength more closely associated with the sample emission.

Procedures

Vesicles containing the phospholipid DMPC and DCQ (molar ratio of 250:1 or less) in 15 mM Tris buffer, pH 7.4 were prepared by sonication by a Model VC250 Sonicator (Sonics and Materials, Inc., Dunbury, CT) set at 40 W and fitted with a microtip. Sonication continued for 30 min at 5-10°C above the lipid phase transition temperature. All sonicated solutions were centrifuged (27000 g for 30 min.) to remove insoluble materials. The correction factor for the emission monochromator and phototube of the SLM 4800 was obtained using quantum counters (solutions of 10^{-4} M of quinine sulphate and 2 x 10^{-4} M of 3-amino-phthalimide in 1 N H_2SO_4)[18]. The fluorescence emission was monitored at right angles with respect to excitation light. Fluorescence decay curves of DCQ were analyzed over at least a 100-fold range of intensity by the method of iterative deconvolution as previously described[19].

Receptor solution containing AChR and 2 mol% NBD-PE was prepared by addition of the NBD-PE during the reconstitution stage of the AChR purification. The appropriate amount of NBD-PE was added to affinity-purified receptor in 2% sodium cholate detergent before dialysis. The sample was centrifuged at 10,900 x g for 15 min. to remove residual

NBD-PE solid. IANBD labelling of the AChR was done according to previous methods[20]. IANBD was added in excess as a solid and the solution was stirred on ice and in the dark for two hours. Controls of soybean lecithin and soybean lecithin/bovine serum albumin (BSA) were prepared identically to the AChR/NBD-PE sample. Dry lecithin was suspended as vesicles by evaporation from chloroform followed by addition of 10 mM sodium phosphate, pH 7.4 and sonication for 2 hours with a probe-tip sonicator. Reagents such as carbamylcholine were added directly to the 1-cm path length quartz cuvettes used in the spectrofluorimeter. All spectral work with AChR was done at room temperature (21 ∓ 1°C). "Poisoning" of the receptor was accomplished by pre-incubation with a minimum three-fold excess of α-BTX for at least 2 hours over ice.

RESULTS AND DISCUSSION

Wavelength and intensity analysis of labelled AChR

The IANBD labelling of the AChR vesicle system was first done in an attempt to reproduce the fluorescence enhancement experiment of Dunn and Raftery[20], and to establish a chemically selective system for investigation of multidimensional analytical characterization. The IANBD labelling of the AChR was by addition of the solid, water insoluble fluorophore to the crude receptor preparation in aqueous solution. The crude preparation contained protein-rich membranes, isolated from bulk tissue by homogenization and centrifugation. The greater solubility of the IANBD in the hydrophobic portion of lipid membranes relative to aqueous solution supports the assumption that most of the probe reaction occurred in the membrane environment. While many reactions are possible, three predominant labelling schemes

are outlined in Fig. 2, depicting covalent fluorophore attachment to nucleophilic sites on protein, the membrane phospholipids and water.

The fluorescence spectrum obtained from the ANBD labelled system (Fig. 2) revealed a broad peak centered at 570 nm. Enhancement was measured as the increase in peak area observed on addition of the agonist carbamylcholine (carb), which is commonly used to generate an ion-gated response from AChR. An asymmetric increase in intensity, favouring the shorter wavelengths, was observed on addition of carbamylcholine and provided an opportunity for application of a multidimensional approach based on wavelength dependence. Peak areas were obtained from the spectra either by integration of the entire peak (500nm to 650nm), by integration of the shorter wavelength component (500nm to 550nm) or by calculation of the ratio of the areas of the shorter and longer wavelength components (500nm to 550nm / 550nm to 650nm). A plot of relative intensity enhancement versus concentration is shown in Fig. 3 where methods of presenting the increase are indicated. The curves indicating enhancement of total intensity represent the integrated areas of the entire peak. This is equivalent to representations of total intensity without spectral information, such as when using filters placed before a detector. The curves indicating enhancement of the shorter wavelength region of the peak represent the integrated area from 500 nm to 550 nm. These results show a much higher percentage of enhancement, and represent an advantage of the sensitivity available through selective spectral analysis. The intensity enhancement curves show poor reproducibility between trials using the same receptor preparation. The inconsistancy in apparent enhancement could be due to many factors, including

changes in the amount and fluorescent yield of fluorophore due to sample inhomogeneity, and variability in biological activity of the receptor from one sample to the next. Other factors, such as instability in the laser source (typical of the nitrogen laser employed) and drift in the photomultiplier, are also possible. The curves in Fig. 4 indicating the enhancement of a ratio value represent the ratio of peak area from 500 nm to 550 nm to the area from 550 nm to 650 nm. This measurement results in much greater reproducibility between samples. The long wavelength side, which contains a constant component, acts as an internal calibration for the system, compensating for the possible variations in intensity mentioned above. To confirm that the observed enhancement was due to the selective response of active receptor, AChR was pre-incubated with the antagonist α-BTX, a highly selective blocker of AChR activity. No fluorescence enhancement was observed for incubated samples. Furthermore, fluorescence enhancement was not observed on the addition of carbamylcholine to ANBD labelled soybean lecithin vesicles without AChR, confirming that the enhancement was due to receptor-agonist interaction.

Wavelength and intensity analysis from pure DMPC vesicles using DCQ

The use of fluorescent lipid membranes as generic transducers necessitates the detection of alterations within membranes that are induced by selective receptor-ligand binding and involves observation of wavelength, intensity and lifetime data. DCQ is a fluorescent probe which is extremely sensitive to its environment, and provides an example of the potential of fluorescence spectroscopy for observing structural alterations within lipid membranes (in the case of DCQ, by

temperature variations[9]). Solubilization of DCQ in DMPC vesicles is manifested through the appearance of an orange tint and an increase in fluorescence quantum yield and decay time as compared to DCQ alone. The fluorescence spectrum of DCQ in vesicles is similar to that in homogeneous solvents and is insensitive to changes in temperature between 10 and 60°C. The absorption and emission spectra of DCQ in DMPC vesicles are shown in Fig. 5. The position of the long wavelength absorption band at 310 nm is sensitive to solvent polarity and shifts to longer wavelengths with increasing solvent polarity. This band is the result of an intra-molecular charge-transfer process originating from the electron lone pair of the amine nitrogen and terminating on the π^* state of the cyano group.

The emission spectrum of DCQ is also highly dependent on solvent polarity and shifts to longer wavelengths with increasing solvent polarity[9]. This is consistent with the assignment of the $S_0 \rightarrow S_1$ transition as an intra-molecular charge-transfer transition. DCQ emits with low to moderate efficiency, depending on solvent polarity and viscosity. Both fluorescence quantum yield (ϕ_f) and single-exponential decay time (τ_f) increase with increasing solvent polarity and viscosity. In addition to the transitions observed in homogeneous solution, an additional absorption band centered around 415 nm appears in vesicular systems. The origin of this transition is not clear. However, it may be due to interactions between the ground state of DCQ and the charged head group of the lipid (i.e., an intermolecular charge-transfer transition). The fact that the probe is located in the head group region of the membrane is also evident from the effect of variation of pH on the absorption spectrum of DCQ[9]. An increase or decrease of proton concentration in the bulk solution could produce

changes in the head group structure or potential, leading to the observed variation in intensities of various transitions. The radiative rate constant (k_r) is relatively insensitive to viscosity and polarity, and variation in Φ_f and τ_f is due to sensitivity of the non-radiative rate constant (k_{nr}) to these parameters. The solvent induced shift of the emission spectrum, and the emission yield and decay time dependence on the solvent indicate that DCQ can be exploited to study the physical properties of lipid membranes[9]. Low values of fluorescence quantum yield and decay time of DCQ in non-viscous, non-polar hydrocarbon solvents is attributed to very fast non-radiative deactivation of the S_1 state due to trans ⇔ cis photoisomerization about the ethylenic double bond. Increasing viscosity (or rigidity) and polarity increases the barrier to rotation, and thus increases the probability of emission at the expense of non-radiative deactivation. Decreasing temperature also increases both fluorescence quantum yield and decay time. Assuming that k_{nr} is the only thermally activated process, it can be expressed in terms of an Arrhenius equation:

$$k_{nr} = A \exp(-E_a/RT) \qquad (1)$$

where E_a is an apparent activation energy, representing all processes contributing to the prevention of rotation about the double bond. Combining equation (1) with the familiar relation (2) leads to (3):

$$\Phi_f = \frac{k_r}{k_r + k_{nr}} \qquad (2)$$

$$\frac{1}{\Phi_f} - 1 = \frac{A}{k_r} \exp(-E_a/RT) \qquad (3)$$

Thus a change in temperature will result in a linear relationship between ln $((1/\Phi_f) - 1)$ and T^{-1}, to the extent that there is a linear relation between ln (η) and T^{-1} [10], (where η is the viscosity). Thermally induced phase transitions in lipid bilayers affects the molecular mobility of lipids. This should affect the emission quantum yield of the probe, and graphs of ln $((1/\Phi_f) - 1)$ vs T^{-1} changes of Φ_f with temperature in DMPC are shown in Fig. 6. A distinct break point is observed near 22.75°C for the DMPC results. This is in agreement with the phase transition temperature of DMPC when in a multilamellar form (23.9°C)[21].

Wavelength and intensity analysis: application to AChR in fluorescent vesicles

The desirability of a generic strategy for transduction of receptor-ligand complexation and recent investigations of the role of membrane lipid components in the function of AChR led us to propose that a fluorescent lipid component could participate in the fluorescence enhancement mechanism. The use of DCQ in pure DMPC vesicles indicated that structural changes within lipid membranes could be monitored with a fluorescent probe located in the headgroup region. However the use of DCQ in practical experiments is limited since it partitions into lipid membranes from bulk solution and is not permanently located in the membrane (i.e. is extractable). One form of fluorescent probe which has been extensively used in lipid membrane studies is fluorescently labelled lipid, which incorporates into the membrane in a relatively irreversible manner. The label is placed on the terminus of the lipid headgroup so that it remains external to the acyl chain region of the membrane. This helps to limit structural

perturbations caused by the presence of the probe. The NBD-PE probe has been used to study phase domain structure in membrane systems by classical spectrofluorometric measurements such as enhancement/self-quenching[22] and by the relatively new technique of fluorescence microscopic imaging of lipid monolayers at an air-water interface[23]. Both techniques are possible as a result of the natural tendency of the NBD-PE molecules to partition between phases in a mixed phase system such that they concentrate in the less ordered domains. When in locally concentrated regions, the NBD moieties will "self-quench", causing a reduction in the overall measured intensity. Any changes in the relative areas of phase structure types will thus result in a change in the overall intensity. Such changes may be proposed for the system under study as the NBD-PE probe has been shown to indicate perturbation of lipid phase structure by incorporated proteins[24], and recently in our laboratory by the presence of AChR[25].

To investigate the response of a system containing fluorescently-labelled lipid only, preparations were made by including fluorescent lipid in the exogenous lipid added to AChR in detergent phase before reconstitution into vesicles. Fluorescence enhancement was observed on agonist addition, as shown in Fig. 7. A simplified approach to quantitation used a linear approximation of the first few data points for curves as shown in Fig. 7. A linear fit yielded a sensitivity of $40\%.\mu M^{-1}$ carbamylcholine and a limit of detection of 300 nM over a dynamic range of 3 uM with a correlation coefficient of 0.978 for the most sensitive systems studied in this work[26]. In addition, it was observed that the fluorescence signal was enhanced by the initial addition of α-BTX at very low concentrations (40% enhancement at 10 nM). This indicated an antagonist-associated conformational change

which may or may not be similar to the change observed for agonist addition, but which may also permit antagonist detection. Selectivity was demonstrated in this system by the elimination of the agonist response after pre-incubation with α-BTX. To further confirm receptor mediation of the enhancement, controls were performed using pure lipid vesicles, vesicles with other protein (bovine serum albumin) and vesicles containing degraded (by extensive sonication) AChR. All of these controls yielded no fluorescence enhancement.

Fluorescence lifetime analysis for DCQ in pure DMPC vesicles

The use of steady-state properties of a probe in lipid membranes such as fluorescence intensity is based on the assumption of the homogeneity of the environment of the probe. However, bilayers are known to be inhomogeneous[27]. We have therefore investigated the decay dynamics of DCQ in DMPC for a limited range of temperatures. Figure 8 shows a typical decay curve of DCQ in DMPC vesicles. The decay is clearly non-exponential and can be best described by a double exponential function.

$$I(t) = \alpha_1 \exp(-t/\tau_1) + \alpha_2 \exp(-t/\tau_2) \qquad \{5\}$$

where τ_1 and τ_2 are the decay times and α_1 and α_2 are the pre-exponential factors. Also shown in Fig. 8 is the calculated decay curve, the weighted residual for each decay channel and the auto-correlation function of the residuals. The decay is well described by a double exponential function as can be judged from the weighted residuals and their auto-correlation function. It is not possible to assign any physical significance to the two individual decay components at this time, and further investigations are required if lipid membrane structural significance is to be assigned to the decay

heterogeneities.

The alteration of quantum yield with the phase structure of DMPC does not indicate that significant changes in the ratios of the pre-exponential factors or the two lifetimes occurs. The pre-exponential factors and lifetimes can be treated as a further set of analytical data channels suitable for transduction. Figure 9 shows the lifetime and pre-exponential data as a function of temperature for an excitation wavelength of 360 nm and emission collected at 570 nm. The two lifetime components show a trend of reduction with increasing temperature from 16 to 26°C, as would be expected if molecular mobility were a primary factor governing lifetime. There is no clearly defined inflection for either of the two lifetime components which would provide evidence for a phase transition in the range of 20 to 24°C. This would indicate that the location and orientation of the probe does not dramatically alter as a function of the phase transition, and presumably the probe remains in the headgroup region of the lipid membrane. The relative contributions to the fluorescence intensity given by the magnitudes of the pre-exponential factors does not clearly identify the structural transition at 20 to 24°C since they tend to alter linearly over a wide temperature range. It is interesting to note that the relative contributions from the two lifetime components as determined by the pre-exponential factors reverses in the temperature range of 20 to 24°C. The general trends observed in Fig. 9 appear again in Fig. 10, where the lifetime and pre-exponential factors due to excitation at a wavelength of 555 nm are plotted across the entire emission range. In this case, however, the reversal of the contributions of the two lifetime components to

the intensity is sharply defined in the temperature range of 21 to 24°C. Excitation at a longer wavelength would alter the excited state dipole moment of DCQ, and, as seen, varies the sensitivity of the probe to environmental interactions.

Examination of the data shown in Fig. 9 indicates that τ_1, τ_2 and α_1 all show a relatively constant decrease as the temperature range increases from 17 to 26°C. The magnitude of α_2 shows a large and relatively constant increase over the same temperature span. For quantitative analysis, an average lifetime is calculated by:

$$\langle\tau\rangle = \Sigma\, \alpha_i\tau_i^2 \,/\Sigma a_i\tau_i \qquad \{6\}$$

Variation of $\langle\tau\rangle$ with temperature is shown in Fig. 11. There is a break point near 21 ± 1°C in the plot of $\ln(1/\langle\tau\rangle)$ vs T^{-1} in DMPC which agrees with expected phase transition temperature.

Fluorescence lifetime analysis: application to AChR in fluorescent vesicles

Analysis of the fluorescence lifetime data obtained from NBD-PE in lipid vesicles containing AChR indicated that the decay could be best described by a double exponential function. No physical interpretation of the origin of the two lifetime components can be assigned at this time. The dependences of the lifetimes and their relative pre-exponential factors on the wavelength used to study the emission process are shown in Figs. 12 and 13 for the selective interaction of α-BTX with AChR in lipid vesicles. The discrete lifetime components of Figs. 12 and 13, and the average lifetimes compiled in Table 1 do not show significant dependence on the selective binding event. Substantial variations of the relative pre-exponential factor distribution (and absolute magnitude as shown in

Fig. 14) are observed. Considering equation 2 and the following relationship:

$$\tau_f = \frac{1}{k_r + k_{nr}} \qquad (7)$$

it would seem that a relative increase in k_r and an equivalent decrease in k_{nr} could cause the fluorescence enhancement with invariant lifetime. A speculative mechanism for the enhancement would involve an average fluidity increase caused by the selective interaction due to aggregative events of the protein. A general increase in the fluid phase at constant surface pressure would imply that little structural alteration of the environment of the probe would occur, but would result in a general fluorescence enhancement.

The fluorescence enhancement is observed for AChR interaction with carbamylcholine, but with substantially less sensitivity than for the interaction with α-BTX. Table 2 provides an indication of the utility of the lifetime analysis, showing that the first discrete lifetime is affected by the interaction of carbamylcholine, while the other three second lifetime parameters remain invariant. Consideration of the absolute magnitude of the pre-exponential factors again shows the enhancement effect. This is a different response than that caused by interaction with α-BTX, and can be used to distinguish between the agonist and antagonist.

CONCLUSIONS

The results of this work indicate a fluorescent lipid membrane may be a generic transducer of selective binding interactions of proteins that can be embedded within lipid matrices. The fluorescence signal may be acquired in both wavelength and time domains, which can

be used to discriminate between different structural alterations induced in lipid membranes by selective interactions of different types. The origin of the fluorescence enhancement effects caused by AChR binding with carbamylcholine and α-BTX are not clear, and further studies using the technique of fluorescence microscopy are being done to directly observe structural alterations which may be caused by the binding events[23]. Three-dimensional plots using wavelength, intensity and lifetime may assist in the interpretation of the mechanism of signal generation, and may provide unique mathematical surfaces for qualitative and quantitative studies of selective and non-selective interactions of AChR in lipid membranes.

Acknowledgements

We thank the Natural Sciences and Engineering Research Council of Canada, the Ontario Ministry of the Environment, the Canadian Defense Research Establishment and Imperial Oil Limited for financial support of this work. We are indebted to Dr. A. Safarzadeh-Amiri for technical assistance with the studies of DCQ.

REFERENCES

1. B. Hille, Ionic Channels of Excitable Membranes, Sinauer Associates, Sunderland, Massachusetts, 1984.
2. P.P.C. Graziadei, in The Ultrastructure of Sensory Organs, I. Friedman (ed.), Ch. 4, Elsevier, New York, 1984.
3. M. Thompson, W.H. Dorn, U.J. Krull, J.S. Tauskela, E.T. Vandenberg and H.E. Wong, Anal. Chim. Acta, 1986, **180**, 251.
4. F.V. Bright, Anal. Chem., 1988, **60**, 1622.
5. W.A. Wyatt, G.E. Poirier, F.V. Bright and G.M. Helftje, Anal. Chem., 1987, **59**, 572.

6. M.J.P. Leiner, M.R. Hubmann and O.S. Wolfbeis, Anal. Chim. Acta, 1987, **198**, 13.

7. U.J. Krull, R.. Brown, R.F. DeBono and B.D. Hougham, Talanta, 1988, **35**, 129.

8. J.L. Tedesco, U.J. Krull and M. Thompson, Biosensors, in press.

9. A. Safarzadeh-Amiri, M. Thompson and U.J. Krull, J. Photochem. Photobiol., in press.

10. J.-P. Changeux, A. Devillers-Thiery and P. Chemouilli, Science, 1984, **225**, 1335.

11. F.B. Abramson, R.B. Barlow, M.G. Mustafa and R.P. Stephenson, Br. J. Pharmac., 1969, **37**, 207.

12. P.I. Ittyerah and F.G. Mann, J. Chem. Soc., 1956, 3179.

13. A. Sobel, M. Weber and J.-P. Changeux, Eur. J. Biochem., 1977, **80**, 215.

14. S. Porter and S.C. Froehner, J. Biol. Chem, 1983, **258**, 10034.

15. J. Lindstrom, R. Anholt, B. Einarson, A. Engel, M. Osame and M. Montal, J. Biol. Chem., 1980, **255**, 8340.

16. R.A. Kohanski, J.P. Andrews, P. Wins, M.E. Eldefrawi and G.P. Hess, Anal. Biochem., 1977, **80**, 531.

17. M.A.K. Markwell, S.M. Haas, N.E. Tolbert and L.L. Bieber, Meth. Enzymol., 1981, **72**, 296.

18. W.H. Melhuish, in Accuracy in Spectroscopy and Luminescence Measurements, R. Mavrodineanu, J.I. Schultz and O. Menis (eds.), pp. 135-150, N.B.S., Washington, D.C., 1973.

19. D.A. Holden, K. Jordan and A. Safarzadeh-Amiri, Macromolecules, 1986, **19**, 895.

20. S.M.J. Dunn and M.A. Raftery, Proc. Natl. Acad. Sci., U.S.A.,

1982, **79**, 6757.

21. S. Mabrey and J.M. Sturtevant, in Methods in Membrane Biology, E.D. Korn (ed.), Vol. 6, pp. 237-269, Plenum Press, New York, 1978.

22. A.E. McGrath, C.G. Morgan and G.K. Radda, Biochim. Biophys. Acta, 1976, **426**, 173.

23. W.M. Heckl, Laterale Organisation von Lipidmonoschichten bei Einbau von amphiphilen Fremdstoffen und Proteinen, Ph.D. Thesis, Department of Physics, Technical University of Munich, 1988.

24. W.M. Heckl, M. Losche, H. Scheer and H. Mohwald, Biochim. Biophys. Acta, 1985, **810**, 73.

25. U.J. Krull, J.D. Brennan, R.S. Brown and E.T. Vandenberg, Proc. SPIE - Int. Soc. Opt. Eng., Vol. 1067, 1989, in press.

26. U.J. Krull, R.S. Brown, K. Dyne, B.D. Hougham and E.T. Vandenberg, in Chemical Sensors and Microinstrumentation, R. Murray (ed.), American Chemical Society Symposium Series, 1989, in press.

27. L. Davenport, J.R. Knutson and L. Brand, Faraday Discuss., 1986, **81**, 81.

TABLES

Table 1. Average lifetime parameters from NBD-PE in lipid vesicles for interaction of 1 μM α-BTX with AChR at various wavelengths of emission

wavelength (nm)	$\langle\tau\rangle$ prior to α-BTX addition (ns)	$\langle\tau\rangle$ after α-BTX addition (ns)
510	2.66	2.48
520	3.44	3.54
530	3.97	3.99
540	4.54	4.45
550	4.82	4.50
560	4.19	4.13
570	3.69	3.85

Table 2. Lifetime parameters from NBD-PE in lipid vesicles for interaction of 100 μM carbamylcholine (carb) and AChR with λ_{em} at 540 nm

	α_1(rel)	α_1(abs)	τ_1(ns)	α_2(rel)	α_2(abs)	τ_2(ns)	$\langle\tau\rangle$
initial	0.79	38	0.9	0.22	12	7.4	5.63
+ carb	0.82	97	0.5	0.18	23	7.3	5.94

Maximum error for values quoted ∓ 10% ; χ^2 approximately 1.5

FIGURE CAPTIONS

Fig. 1. Structure of the fluorescent probe 4-dicyanomethylene-1,2,3,4-tetrahydromethylquinoline (DCQ)

Fig. 2. Major chemical products resulting from the use of IANBD in the labelling of crudely purified AChR.

Fig. 3. Concentration-response curves showing relative fluorescence intensity enhancement for AChR interaction with carbamylcholine using integrated response calculated from three different wavelength windows (two experiments demonstrating irreproducibility shown for each window); (◇,□) 500 to 550 nm, and (△,+) 500 to 650 nm.

Fig. 4. Concentration-response curves showing reproducibility of relative fluorescence intensity enhancement derived form data shown in Fig. 3. The variability between experiments is largely eliminated by dividing the results from the 500 to 550 nm wavelength window by the results from the 500 to 650 nm wavelength window.

Fig. 5. The absorption and emission spectra of DCQ in DMPC vesicles.

Fig. 6. Variation of fluorescence quantum yield of DCQ in DMPC vesicles with temperature.

Fig. 7. Concentration-response curve for AChR interaction with carbamylcholine as determined by fluorescence intensity enhancement from lipid vesicles containing 2 mole% NBD-PE. Enhancement was measured for a wavelength window of 500 to 650 nm; A - response curve, B - control in absence of AChR.

Fig. 8. A typical fluorescence decay curve of DCQ in DMPC at 21.5°C. Excitation was at 555 nm and emission was collected across

all wavelengths. A double exponential fit provided lifetimes of 2.12 and 3.78 ns. The points are experimental data and the solid curve is calculated. Also shown are the weighted residuals and their autocorrelation function. The χ^2 value was 1.45.

Fig. 9. Variations of the two lifetime components and the associated relative pre-exponential factors ($\alpha_1 + \alpha_2 = 1$) for DCQ in DMPC at various temperatures. Excitation was at 360 nm and emission was collected at 570 nm. The maximum error was ±10% and the χ^2 value was between 1.2 to 1.5 for all results. τ_1 - ●, α_1 - ■ , τ_2 - o, α_2 - □ .

Fig. 10. Temperature dependence of the lifetime components and pre-exponential factors of DCQ in DMPC as described in Fig.9. Excitation was at 555 nm and emission was collected across all wavelengths.

Fig. 11. Temperature-dependent variation of average fluorescence decay of DCQ in DMPC.

Fig. 12. Variations of the first lifetime components and the associated relative pre-exponential factor ($\alpha_1 + \alpha_2 = 1$) of NDB-PE in soybean lecithin vesicles containing AChR due to the introduction of 1 μM α-BTX. Before toxin addition : τ_1 - ●, α_1 - ■ . After toxin addition : τ_1 - o, α_1 - □.

Fig. 13. Variations of the second lifetime components and the associated relative pre-exponential factor of NDB-PE in soybean lecithin vesicles containing AChR due to the introduction of 1 μM α-BTX. Before toxin addition : τ_1 - ●, α_1 - ■ . After toxin addition : τ_1 - o, α_1 - □ .

Fig. 14. Variations of the pre-exponential factors as absolute quantities (ie. not normalized to $\alpha_1 + \alpha_2 = 1$) for NBD-PE in soybean lecithin vesicles containing AChR due to the introduction of 1 μM α-BTX. Before toxin addition : α_1 - ●, α_2 - ■ . After toxin addition : α_1 - ○, α_2 - □ .

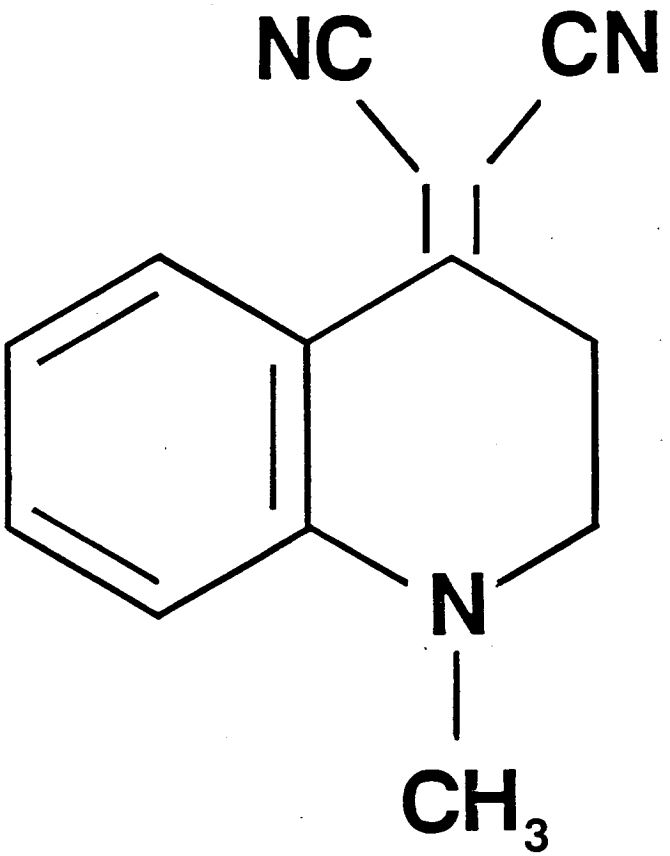

Fig 1

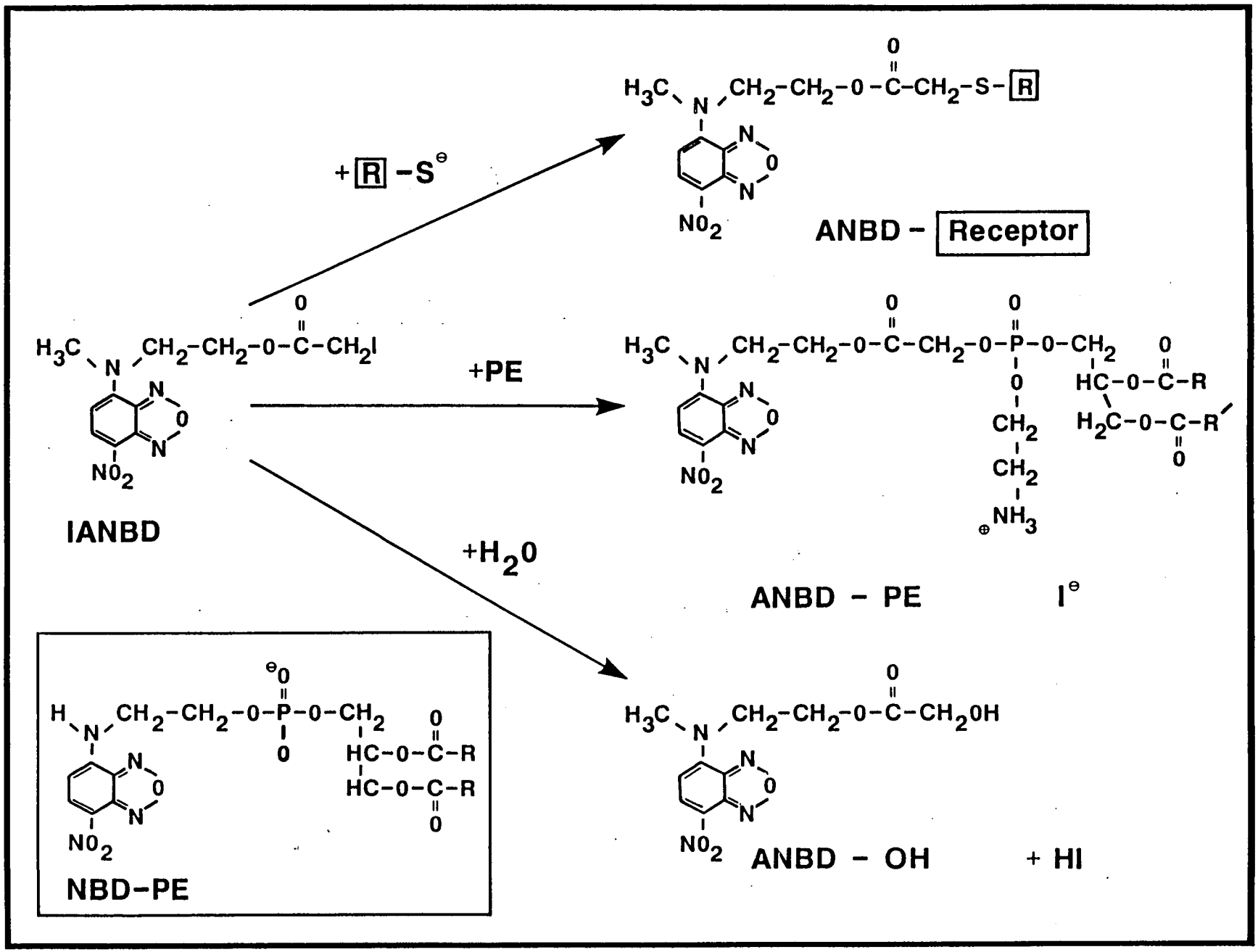

Fig 2

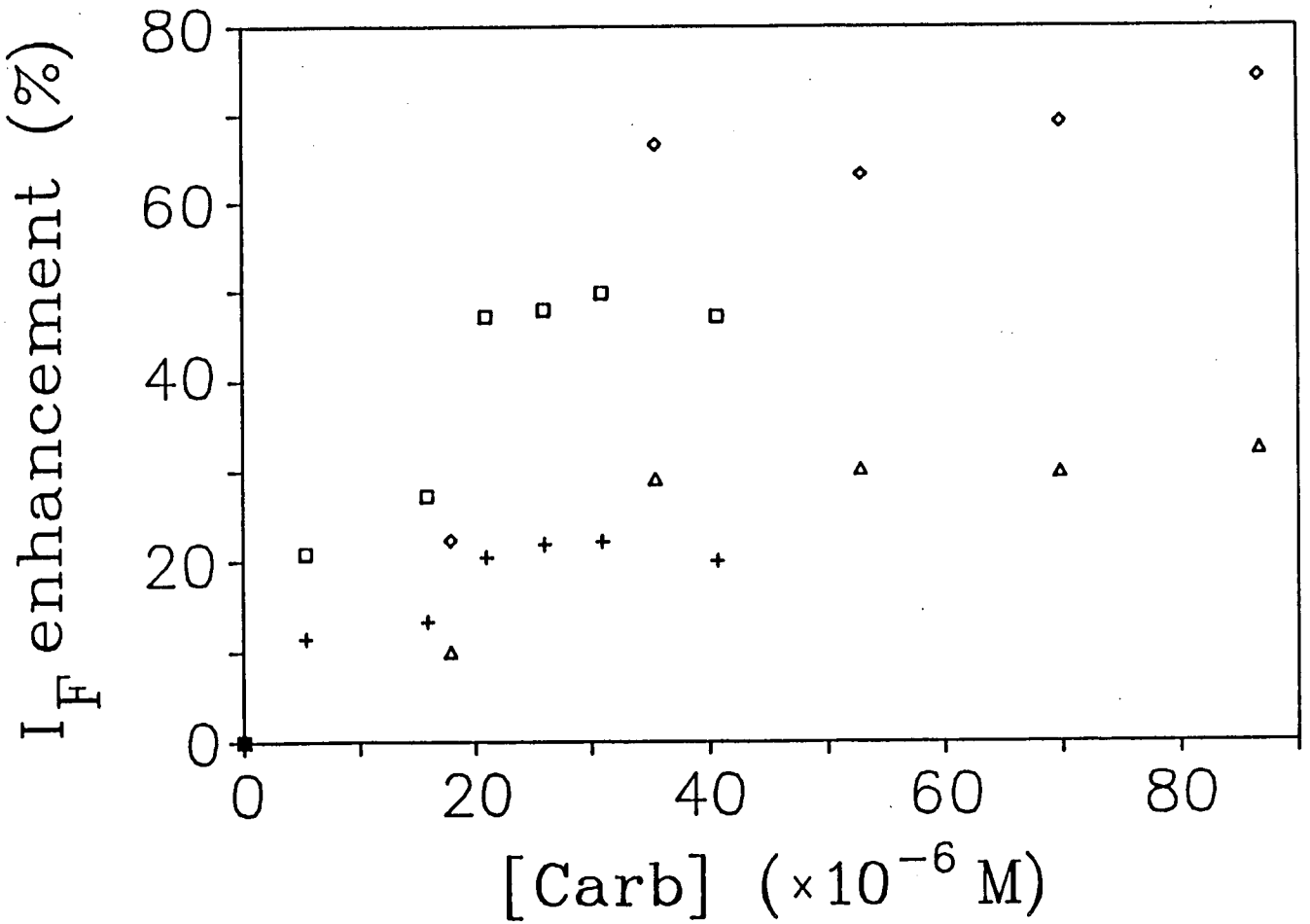

Fig 3

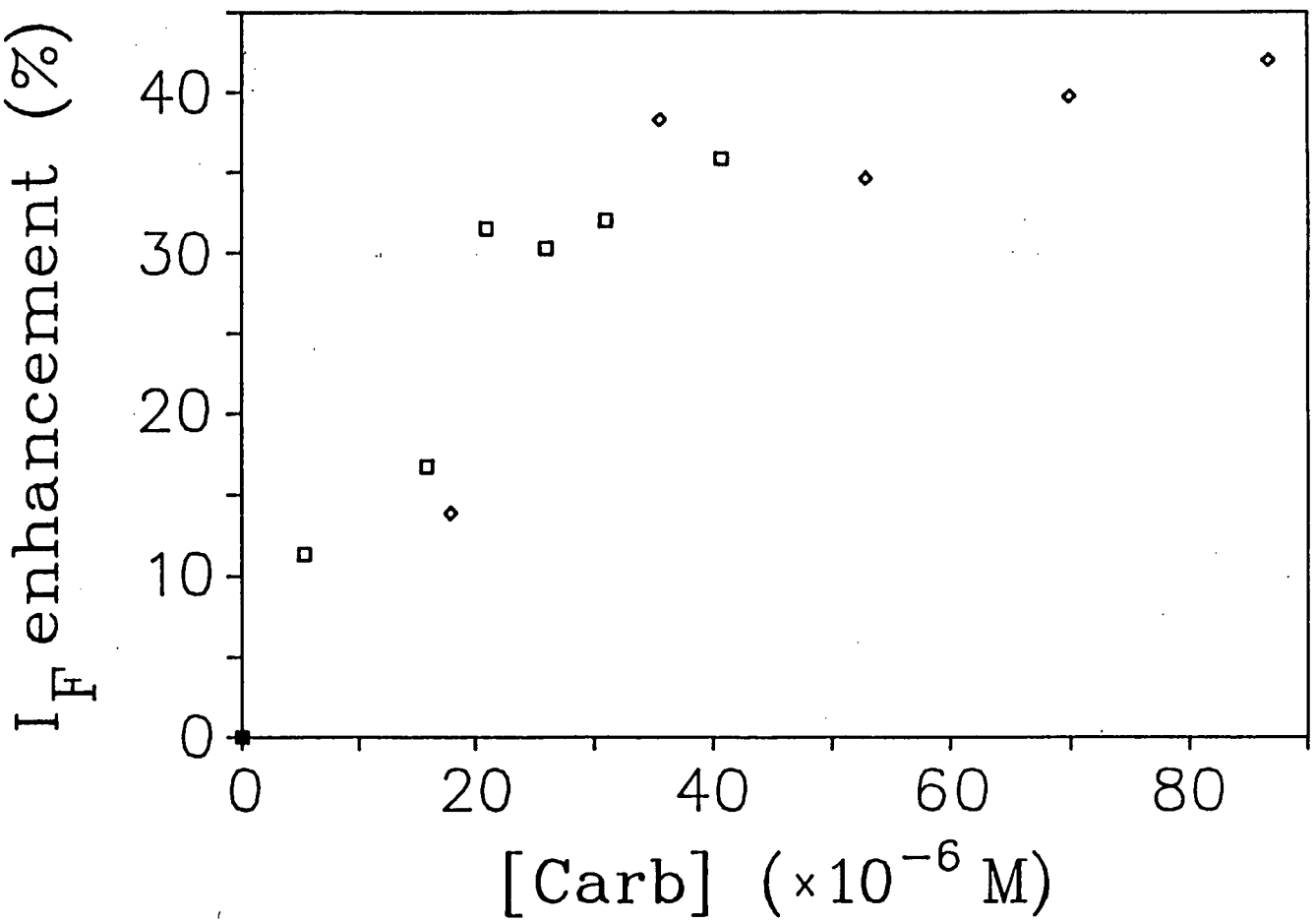

Fig 4

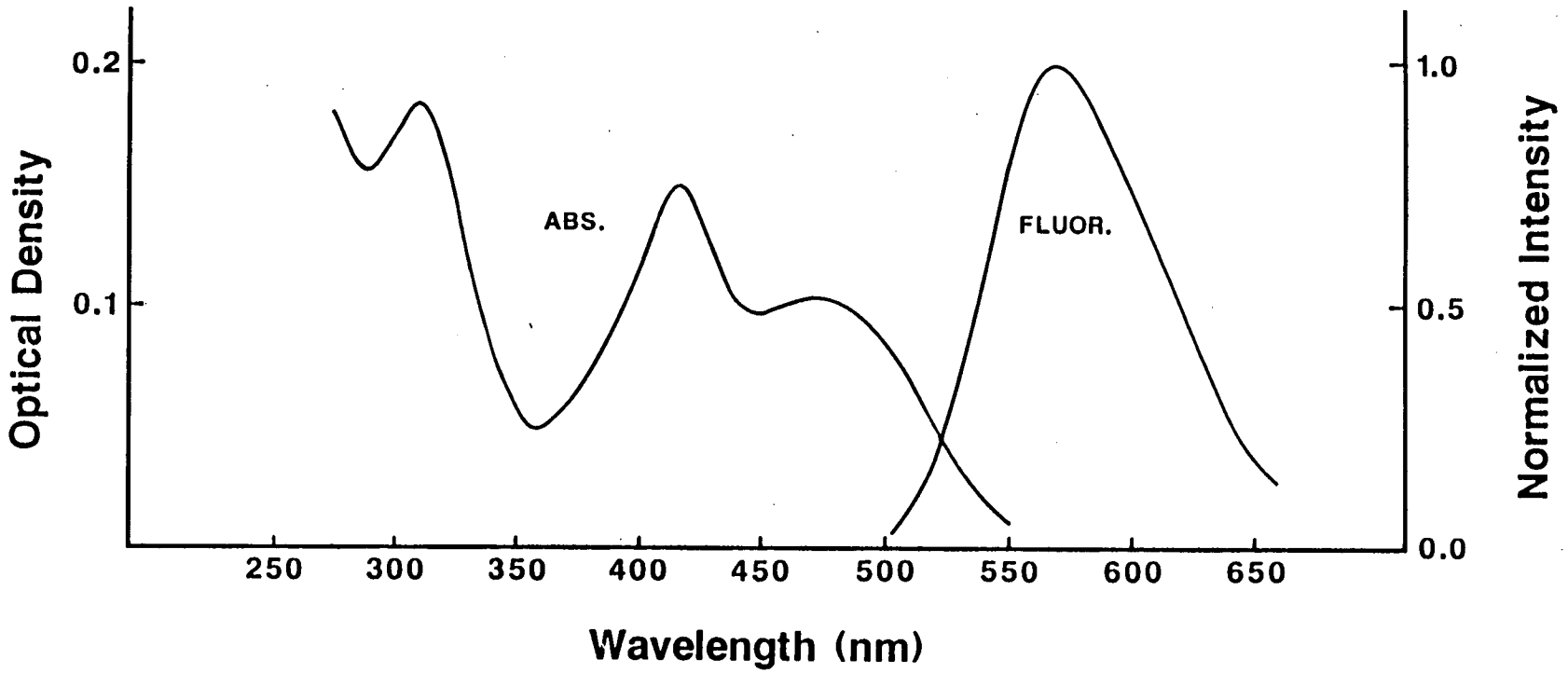
Optical Density
0.2
0.1
ABS.
FLUOR.
1.0
0.5
0.0
Normalized Intensity
250
300
350
400
450
500
550
600
650
Wavelength (nm)

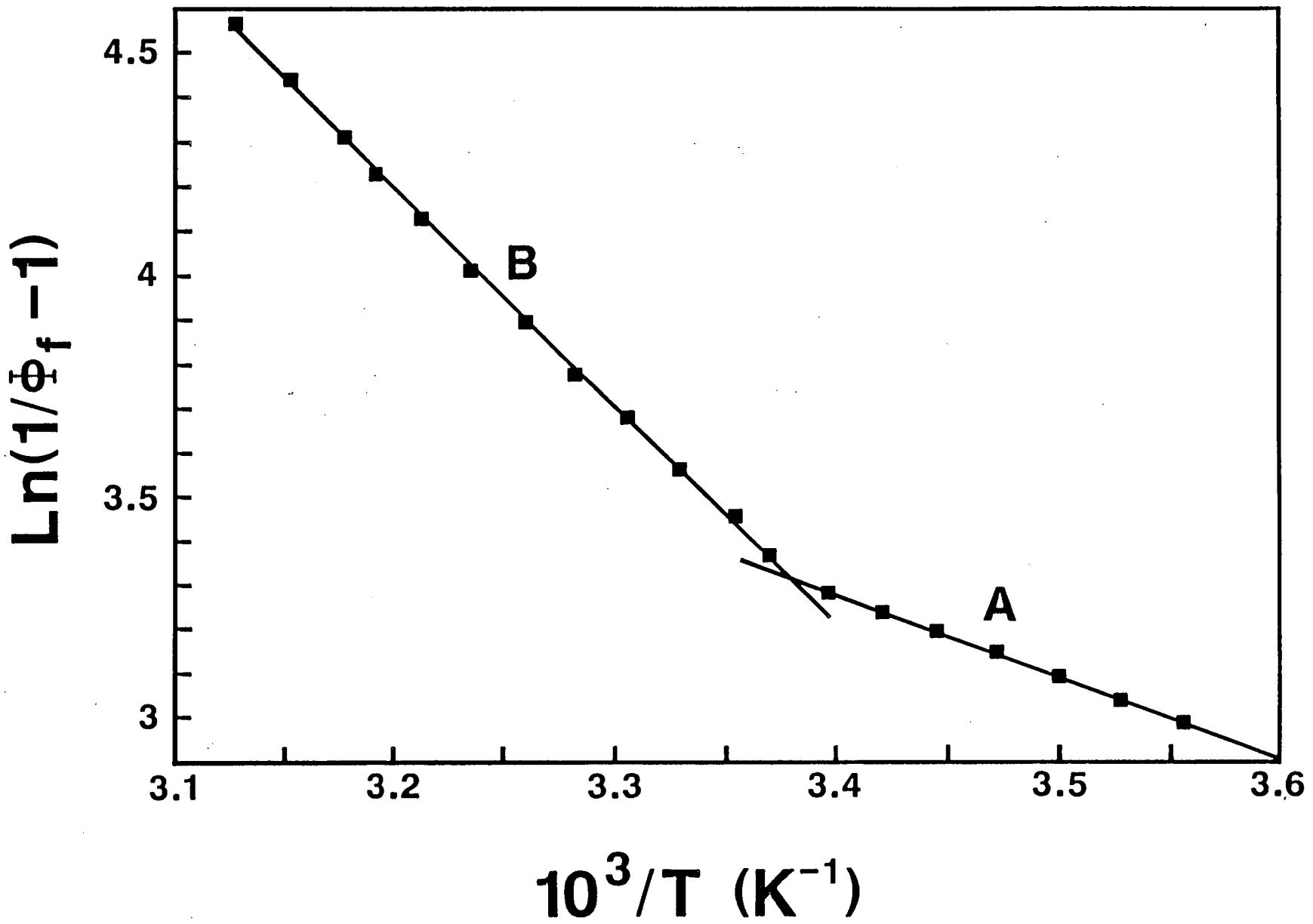
4.5
4
3.5
3
3.1
3.2
3.3
3.4
3.5
3.6
B
A
Ln(1/Φf −1)
10³/T (K⁻¹)

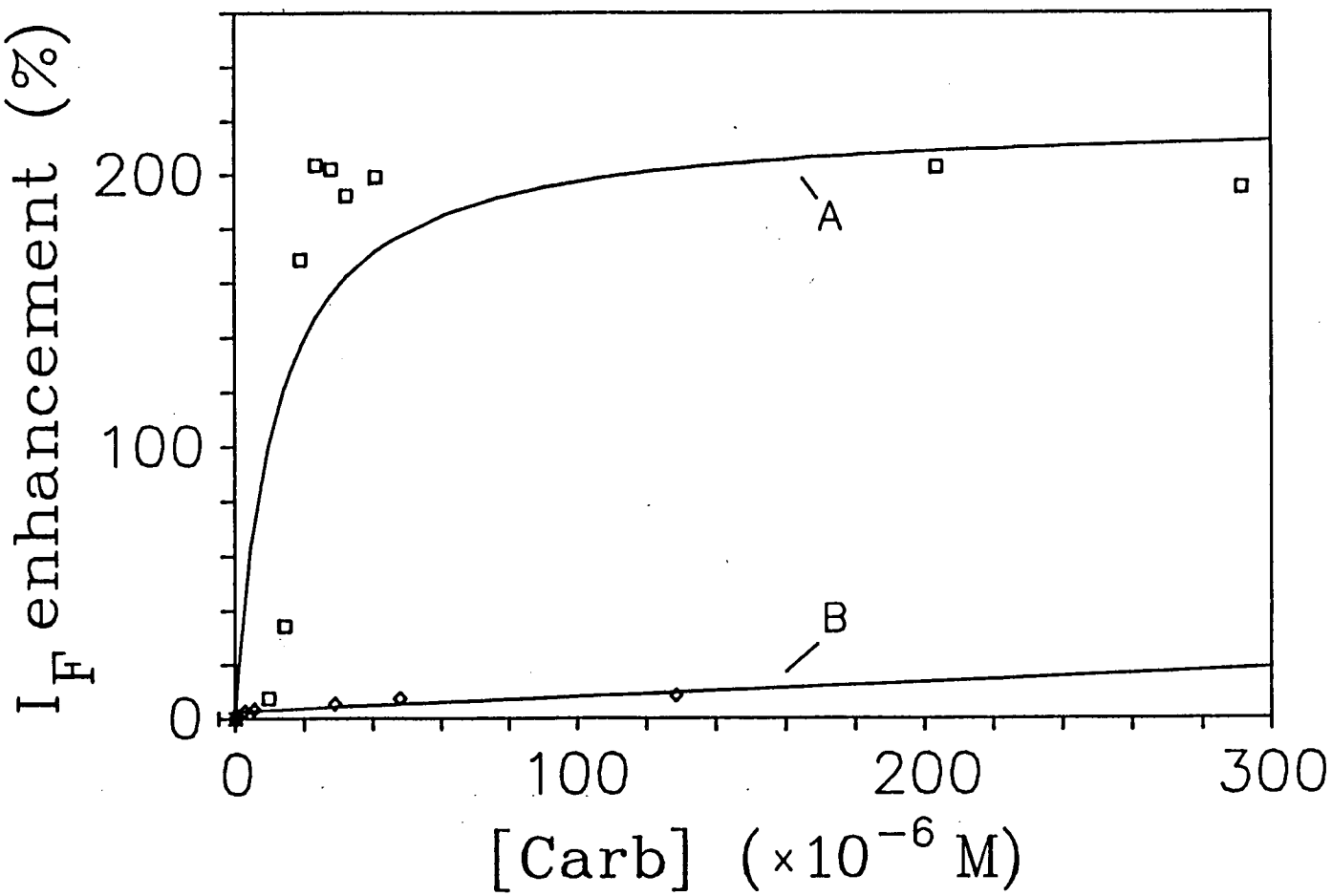

Fig. 7.

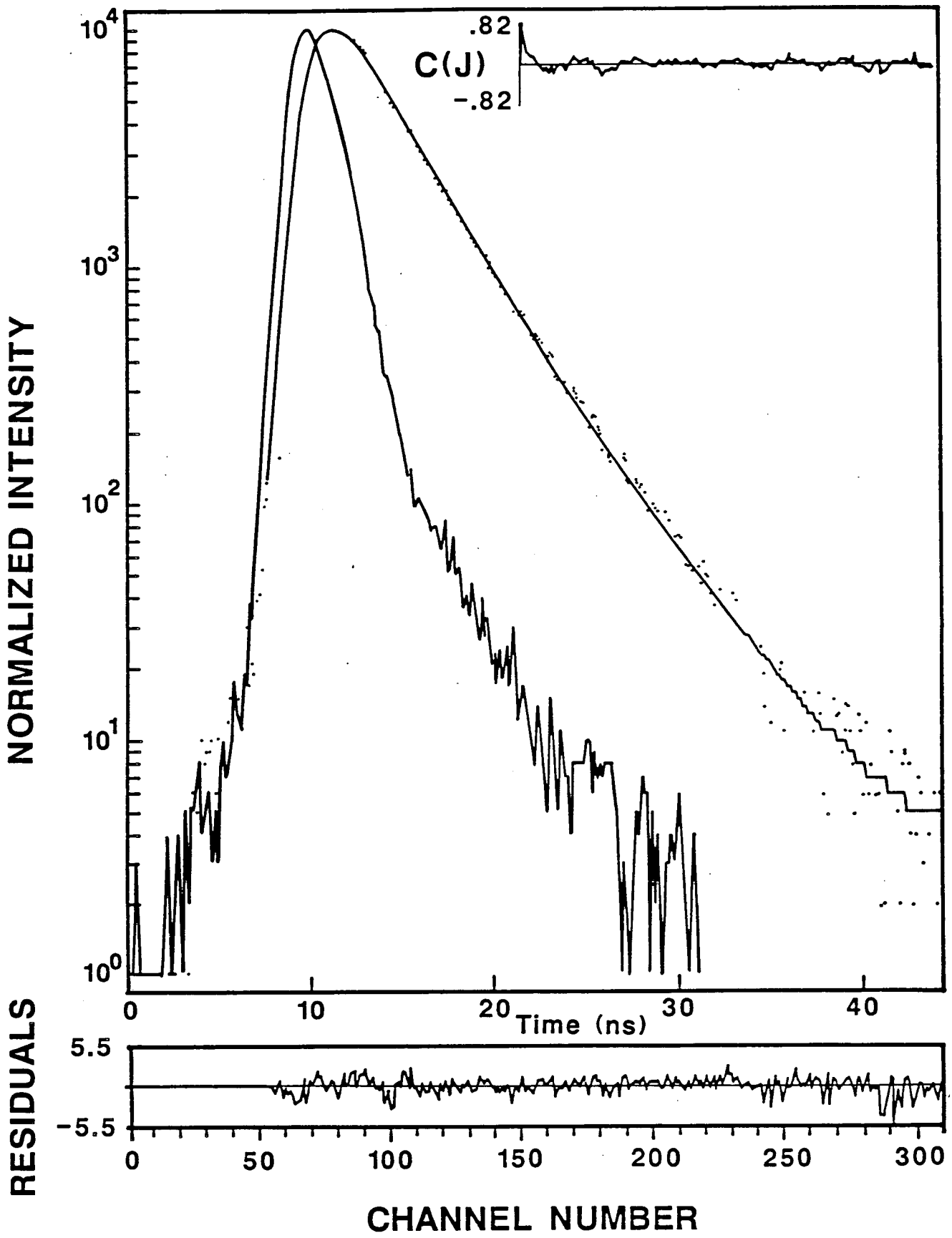
NORMALIZED INTENSITY
10^4
10^3
10^2
10^1
10^0
.82
C(J)
-.82
0
10
20
30
40
Time (ns)
RESIDUALS
5.5
-5.5
0
50
100
150
200
250
300
CHANNEL NUMBER

Fig. 8

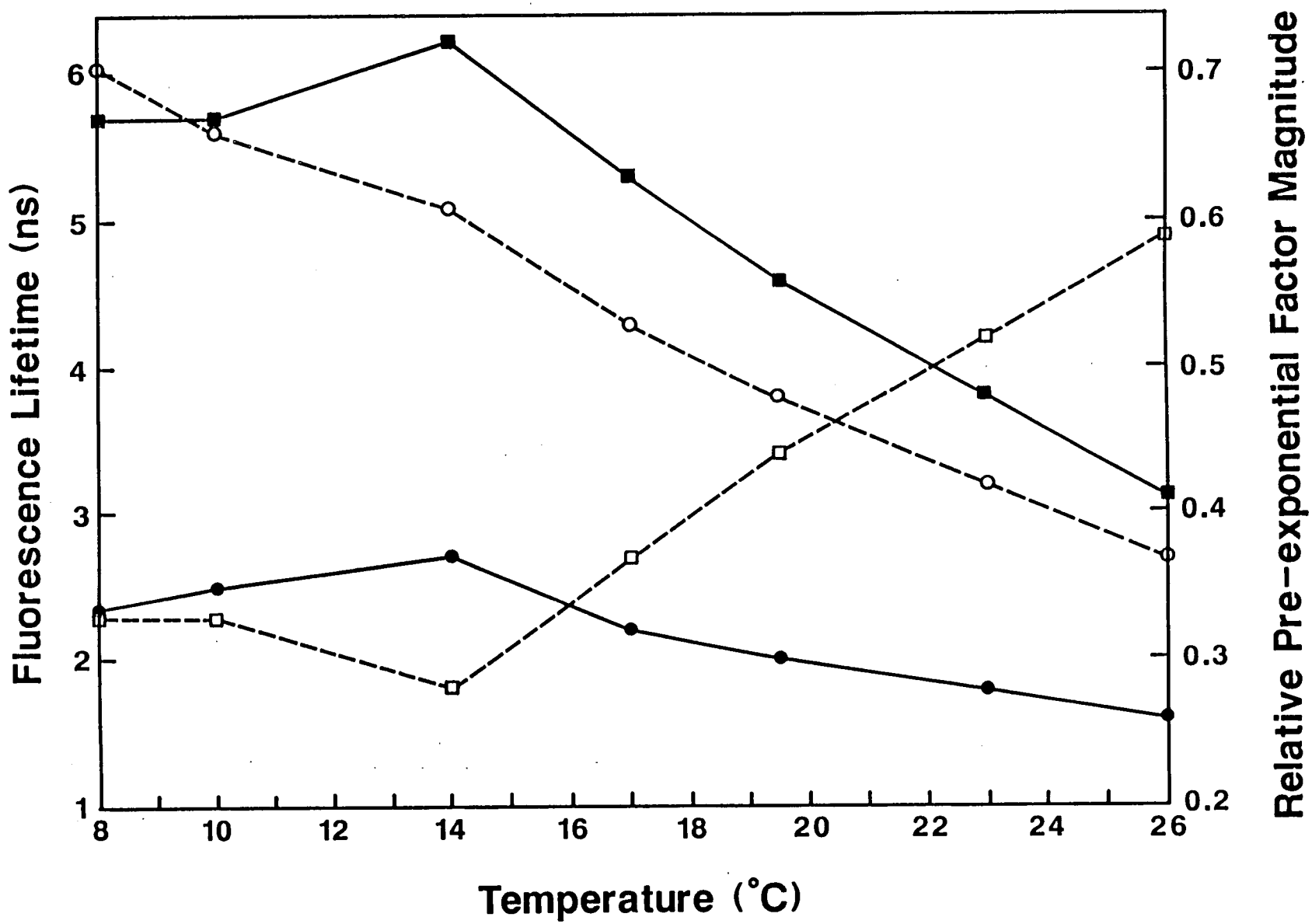
Fluorescence Lifetime (ns)
Relative Pre-exponential Factor Magnitude
Temperature (°C)
1
2
3
4
5
6
0.2
0.3
0.4
0.5
0.6
0.7
8
10
12
14
16
18
20
22
24
26

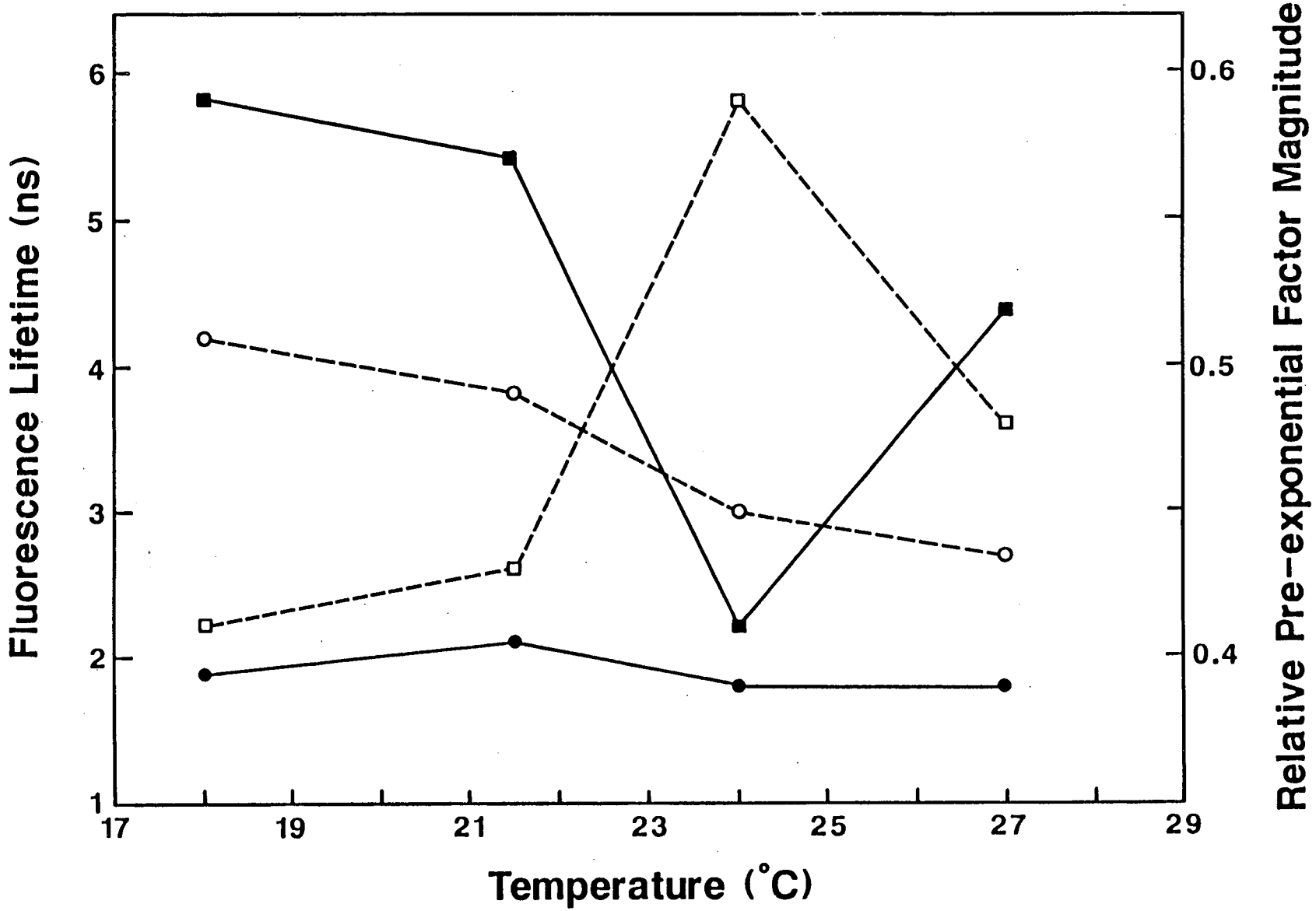
Fluorescence Lifetime (ns)
Relative Pre-exponential Factor Magnitude
Temperature (°C)
6
5
4
3
2
1
0.6
0.5
0.4
17
19
21
23
25
27
29

Fig. 10.

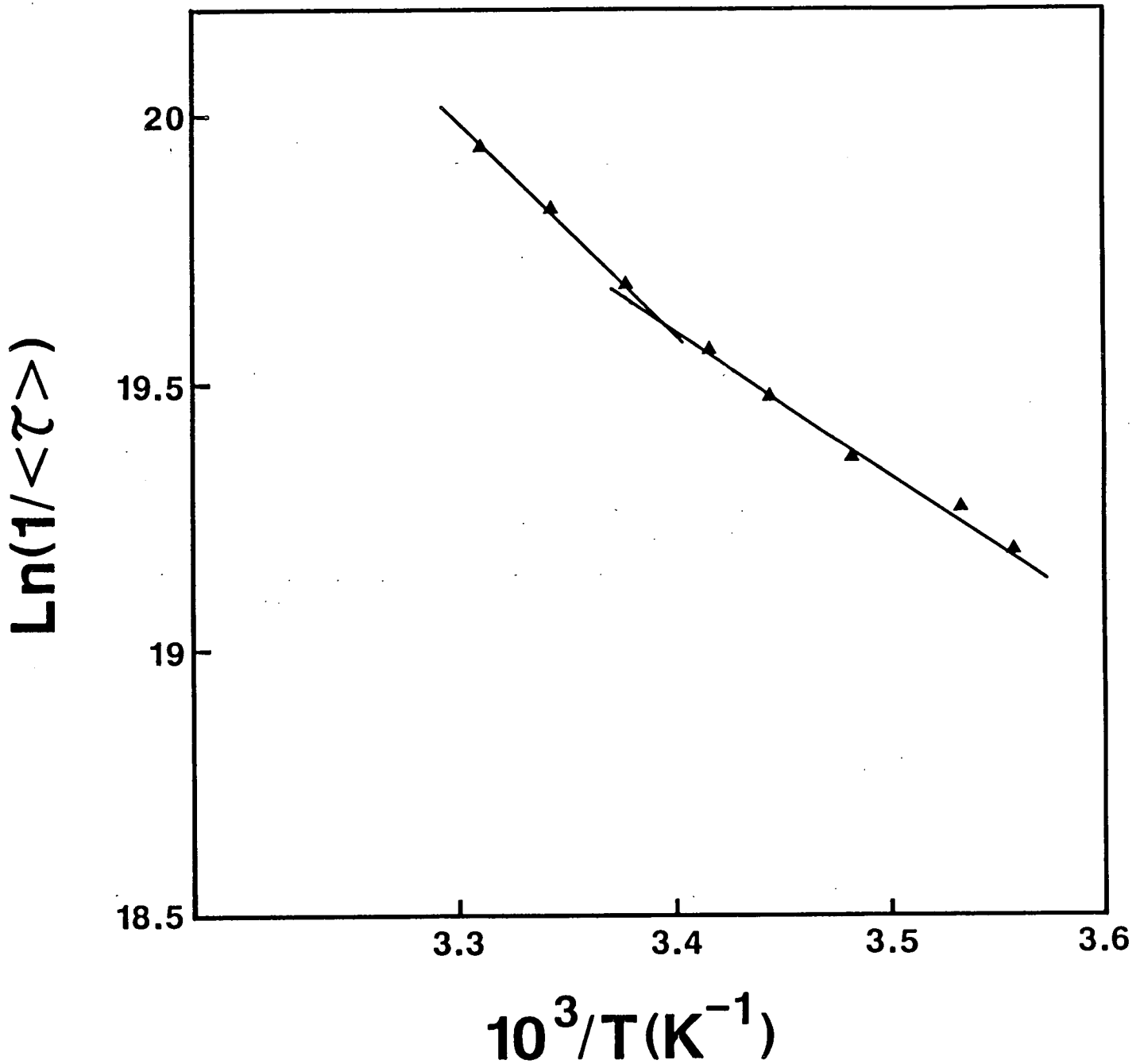

Fig. 11

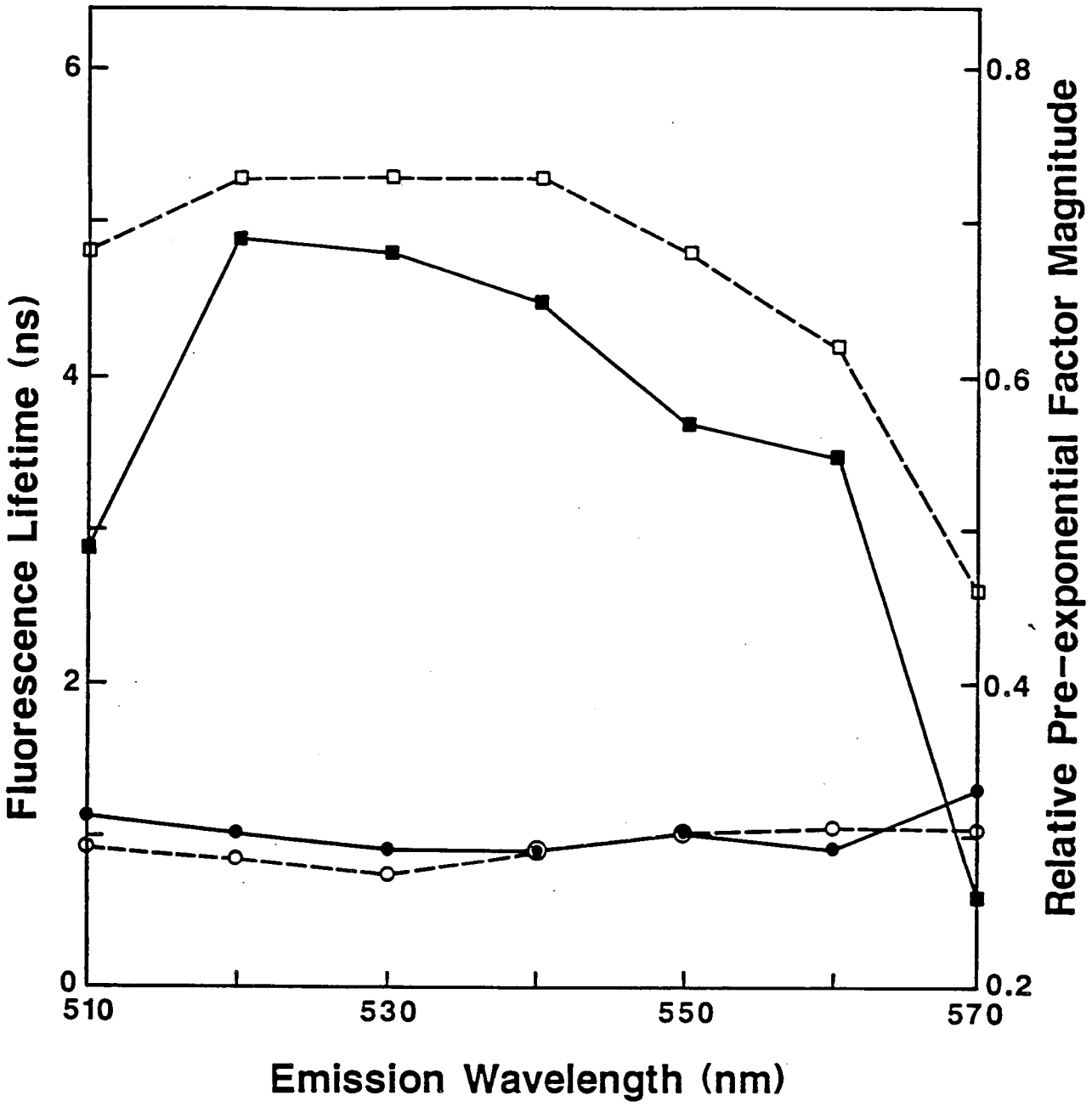
Fluorescence Lifetime (ns)
Relative Pre-exponential Factor Magnitude
Emission Wavelength (nm)
0
2
4
6
0.2
0.4
0.6
0.8
510
530
550
570

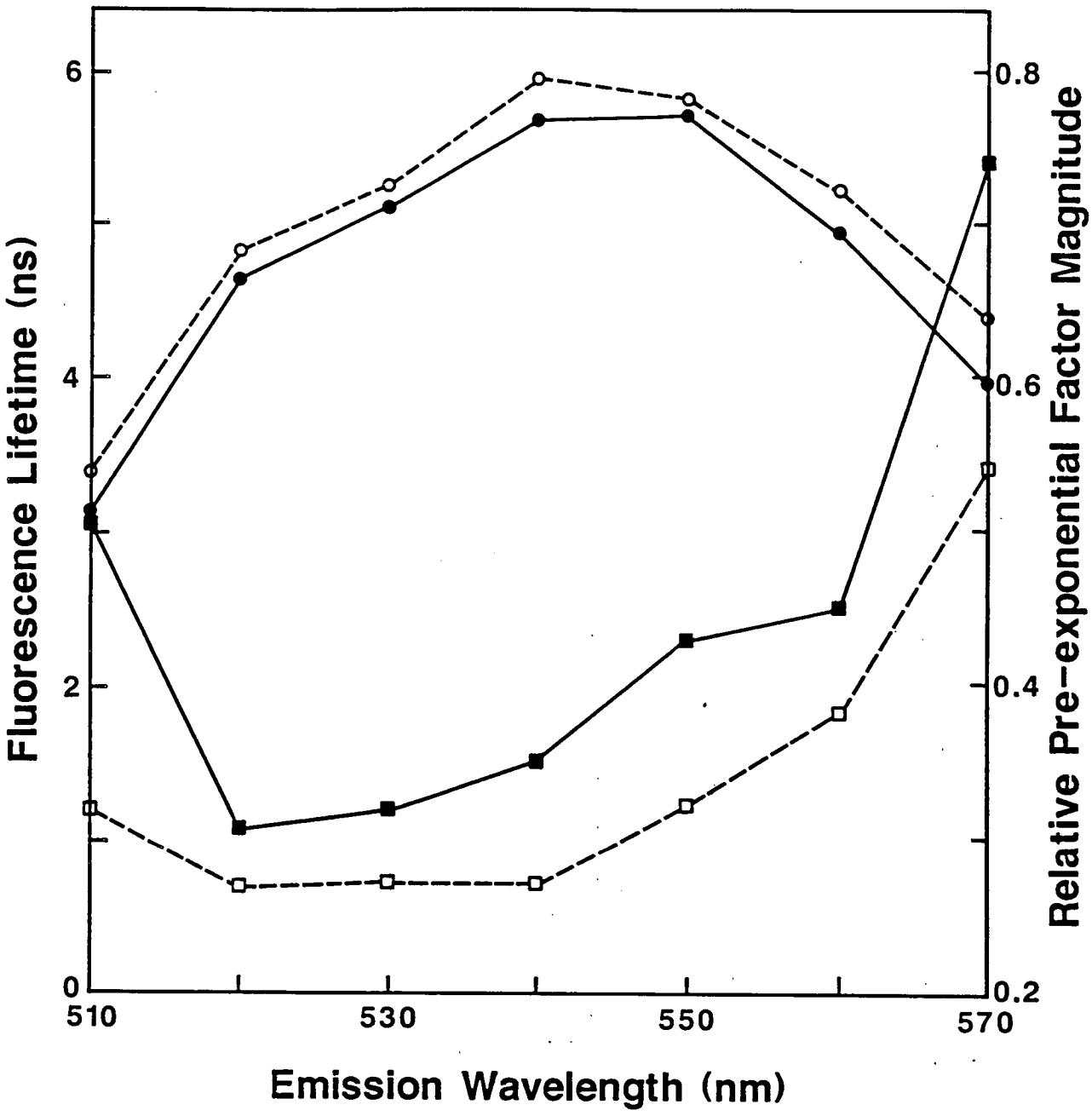
Fluorescence Lifetime (ns)
Relative Pre-exponential Factor Magnitude
Emission Wavelength (nm)
0
2
4
6
0.2
0.4
0.6
0.8
510
530
550
570

Fig 13

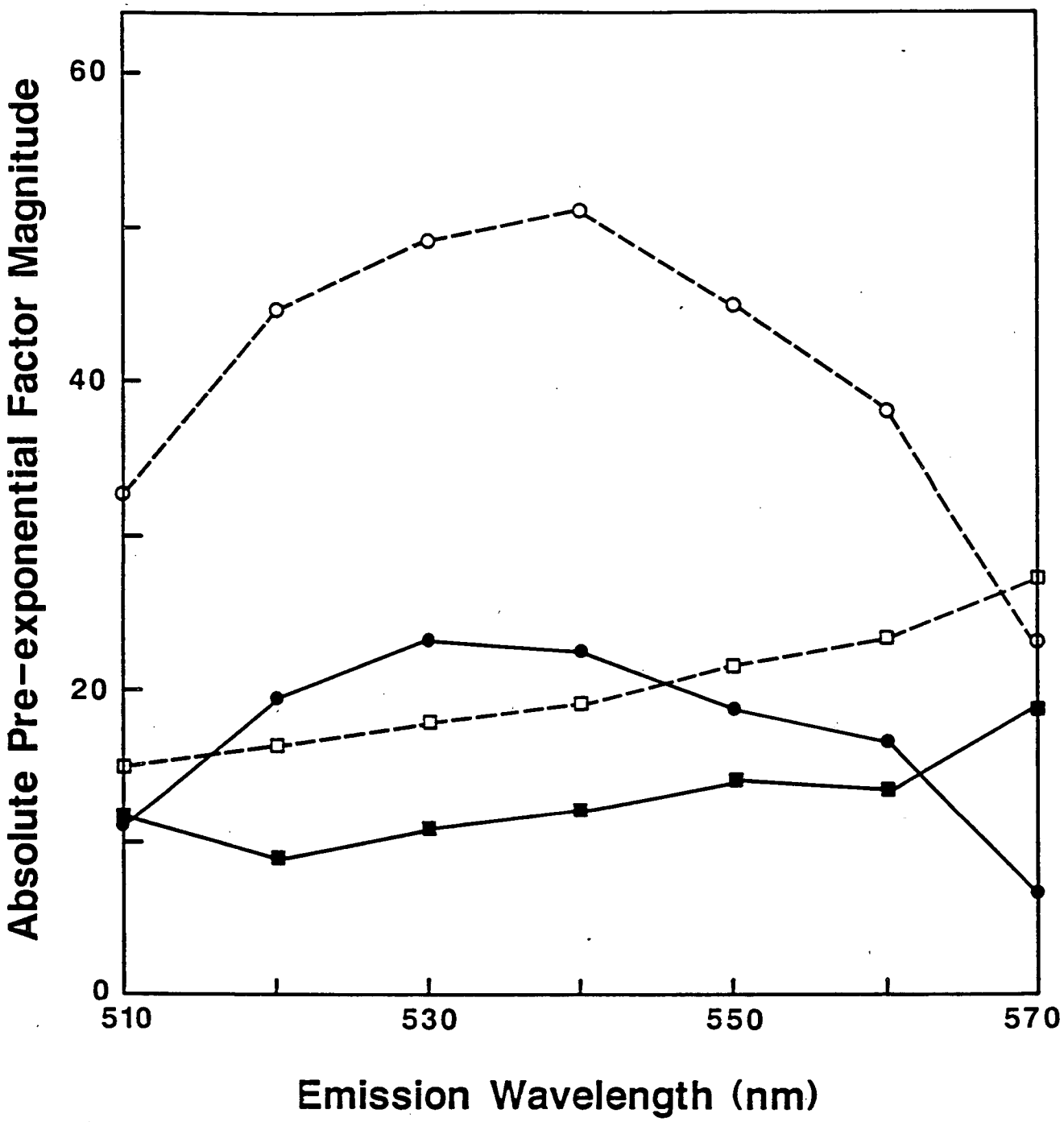
Absolute Pre-exponential Factor Magnitude
60
40
20
0
510
530
550
570
Emission Wavelength (nm)

Fig 14